

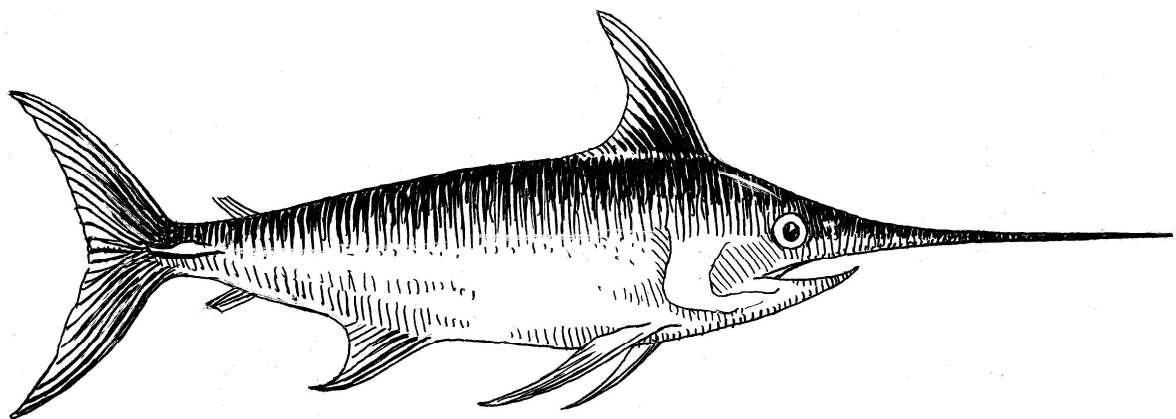


Australian Government
Australian Fisheries Management Authority

R 2014/0821 | April 2016



Determination of swordfish growth and maturity relevant to the southwest Pacific stock



Jessica Farley, Naomi Clear, Dale Kolody,
Kyne Krusic-Golub, Paige Eveson, Jock Young



www.afma.gov.au

 Protecting **our** fishing future

Determination of swordfish growth and maturity relevant to the southwest Pacific stock

Jessica Farley, Naomi Clear, Dale Kolody, Kyne Krusic-Golub, Paige Eveson, Jock Young
R 2014/0821
April 2016



Australian Government
Australian Fisheries Management Authority



Western and
Central Pacific
Fisheries
Commission



Fish Ageing Services Pty Ltd

Copyright

© Commonwealth Scientific and Industrial Research Organisation 2016. To the extent permitted by law, all rights are reserved and no part of this publication covered by copyright may be reproduced or copied in any form or by any means except with the written permission of CSIRO.

Important disclaimer

CSIRO advises that the information contained in this publication comprises general statements based on scientific research. The reader is advised and needs to be aware that such information may be incomplete or unable to be used in any specific situation. No reliance or actions must therefore be made on that information without seeking prior expert professional, scientific and technical advice. To the extent permitted by law, CSIRO (including its employees and consultants) excludes all liability to any person for any consequences, including but not limited to all losses, damages, costs, expenses and any other compensation, arising directly or indirectly from using this publication (in part or in whole) and any information or material contained in it.

CSIRO is committed to providing web accessible content wherever possible. If you are having difficulties with accessing this document please contact enquiries@csiro.au.

ISBN 978-1-4863-0688-6

Determination of swordfish growth and maturity relevant to the southwest Pacific stock. By Jessica Farley, Naomi Clear, Dale Kolody, Kyne Krusic-Golub, Paige Eveson, Jock Young – print
CSIRO Oceans & Atmosphere, Hobart, 2016.

Contents

Acknowledgments.....	10
Executive summary	11
1 Background	14
1.1 Age and growth	14
1.2 Maturity.....	15
1.3 Resolving the uncertainty.....	15
2 Need	17
3 Objectives	18
4 Inter-lab comparison of methods to estimate age and maturity of Pacific swordfish	19
4.1 Age estimation.....	19
4.2 Ovary classification.....	21
4.3 Conclusions.....	22
5 Age and growth of swordfish in the SW Pacific.....	23
5.1 Introduction.....	23
5.2 Methods	23
5.3 Results and Discussion.....	35
5.4 Conclusions.....	52
6 Maturity of swordfish in the SW Pacific	54
6.1 Introduction.....	54
6.2 Methods	54
6.3 Results and Discussion.....	61
6.4 Conclusions.....	69
7 Implications of new growth, maturity and natural mortality estimates for the stock assessment.....	70
7.1 Introduction.....	70
7.2 Methods	71
7.3 Results and Discussion.....	77
7.4 Conclusions.....	78
8 Recommendations for future assessments.....	83
References	85

Appendix A	Distally ground A) sagittae and B) lapilli and C) transverse ground sagittae from the same fish. The clearest count path is shown at higher magnification	91
Appendix B	Examples of the variability in swordfish sagittal otolith morphology among similar sized fish.	94
Appendix C	Daily age estimates versus annual age estimates from otoliths (transverse sections read at 640-1000x magnification with transmitted light).	95
Appendix D	Example images for some otoliths prepared for annual (left) and daily (right) examination. White line represents transect A (distance and count to a point that corresponds to either the marked change in microincrement structure or as indicated on the annual images, the first assumed annual zone).	98
Appendix E	Examples of the transition point in otoliths.....	102
Appendix F	Age bias plots (+/- CI) between readers (R1-R4) of rays and otoliths.....	105
Appendix G	Comparison of von Bertalanffy growth curves to otolith-based age data from three readers (R1, R2 and R3).	107
Appendix H	Examples of the marginal state of clear otoliths and fin rays for each month that samples are available for. Where possible, hardparts were selected from the same fish.	108

Figures

Figure 1 Age bias plots for comparisons of counts of translucent zones in fin rays by reader 1 (R1) (left) and reader 2 (R2) (right) and the median age obtained by 4 labs in an inter-laboratory study (DeMartini et al. 2007).	20
Figure 2 Map indicating the capture locations of swordfish sampled for otoliths (from Young & Drake 2004).	24
Figure 3 Swordfish #148 (female, 195 cm OFL, October) fin ray prepared for annual ageing with the outer edge of translucent zones indicated by red dots.	26
Figure 4 The cycle of edge classifications used for swordfish rays.	27
Figure 5 The three different otolith structures of swordfish, indicating their size and shape.	28
Figure 6 Illustration of the individual grinding process for preparation transverse otolith thin sections (Source: Robbins & Choat 2002).	29
Figure 7 Transverse preparation of a swordfish sagittae (#224) prepared for annual reading showing the reasonably clear alternating opaque and translucent zones with the outer edge of translucent zones (or start of the opaque zones) indicated by red dots. Note the double banding (grey arrows) in the opaque zones in the first 5 or 6 assumed annual increments.	30
Figure 8 Example of assumed daily increments in a transverse sectioned otolith and also the approximate position (white arrow) where there is a noticeable change in the pattern and clarity of the DGZs.	31
Figure 9 Transverse section of an otolith indicating the locations of measurements taken. Blue line measurement A, red line measurement B and black line measurement C. The transverse section prepared for annual age estimation is also shown for comparison (right). The yellow crosses indicate the primordium, the first assumed opaque zone and the otolith edge.	31
Figure 10 Swordfish otolith (#228; 230 cm OFL, female) prepared for annual ageing with two presumed annual opaque zones indicated by arrows. The blue arrow is at 0.550 mm and the green arrow at 0.750 mm from the primordium.	32
Figure 11 Swordfish otolith (#589, 161 cm OFL, male) prepared for annual ageing with presumed annual opaque zones indicated by arrows. The blue arrow is at 0.612 mm. The green and subsequent white arrows indicate the presumed 2 nd to 6 th opaque zones.	33
Figure 12 Swordfish otolith (#196, 257 cm OFL, female) otolith prepared for annual ageing with presumed annual opaque zones indicated by crosses. The primordial and edge are also marked with a cross.	33
Figure 13 Cycle of edge classifications used for swordfish otoliths.	34
Figure 14 Relationship between fish size and: fin ray diameter (n=390) (A), otolith weight (n=305) (B) and otolith transverse section (TS) length (n=296) (C) for male and female swordfish.	35
Figure 15 Transverse section of an otolith (108 cm OFL). Blue arrow indicates 100 increments and the black arrow indicates 150 increments. The total count was 299 increments.	39

Figure 16 Highlighted area under higher magnification (100x) of the transition point in the otolith (other examples are shown in Appendix E).	39
Figure 17 Comparison of daily and annual counts from transverse sectioned otoliths sampled from the same fish.	40
Figure 18 Relationship between orbital fork length (OFL, cm) and daily counts from transverse sectioned otoliths obtained in the current study (•) and the study by Young & Drake (2004) (x) for fish sampled in the SW Pacific.....	40
Figure 19 The relationship between otolith weight and annual age for swordfish in the SW Pacific (n=290). $R^2 = 0.7698$	41
Figure 20 Mean (+/- SE) monthly ray marginal increment ratio (MIR) for male and female swordfish (n = 318). Sample size is shown next to the mean; only months where n ≥ 5 are shown.	43
Figure 21 Mean (+/- SE) monthly otolith marginal increment ratio (MIR) for male and female swordfish (m = 263). Sample size is shown next to the mean; only months where n ≥ 5 are shown.	44
Figure 22 Age bias plots by sex comparing final age estimates from otoliths and rays from the same fish. R1 = reader 1, R3 = reader 3.	45
Figure 23 Swordfish #224 (female, 219 cm OFL) fin ray and otolith prepared for annual ageing. The red dots indicate the outer edge of the translucent zones counted, giving a slightly higher age from the ray (11 years) compared to the otolith (10 years).	47
Figure 24 von Bertalanffy growth curves fitted to length at age (count) from otoliths (top) and rays (i.e., spines) (bottom) by sex (○= females; Δ = males).	50
Figure 25 Comparison of sex-specific VB growth curves estimated using otolith and ray (i.e., spine) count data.	51
Figure 26 von Bertalanffy growth curves estimated by sex for swordfish in the current study compared to previous studies by DeMartini et al. (2007) and (Young & Drake 2004). The curves only cover the age range of the data.	52
Figure 27 Map indicating the capture locations of swordfish sampled for gonads (from Young & Drake 2002).	55
Figure 28 Oocyte development classes in fresh (left) and frozen (right) fixed swordfish ovaries. A: unyolked (UY). B: early yolked (EY). C: advanced yolked (AY). D: migratory nucleus (MN). E: Hydrated. Bar equals 500 μm.	57
Figure 29 Postovulatory follicles degeneration in fresh (left) and frozen (right) fixed swordfish ovaries. A: Early stage POF which has a clear convoluted shape and two distinct layers (T = thecal; G = granulosa). B: later stage POF which has a smaller lumen (L) and the thickness of the thecal and granulosa layers has increased. C: old POF where the folds have shrunk and convoluted shape is disappearing. Bar equals 100 μm.	58
Figure 30 Atresia of advance yolked oocytes in fresh- (left) and frozen (right) fixed swordfish ovaries. A-B: Late stage alpha (α) with some yolk granules remaining. C-D: Beta (β). Bar equals 200 μm.	59

Figure 31 Histological sections of ovaries containing maturity markers considered in this study including (A) well defined muscle bundles (black arrows), (B-D) “brown bodies” (black arrows), and (E-F) clumps of residual hydrated oocytes (RHO). Black bar equals 1000 μm , grey bar equals 500 μm white bar equals 100 μm 60

Figure 32 Examples of residual hydrated oocytes (RH, black arrows) in the ovary lumen (A, B) and connective tissue (C, D) of swordfish <125 cm OFL. A = 121 cm OFL, B = 97 cm, C = 111 cm, B = 80 cm. 62

Figure 33 Proportion of mature female swordfish by reproductive phases sampled by month (n=432). 63

Figure 34 Box plot of gonadosomatic index (GSI) by month for female swordfish. The horizontal line through a box indicates the median, the length of a box represents the inter-quartile range, and the vertical lines extend to the 10th and 90th percentiles. 63

Figure 35 Observed ovary weight at orbital fork length (OFL) for female swordfish (n=656). 65

Figure 36 Comparison of maturity curves estimated using three different link functions (cloglog = complementary log-log). Also shown is the observed proportion of mature females in each 5-cm length class (filled red circles) ± 2 standard errors. 66

Figure 37 The fitted maturity curve from the best-fitting complementary log-log model (solid black line) with approximate 95% confidence region (grey shaded region), calculated as the estimated proportion mature ± 2 standard errors. Also shown is the observed proportion of mature females in each 5-cm length class (filled red circles) ± 2 standard errors. 66

Figure 38 The fitted maturity at age curve from the best-fitting logit model (solid black line), where age was estimated from length using the female VB growth curve derived from ray (i.e., spine) data. The grey shaded region is the approximate 95% confidence region, calculated as the estimated proportion mature ± 2 standard errors. Also shown is the observed proportion of mature females in each age class (filled red circles) ± 2 standard deviations. 67

Figure 39 The fitted maturity at age curve from the best-fitting logit model (solid black line), where age was estimated from length using the female VB growth curve derived from otolith data. The grey shaded region is the approximate 95% confidence region, calculated as the estimated proportion mature ± 2 standard errors. Also shown is the observed proportion of mature females in each age class (filled red circles) ± 2 standard deviations. 68

Figure 40 Sex-aggregated growth curves (A) and female maturity ogives (B) used in the Davies et al. (2013) assessment, and the otolith-derived and spine-derived age estimates from this study, used for evaluating stock assessment implications. Note that the term spine is used here rather than ray. 73

Figure 41 Comparison of age-specific length frequency distributions assuming equal numbers of males and females using the otolith-based LJFL growth curves from this study (black line), and the combined sex-aggregated approach (red line). The indicated SD applies to both distributions within each age class. 74

Figure 42 The eight natural mortality (*M*) vectors explored in the Davies et al. (2013) assessment (A) and analogous *M* vectors derived from otolith-based and spine-based growth/maturity estimates from this study (B). Scenario H-HS represents the reference case

mortality assumption from the 2013 assessment (relatively high M , with a spawning-related component, derived for the Hawaiian growth and maturity estimates from DeMartini et al (2000; 2007), referred to as GHMHS in Davies et al. 2013); A-HS is the analogous model from the 2013 assessment based on the Australian growth and maturity estimates from Young & Drake (2002; 2004) (GAMHS in Davies et al. 2013); S-HS (spine-based) and O-HS (otolith-based) represent the analogous M assumptions derived from this study. M abbreviations are explained in Table 13 and Table 14. Note that the term spine is used here rather than ray. 75

Figure 43 Time series of estimated stock status reference points for the Davies et al. (2013) reference model (derived from the Hawaiian life history parameters HHH-HS), and the analogous models (in terms of M) derived from the Australian life history parameters in 2013 (AAA-HS), the otolith-based (OOO-HS) parameters from this study, and the ray/spine-based (SSS-HS) parameters from this study. Model abbreviations are explained in Table 13 and Table 14. 80

Figure 44 Time series of estimated stock status reference points for the Davies et al. (2013) reference model (derived from the Hawaiian life history parameters HHH-HS), and the analogous models (in terms of M) derived from the Australian life history parameters in 2013 (AAA-HS), and mixed combinations of Australian and Hawaiian life history parameters from the 2013 assessment. The mixed combinations are not considered realistic, but provide insight into the relative importance of growth, maturity and M . Model abbreviations are explained in Table 13 and Table 14. 81

Figure 45 Time series of estimated stock status reference points for a range of models using the otolith-based and ray/spine-based growth and maturity estimates from this study, combined with the full range of M assumptions analogous to the assessment uncertainty grid from Davies et al. (2013). The otolith-based (OOO-HS) and ray/spine-based (SSS-HS) models are the closest analogues to the reference case model from 2013. Model abbreviations are explained in Table 13 and Table 14. 82

Tables

Table 1 Comparison of maturity status of swordfish from the SW Pacific based on histological evaluation. Imm/rest = immature/resting. 21

Table 2 Number of rays and otoliths available and those selected for ageing by month. 25

Table 3 Number of age estimates obtained from rays and otoliths by age class and by sex. 36

Table 4 Mean radius of the distal edge of each translucent zone in rays for male and female swordfish caught in the ETBF. SD = standard deviation. Increment = increase in the mean radii from the preceding increment. 37

Table 5 Precision for age estimates (counts) between readers and hardparts. 42

Table 6 Summary table of paired t-test results for age estimates obtained from otoliths and rays from the same fish. The results are shown by sex and otolith-age. Significant differences among ages are indicated by *. 45

Table 7 Sex-specific VB growth parameters estimated using otolith and ray count data.	49
Table 8 Number of swordfish by histological classification. MAGO = most advanced group of oocytes, POF = postovulatory follicle.....	62
Table 9 Comparison of maturity at length model results using the logit, probit and complementary log-log (cloglog) link functions. L_{50} denotes the length at which 50% of females are estimated to be mature.	66
Table 10 Comparison of maturity at age model results using the logit, probit and complementary log-log (cloglog) link functions. Age was estimated from length using the female VB growth curve derived from ray and otolith data.....	67
Table 11 Estimated length at 50% maturity (L_{50}) for female swordfish. The estimate for the current study and DeMartini are shown in OFL and lower jaw fork length (LJFL) for comparison with other studies.	69
Table 12 Multifan-CL growth parameters for the sex-aggregated growth curves derived from this study.....	73
Table 13 M vectors (instantaneous annual) analogous to those used in 2008 and 2013 assessments, derived from the otolith-based and spine-based growth and maturity estimates in this study (shown in Figure 42). Note that the term spine is used here rather than ray.....	76
Table 14 Suite of MFCL assessment models exploring the implications of a range of growth, maturity and M assumptions, including the reference case model defined in Davies et al. (2013) with Hawaiian-based life history assumptions from DeMartini et al. (2000; 2007), the analogous model with the Australian life history assumptions from Young & Drake (2002; 2004), analogous models with the new otolith-based and spine-based growth and maturity estimates from this study (3-4), intermediate model configurations that partition the relative effects of growth, maturity and M from the 2013 assessment (models 5-10), and a suite of models using the growth and maturity estimates from this study and spanning the range of M uncertainty from the assessment (i.e., using M vectors analogous to those used in the assessment, but derived for the growth and maturity estimates from this study) (models 11-16). Assessment assumptions other than growth, maturity and M correspond to the reference case from the 2013 assessment. A = Australian studies (Young & Drake 2002, 2004), H = Hawaiian studies (DeMartini et al. 2000, 2007), O = this study Otoliths, S = this study Spines; M definitions are explained in the text and shown in Figure 42. Note that the term spine is used here rather than ray.....	77
Table 15 Convergence and stock status statistics from the suite of MFCL assessment defined in Table 14. The negative log-likelihood-based objective function has been rescaled relative to the lowest (best fit) value. A = Australian studies (Young & Drake 2002, 2004), H = Hawaiian studies (DeMartini et al. 2000, 2007), O = this study Otoliths, S = this study Ray/Spines; M definitions are described in the text and shown in Figure 42.	79

Acknowledgments

We would especially like to thank Ed DeMartini and Bob Humphreys at NOAA Pacific Islands Fisheries Science Center (PIFSC) for hosting our visit to Hawaii and providing guidance and assistance on fin ray and ovary interpretation. Thanks also to Andrew Brown (Fish Ageing Services Pty Ltd) who assisted with the initial otolith investigation and prepared the majority of the otolith samples for annual ageing; and to Anita Drake, Tonya van der Velde and Michael Barlow for preparing the ovary histology and ray sections as part of the FRDC projects 1999/108 and 2001/014. Thanks to Nick Davies and the Secretariat of the Pacific Community for providing the 2013 swordfish stock assessment configuration files and software. We also gratefully acknowledge all the field people and fish processors involved in collecting the fin rays, otoliths and gonads for the project. Finally we thank Malcolm Haddon and Shane Griffiths for reviewing this report. This work was funded by the Australian Fisheries Management Authority (AFMA), the Western and Central Pacific Fishery Commission (WCPFC), and CSIRO Oceans and Atmosphere.

Executive summary

This project was developed in response to concern expressed by the Western and Central Pacific Fisheries Commission Scientific Committee regarding biological aspects of the 2013 South Pacific Swordfish (*Xiphias gladius*) stock assessment. The stock status estimates had a high degree of uncertainty that was attributed to uncertainty in the accuracy of growth and maturity parameters. The Scientific Committee recommended that additional work on age, growth and age validation should be undertaken to reduce the uncertainty in future assessments.

The aim of the project was to (i) determine the degree to which differences in swordfish growth and maturity parameters obtained by Young & Drake (2002; 2004) and DeMartini et al. (2000; 2007) for swordfish in the southwest (SW) Pacific off Australia and the central North Pacific around Hawaii, respectively, were methodological or due to spatial variation in life-history, and (ii) to develop standardised protocols for interpreting fin rays (spines), otoliths and ovaries to re-estimate growth and maturity parameters for swordfish in the SW Pacific. The project also aimed to examine the effect of the different growth curves and maturity ogives on swordfish assessments and to make recommendations for future assessment and harvest strategy evaluation activities.

The project met all of its objectives, including the evaluation of otoliths to estimate the annual age of swordfish in the SW Pacific. Although direct validation of the ageing method was not possible in this project, the results of the otolith analysis suggest that swordfish live longer and grow slower than previously estimated. The project also evaluated ovaries and estimated a maturity ogive. The new estimate of length at 50% maturity is substantially lower than the preliminary estimate obtained by Young & Drake (2002) for swordfish in the SW Pacific.

The main findings of the project are:

Growth

1. Methodological differences did exist between previous studies to estimate the age of swordfish in the SW Pacific and Hawaiian regions using counts of increments in fin rays (i.e., the studies of Young & Drake 2004 and DeMartini et al. 2007). The methodological differences could explain the different growth parameter estimates obtained by the studies.
2. The new ray-based age interpretations presented here are consistent with other international labs in the Pacific, including the NOAA PIFSC lab in Hawaii.
3. The otolith-based age interpretations presented here are consistent with the interpretations of otoliths by the NOAA PIFSC lab in Hawaii. While the PIFSC study rejected the use of otoliths for a number of reasons, indirect validation work undertaken in this study suggests that otolith-based age estimates should be considered in future assessments.
4. Age estimates from fin rays and otoliths sampled from the same fish produce different growth curves for both male and female swordfish in the SW Pacific. A clear discrepancy is evident in age classes >7 years for females and >4 years for males, where ray counts are lower on average compared to otolith counts.

5. The otolith-based growth curves indicate slower growth and a higher maximum age for both males and females, compared to the ray-based growth curves of Young & Drake (2004) and DeMartini et al. (2007). The maximum estimated age for (female) swordfish was 14 years from rays and 21 years from otoliths.
6. Age estimates from otoliths are likely to be more reliable than for rays, especially in larger/older fish, as rays are subject to resorption and vascularisation of the core. However, due to the precision required when sampling and sectioning otoliths, fin rays may be the more practical structure for ageing smaller fish up to approximately 170 cm orbital fork length (OFL) for females and 120 cm OFL for males. These lengths correspond to the ages up to which otoliths and rays give similar results.
7. Direct validation of the age estimation methods are required.

Maturity

8. Methodological differences did exist between the previous studies to estimate the maturity of swordfish in the SW Pacific and Hawaiian regions (i.e., the studies of Young & Drake 2002 and DeMartini et al. 2000). These methodological differences could explain the different parameter estimates of the maturity ogive obtained by the studies.
9. Methodological differences still exist between DeMartini et al. (2000) and the current study to differentiate immature from mature-regenerating females. However, these differences are unavoidable because the majority of ovary material collected in the SW Pacific was frozen before being fixed, resulting in poorer quality histological sections. It was agreed that the histological classification system used in the current study was appropriate and was successfully identifying mature and immature female swordfish.
10. The new estimate of length at 50% maturity for female swordfish in the SW Pacific is 161.5 cm OFL. This is higher than estimated by DeMartini et al. (2000) for swordfish around Hawaii (143.7 cm OFL), but substantially lower than the preliminary estimate obtained by Young & Drake (2002) (193.6 – 199.7 cm OFL) and is within the range for swordfish worldwide.
11. The new estimate of age at 50% maturity for female swordfish in the SW Pacific is 4.34 years using ray-based ages and 4.42 years using otolith-based ages. These estimates are very similar because the divergence observed in length-at-age from rays and otoliths occurs well after this age in females.

Implications for the stock assessment

12. The new life-history parameters estimated for swordfish in the SW Pacific appear to differ from those estimated for the Hawaiian region. This supports the hypothesis of geographically separate populations. Given this, we recommend that the life-history parameters of DeMartini et al. (2000) and DeMartini et al. (2007) should no longer be used for (at least the western part of) the SW Pacific.
13. Both otolith and ray-based age estimates for swordfish require direct validation; however, there are strong arguments why otolith-based age estimates should be preferable, particularly for older individuals. Therefore, we recommend that otolith-based estimates of growth and maturity should be included in future assessments.

14. A range of models resembling key 2013 stock assessment configurations were examined to compare the stock status implications and relative importance of different growth, maturity and natural mortality (M) assumptions (M estimates were not part of the study, but were parameterized as a function of growth and maturity in the assessment). The results suggest that: i) growth and M uncertainties are considerably more influential than maturity, ii) stock status estimates from the ray-based age estimates in this study tend to be pessimistic (recent $F > F_{MSY}$) and resemble the scenarios from 2013 based on life history parameters from Young and Drake (2002; 2004), iii) stock status estimates from the otolith-based age estimates in this study tend to be more optimistic, and resemble the scenarios from 2013 based on life history from DeMartini et al. (2000; 2007) (though one out of four scenarios suggested recent overfishing depending on the M assumption). A number of recommendations for future assessments are provided.

1 Background

Broadbill swordfish (*Xiphias gladius*) are a large pelagic species distributed between ~50°N and 50°S in all of the major oceans. In the Pacific, there is genetic evidence of three independent populations (north, southwest and southeast) with no mixing across the equator in the western Pacific (Reeb et al. 2000). Recent tagging work suggests there may be structure within the southwest (SW) population as fish tagged off eastern Australia showed little propensity to move eastward, remaining instead within the western half of the Coral and Tasman Seas (Evans et al. 2014). While the tag numbers and release durations are not large, they suggest that there may be a distinct 'Australian population' that range from the east coast to approximately 165°E.

In the mid-to-late 1990s, the swordfish fishery expanded off eastern Australia and New Zealand. Concerns were raised about the sustainability of catches since catch rates and the size of fish caught were both declining. There was an urgent need to determine the status of the stock and develop a stock assessment for the region. Unfortunately, life-history parameters for input to stock assessments of swordfish were not available at the time. In response, two studies were undertaken in the early 2000s to estimate key parameters such as length-at-age, longevity, sex ratio, maturity, spawning frequency and fecundity for fish in the SW Pacific (Young & Drake 2002; 2004). The growth and maturity parameters obtained in these studies were very different to those obtained by DeMartini et al. (2000; 2007) for swordfish caught in the central North Pacific around Hawaii. As it was not known if the differences were methodological or due to spatial variation in life-history, the alternative growth and maturity parameters were both admitted into SW Pacific stock assessments as equally likely alternative hypotheses (Kolody et al. 2008; Davies et al. 2013). The different biological assumptions, however, have important implications for the stock status advice (Davies et al. 2013).

1.1 Age and growth

The traditional method to estimate the annual age of swordfish is to count (assumed) annuli in sectioned anal fin rays (spines). Otoliths were considered too small to be useful in age determination studies (Tserpes & Tsimenides 1995). In the Pacific, the age of swordfish was estimated using rays by both Young & Drake (2004) and DeMartini et al. (2007). These studies used indirect validation methods to verify the age estimates obtained, and estimated growth parameters for male and females by fitting the von Bertalanffy growth model to the data. Young & Drake (2004) fitted the model to the raw length-at-age data and DeMartini et al. (2007) fitted it to back-calculated length-at-age.

As noted above, the growth parameters estimated by the two studies were very different, with a slower growth rate (k) and higher mean asymptotic length (L_{∞}) for both males and females in the SW Pacific relative to Hawaiian waters. It was unknown whether the difference in growth curves was due to genuine differences in swordfish growth between regions and/or differences in fin ray interpretation (methodological) as suggested by Young et al. (2008). Fin rays often contained split

translucent growth zones, which are difficult to interpret, and rays are subject to resorption and vascularisation of the core area making age estimation for older fish difficult.

1.2 Maturity

Maturity schedules for fish are typically obtained by examining gonads using histological techniques to determine maturity status of individuals, and applying statistical models to determine the proportion mature as a function of length or age. Estimates of length and/or age at which 50% of the individuals are sexually mature (L_{50} , A_{50}) are the biological parameters often reported in maturity studies. For many species, maturity schedules are estimated for females only as it is assumed that male sperm production is much less limiting.

Similar to the direct ageing work, maturity parameters were estimated for female swordfish by Young & Drake (2002) and DeMartini et al. (2000) Both studies prepared histological sections of the ovary material and used standard (although slightly different) classification schemes to determine the maturity status of each fish. Predicted L_{50} for fish from the SW Pacific was 194-200 cm orbital fork length (OFL; the distance from the posterior edge of the eye orbit to fork of tail) depending on the analytical model used, compared to only 144 cm OFL for females from Hawaii. Using the corresponding length-at-age data, A_{50} was predicted at 8-10 years for fish in the SW Pacific (Young et al. 2008) compared to only 4-5 years for Hawaiian fish (DeMartini et al. 2000).

The different maturity schedules obtained may be due to regional variation in length-at-maturity; however, different interpretations of the maturity status of individuals from the histological sections is also likely (Young et al. 2008). A difficulty occurs when trying to differentiate immature (virgin) from mature-resting (post-spawning) females because after spawning, females absorb all their yolked eggs (oocytes) and appear histologically similar to immature females. Young & Drake (2002) classified all females with unyolked or early yolked oocytes (as the most advanced present in the ovary) and no alpha or beta atresia as “immature or resting” and subsequently included them as immature in the maturity analysis. Yet the maturity status of immature and resting females is fundamentally different. If a proportion of these fish were truly mature (especially the large fish), it could explain the relatively high L_{50} estimate obtained by Young & Drake (2002) compared to DeMartini et al. (2000), which used specific histological criteria to identify mature-resting females. It was also suggested that much of the histological material examined by Young & Drake (2002) was inadequate for studying maturity due to cell lysis, possibly due to the freezing/thawing of the ovaries prior to tissue fixation (Young et al. 2008), further complicating the process of differentiating immature from mature-resting females.

1.3 Resolving the uncertainty

Work over the last decade has shown that age estimates from otoliths are more accurate than those from other hardparts including rays, vertebrae and scales for large pelagic species such as tunas (see Farley et al. 2013a and references therein). A study by Nishimoto et al. (2006) also suggests that sectioned sagittal otoliths may be useful to estimate the annual age of swordfish in the Pacific. Although over 500 otoliths were collected by Young & Drake (2004) in the SW Pacific, only 22 were used to estimate the (assumed) daily age of small fish and to verify the location of the first annuli in fin rays. The remaining otoliths were archived at CSIRO. Recent reproductive

work on tuna has also shown that it is possible to differentiate mature-resting from immature females by the presence 'maturity markers' in histological sections of frozen-fixed ovaries (e.g., Farley et al. 2013b).

Given the difference in the life-history parameter estimates between studies in the Pacific, and their ramification for management (see Needs), the aim of the current study was to re-examine swordfish age, growth and maturity in the SW Pacific using ray and gonad samples already collected and prepared by Young & Drake (2002; 2004). Additional length-at-age information would be obtained from the analysis of sectioned otoliths. Finally, the effect of the different growth curves and maturity ogives on population models would be assessed and recommendations made for future assessment and harvest strategy evaluation activities.

2 Need

Uncertainty in the accuracy of growth and maturity parameters for swordfish in the SW Pacific led to a high degree of uncertainty in the 2013 stock assessment and estimates of stock status (Davies et al. 2013). The stock assessment noted that “the overwhelming source of uncertainty in the assessment is attributed to the assumptions for the growth, maturity and mortality at age schedules” (Davies et al. 2013). Using the growth curve of Young & Drake (2004), the assessment indicated that “overfishing was occurring but that the stock was not in an overfished state” while the growth curve of DeMartini et al. (2007) indicated “that no overfishing is occurring and that the stock is not in an overfished state”. In 2013, the WCPFC SC acknowledged the inconsistencies in the two growth schedules and “recommended that additional work on age, growth and age validation be undertaken” as a high priority project.

The Australian Eastern Tuna and Billfish Fishery Harvest Strategy for swordfish also requires growth and maturity schedules. While the initial harvest strategy evaluation admitted this source of uncertainty, it should benefit from improved accuracy and precision in these estimates (Kolody et al. 2010).

3 Objectives

1. Evaluate the use of otoliths to estimate the annual age of swordfish in the southwest Pacific.
2. Re-examine ageing methodology of Young & Drake (2004) and confirm age estimates obtained for a representative sample of fin ray sections.
3. Re-examine the ovary histology from Young & Drake (2002) and use new methods to estimate the maturity status of females.
4. Undertake a range of verification and/or indirect validation methods to determine the accuracy of age and maturity interpretations from fin rays, otoliths and ovaries.
5. Examine the effect of the different growth curves and maturity ogives on population models and make recommendations for future assessment and harvest strategy evaluation activities.
6. Collaborate with NOAA PIFSC scientists (Hawaii) to resolve possible methodological differences in direct age and maturity estimation.

4 Inter-lab comparison of methods to estimate age and maturity of Pacific swordfish

Meetings were held with Dr. Edward DeMartini and Dr. Robert Humphreys at the NOAA PIFSC in Hawaii in January 2015. The purpose was to undertake direct collaborative work to resolve possible methodological differences in estimates of age and maturity of swordfish in the SW Pacific and Hawaiian regions. The specific objectives were to:

- Compare ray, otolith and ovary histology interpretation methods between laboratories.
- Examine the ray inter-laboratory calibration study data.
- Undertake cross-readings of a subset of rays, otoliths and ovary histology.
- Discuss age validation methods.

4.1 Age estimation

4.1.1 Rays

Prior to the meeting in Hawaii, digital images of 100 sectioned swordfish anal fin rays were provided from an age inter-laboratory calibration exercise undertaken in the early 2000s (see DeMartini et al. 2007). In that study, the precision and bias of annual age estimates were examined among five laboratories – the National Marine Fisheries Service, Hawaii USA; the Centro de Investigacion Cientifica y de Educacion Superior de Ensenada, Mexico; the Instituto de Fomento Pesquero, Chile; the National Research Institute of Far Seas Fisheries, Japan; and the National Taiwan University, Taiwan. The coefficient of variation (CV) among and between the readers ranged from 9.7 to 15.7% and was considered ‘adequately precise’ (DeMartini et al. 2007). The analysis showed that one laboratory was underestimating age and it was recommended that these data be removed from our analysis (DeMartini, pers comm).

The images were read by two readers (R1 and R2) to determine if their reading methods were consistent with the other laboratories in the region. For each image, the number of translucent zones was counted using the criteria of Ehrhardt et al. (1996) and Quelle et al. (2014) (also see section 5.2 below). All readings were undertaken without knowledge of the size of fish or date of capture. The precision (consistency) of readings was assessed using the coefficient of variation (CV) (Chang 1982). Age-bias and age difference plots were used to detect systematic disagreement between age estimates from different readers and structures (Campana et al. 1995).

The CV between counts by R1 and R2 was 12.4%. The CV between the counts of these readers and the median count obtained by the four Pacific laboratories (DeMartini et al. 2007) was 13.71% (R1) and 13.33% (R2). The plots in Figure 1 suggest no or very little bias in the counts, and the results indicate good overall precision and consistency in readings between laboratories in the Pacific.

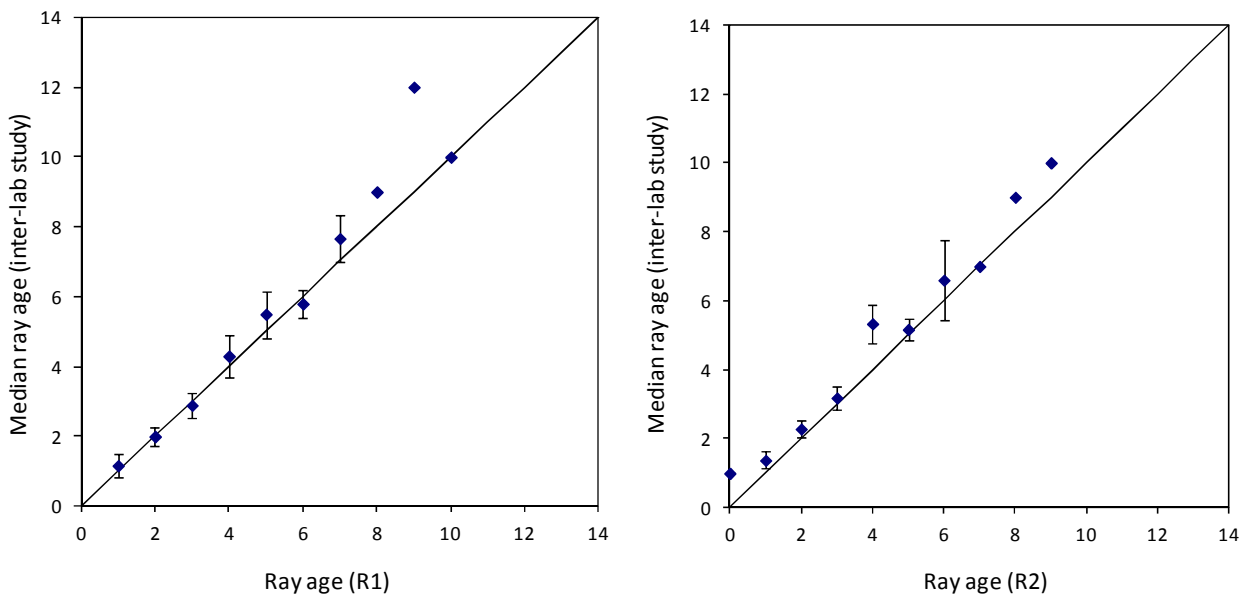


Figure 1 Age bias plots for comparisons of counts of translucent zones in fin rays by reader 1 (R1) (left) and reader 2 (R2) (right) and the median age obtained by 4 labs in an inter-laboratory study (DeMartini et al. 2007).

Examination of digital images of individual ray sections from the inter-lab comparison study and from Young & Drake (2004) highlighted potential areas of disagreement between readers. Differences can occur:

1. in assigning the first increment,
2. interpreting the ray margin (important for determining the marginal increment), and
3. interpreting doublets, triplets or “ghosts” increments.

It was recommended that: (i) the mean and standard deviation of the position of the first few increments (i.e., distance from the primordium collected during the reading process) is used to identify if any have been obscured due to resorption or vascularisation (and hence age would be underestimated); (ii) protocols are established for identifying and describing the opaque and translucent zones on the margin; (iii) digital images are marked where increments are located/counted.

4.1.2 Otoliths

The interpretation of sectioned otoliths was also discussed. Digital images of otoliths and preliminary daily and annual age estimates for fish in the SW Pacific (see section 5.2 below) were examined and compared to otoliths from Nishimoto et al. (2006) collected around Hawaii. Counts of increments in otoliths and rays from the same fish were often different. Otolith counts were generally higher with a maximum age of 21 years for otoliths from the SW Pacific and 23 years for otoliths from Hawaii. As expected, otolith and fin ray counts produced very different growth curves. The results of the analysis of otoliths from the SW Pacific are given in section 5 below. It was noted during the meeting that the otoliths prepared in the current study were clearer than those prepared by Nishimoto et al. (2006) which is probably due to improved accuracy and quality of the sectioning process.

4.2 Ovary classification

During the meeting, the ovary histology classification schemes used for swordfish were also discussed and compared. The classification scheme used in the current study was developed based on recent work on albacore tuna (*Thunnus alalunga*) by Farley et al. (2013b), which uses the presence of maturity markers such as muscle bundles and “brown bodies” to differentiate immature from mature-resting females (see section 6). These maturity markers are particularly obvious in ovary histology that has been prepared from material frozen prior to fixation. The classification scheme used is slightly different to that of DeMartini et al. (2000), which used alpha (α), beta (β) and later stage atresia of yolked oocytes to identify mature-resting females.

Histological sections of 19 ovaries prepared by Young & Drake (2002) were scored independently using the new classification scheme. These sections were scored previously by PIFSC and Young & Drake (2002) during a comparative study (see Young et al. 2008). Table 1 indicates that of the 12 fish that could be classified by PIFSC, 11 (91.7%) were given the same maturity classification as the current study, compared to only 50% by Young & Drake (2002). It was agreed that the new histological classification system used in this study was appropriate and successfully differentiated mature from immature female swordfish.

Table 1 Comparison of maturity status of swordfish from the SW Pacific based on histological evaluation. Imm/rest = immature/resting.

FISH NUMBER	OFL (CM)	PIFSC	YOUNG & DRAKE (2002)	AGREE WITH PIFSC	CURRENT STUDY	AGREE WITH PIFSC
161	250	Mature	Mature	Yes	Mature	Yes
185	212	Mature	Mature	Yes	Mature	Yes
417	263	Mature	Mature	Yes	Mature	Yes
587	180	Mature	Mature	Yes	Mature	Yes
597	190	Indeterminate	Imm/rest	-	Mature	-
718	160	Indeterminate	Imm/rest	-	Immature	-
736	145	Indeterminate	Imm/rest	-	Immature	-
829	197	Indeterminate	Imm/rest	-	Mature	-
840	205	Mature	Mature	Yes	Mature	Yes
1310	165	Mature	Imm/rest	No	Mature	Yes
1311	179	Immature	Imm/rest	No	Immature	Yes
1313	178	Mature	Imm/rest	No	Mature	Yes
1316	201	Mature	Imm/rest	No	Mature	Yes
1317	140	Mature	Imm/rest	No	Mature	Yes
1318	153	Indeterminate	Imm/rest	-	Immature	-
1319	183	Indeterminate	Imm/rest	-	Mature	-
1357	270	Indeterminate	Imm/rest	-	Mature	-
1380	237	Mature	Mature	Yes	Mature	Yes
1401	210	Immature	Mature	No	Mature	No
% agreement¹				50.0		91.7

¹ comparisons could not be made for the 7 fish classified as indeterminate by PIFSC.

4.3 Conclusions

After the comparison work was undertaken, it was concluded that:

1. No major methodological differences exist between DeMartini et al. (2002) and the methods used in the current study to age swordfish using fin rays. However, examination of images of individual rays highlighted potential areas of disagreement, especially in assigning the first increment and at the ray margin.
2. Given the above, re-reading a subset of rays prepared and aged by Young & Drake (2004) should determine if the differences in growth rates between the ageing studies of DeMartini et al. (2002) and Young & Drake (2004) are methodological or due to spatial variation in growth rates.
3. No major methodological differences exist between Nishimoto et al (2006) and the methods used in this study to age (annual) swordfish using otoliths.
4. Slight methodological differences exist between DeMartini et al. (2000) and the current study to differentiate immature from mature swordfish. However, these differences are unavoidable because the majority of ovary material collected in the SW Pacific was frozen before being fixed, resulting in poorer quality histological sections. It was agreed that the histological classification system used in the current study was appropriate and successfully differentiated mature from immature females.

5 Age and growth of swordfish in the SW Pacific

5.1 Introduction

Fin rays have been the preferred structure for ageing swordfish due to ease of sampling and preparation (Quelle et al. 2014). Sagittal otoliths have, however, been used in several studies. DeMartini et al. (2007) used the microstructure on the surface of the sagittal otoliths collected from the Hawaii-based pelagic longline fishery to verify the annual growth zones of anal rays by comparing against the daily growth increments. Sun et al. (2002) and Megalofonou et al. (1995) both observed micro-increments from sagittae sectioned in a transverse plane using light and scanning electron microscopy. This microstructure was counted to provide age estimates of juvenile swordfish from waters from Taiwan and the Mediterranean respectively. Esteves et al. (1995) and Uchiyama et al. (1998) both investigated a number of different ageing structures including anal and dorsal rays, vertebrae and sagittal otoliths. Neither study directly focused on the comparison of the individual zone counts from each structure to one another; rather the results were directed towards estimating the precision of readings and suitability of each structure for age estimation. Interestingly, the estimates from the sagittal otoliths were made from reading the growth ridges on the proximal surface of the whole otoliths, even though many studies on other fish species have shown whole otoliths to underestimate longevity (Dwyer et al. 2003; Brouwer & Griffiths 2004; Beamish 1979). Both studies did note the potential of sagittae for ageing, however, due to their extremely small size, fragile nature and inconsistent “banding”, they recommended the fin ray method as the preferred method. Esteves et al. (1995) did go as far as suggesting that this structure merited further research and should now be analysed as sections in order to establish criteria for age determination.

The suitability of using ridges on rostrums, and annuli in whole and sectioned sagittae, to age swordfish was examined further by Nishimoto et al. (2006). Their results indicated that internal growth structures in thin transverse sections were easier to interpret than the external ridges. Consequently they were able to compare zone counts from transverse sagittal sections against those made from fin rays. Age-bias plots based on annuli counts in sectioned sagittae and fin rays from the same swordfish indicated that ages estimated from otoliths were generally older than ages estimated using fin rays for all age groups and for females and males separately.

In this study, we aim to investigate the rays and otoliths sampled from the Australian Eastern Tuna and Billfish Fishery in the SW Pacific and determine the most appropriate structure and method for providing both daily and annual age estimates.

5.2 Methods

5.2.1 Study material

Sectioned anal fin rays (n=1588) and whole sagittal otoliths (n=504) were obtained from Young & Drake (2004) for swordfish caught in the ETBF between 1995 and 2003 (Figure 2; Table 2). Orbital

fork length (OFL), sex and date of capture were obtained for all fish (Table 2). Only 363 fish had both the sectioned ray and otolith available for analysis. Of these, 311 fish were initially selected for analysis. Fish were chosen based on OFL, sex and month of capture to obtain fish from the full size range by sex and from as many months as possible. To obtain at least 10 fish per month per sex where possible, an additional 112 fin rays were selected from the months where no ray/otolith pairs were available. Additional otoliths could not be selected as none were available for months with low sample sizes. Ray-based age estimates were obtained from Young & Drake (2004). All undamaged sagittal otoliths were weighed to the nearest 0.001 g.

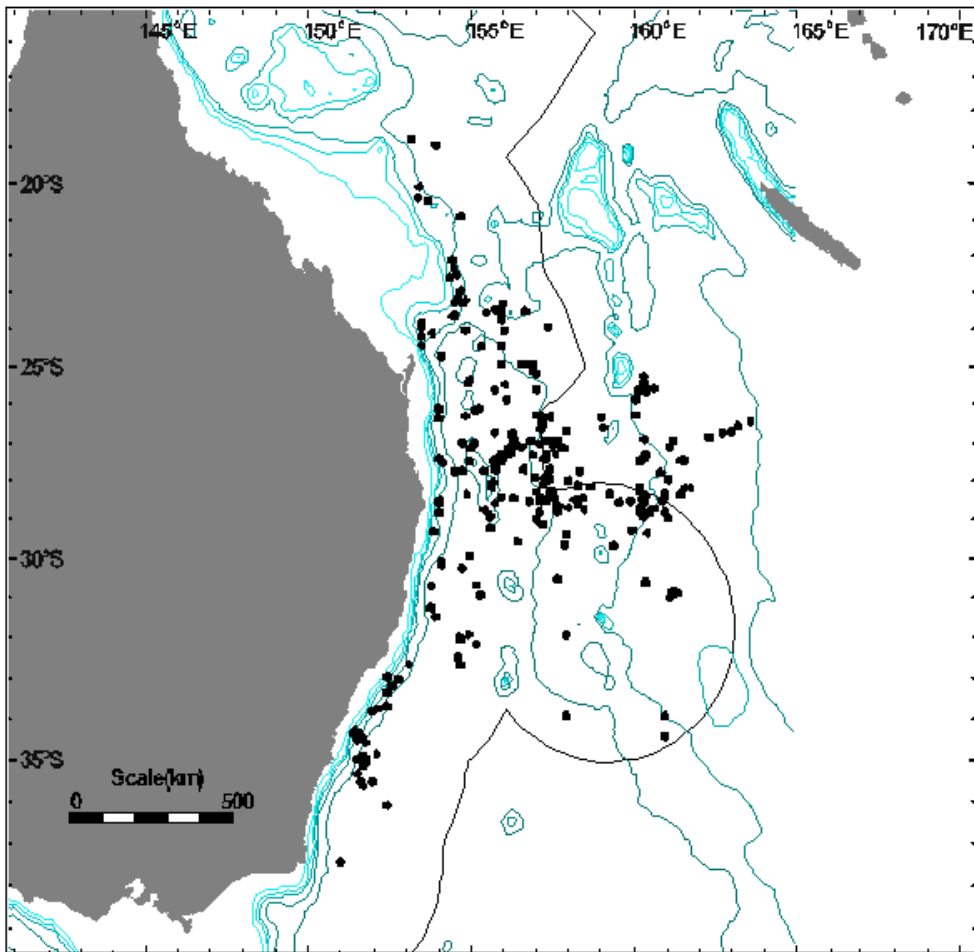


Figure 2 Map indicating the capture locations of swordfish sampled for otoliths (from Young & Drake 2004).

Table 2 Number of rays and otoliths available and those selected for ageing by month.

MONTH	RAYS AVAILABLE		OTOLITHS AVAILABLE		SELECTED FOR ANALYSIS (RAY & OTOLITHS FROM SAME FISH)		ADDITIONAL RAYS SELECTED FOR ANALYSIS	
	Female	Male	Female	Male	Female	Male	Female	Male
Jan	104	61	27	14	20	12		5
Feb	165	81	96	56	64	40		
Mar	90	57					10	10
Apr	31	10					10	3
May	84	36	4	6	4	6	8	7
Jun	48	10					10	10
Jul	67	22	1		1		9	10
Aug	99	40	13	6	7	6	5	8
Sep	116	45	19	9	17	9		5
Oct	128	51	37	22	31	21		
Nov	126	41	27	13	19	12		1
Dec	53	23	34	14	28	13		1
Total	1111	477	258	140	191	119	52	60

5.2.2 Fin rays

Young & Drake (2004) cut multiple cross-sections from each fin ray. The bilaterally paired ray was split in two and the distance (D) was measured across the widest section of the condyle and a minimum of four transverse sections ~1.0 mm in width were taken along the length of the ray at locations equivalent to distances $\frac{1}{4}D$, $\frac{1}{2}D$, $\frac{3}{4}D$ and D. Cuts were made using a diamond saw at either a high or low-speed, depending on the size of the ray, placed in small plastic vials labelled with a unique identification (ID) number and the section type (i.e., $\frac{1}{4}D$, $\frac{1}{2}D$, etc.), and immersed in 70% ethanol for one hour, before being rinsed with distilled water and placed in dichloromethane for an additional hour to improve band clarity (Berkeley and Houde 1983). Sections were air-dried, mounted with crystal bond on glass slides labelled with the ID number and section type, and stored for later reading.

We selected the $\frac{1}{2}D$ section for reading as this is most commonly used in ageing studies of swordfish. Occasionally the D or $\frac{3}{4}D$ section was used if $\frac{1}{2}D$ was unreadable or not present. Each section was examined using a stereo-microscope under reflected light. A digital image of the section was captured and a calibrated scale was set into each image. The images were enhanced using Photoshop Elements. All interpretations and measurements were done using the digital images.

Each ray was read twice by reader 1 (R1; primary ray reader) without reference to the size of fish or capture date. The number of translucent zones (which appear dark under reflected light) was counted using the criteria of Ehrhardt et al. (1996) for Atlantic swordfish. This method was also used by Sun et al. (2002) and DeMartini et al. (2007) for North Pacific swordfish. As noted previously, the sectioned rays often contained split translucent growth zones, which were difficult to interpret. Translucent zones were only counted if it could be followed around the whole section and did not appear to split (Ehrhardt et al. 1996). Translucent zones at the terminal edge were

counted only if opaque material was evident after the translucent zone following Quelle et al. (2014). Figure 3 shows an example of a sectioned fin ray with the outer edge of the presumed annual translucent zones marked. Note a translucent zone on the terminal edge is visible in places, but was not counted. The radius to the outer edge of each complete translucent zone and the ray margin was measured. Estimates of the number of translucent zones missing due to vascularisation (if present) were determined based on (i) the mean radius of the translucent zones in rays where vascularisation did not obscure the first translucent zones (see Table 4 in section 5.3.2 for measurements), and (ii) the distribution pattern of the visible translucent zones to infer the number missing. Each reading was assigned a confidence score of 0-5 (poor-good). If no obvious pattern could be seen in the otolith section, a count was not made (confidence 0). If the successive readings were in agreement, this estimate was used as the final count for the fin ray. However, if the readings differed, a further reading was conducted with knowledge of the previous readings to decide on a final count and confidence score. The edge classification (narrow, intermediate or wide) was calculated for each ray following the criteria shown in Figure 4. Edge type was also recorded as either opaque or translucent.

To examine precision, the rays were read by a second reader (R2) using the protocols described above. The number of zones missing due to vascularisation was estimated based on the mean radius of the translucent zones measured by R1 and the distribution pattern of visible zones. Only the 310 rays with matching otoliths were read by R2.

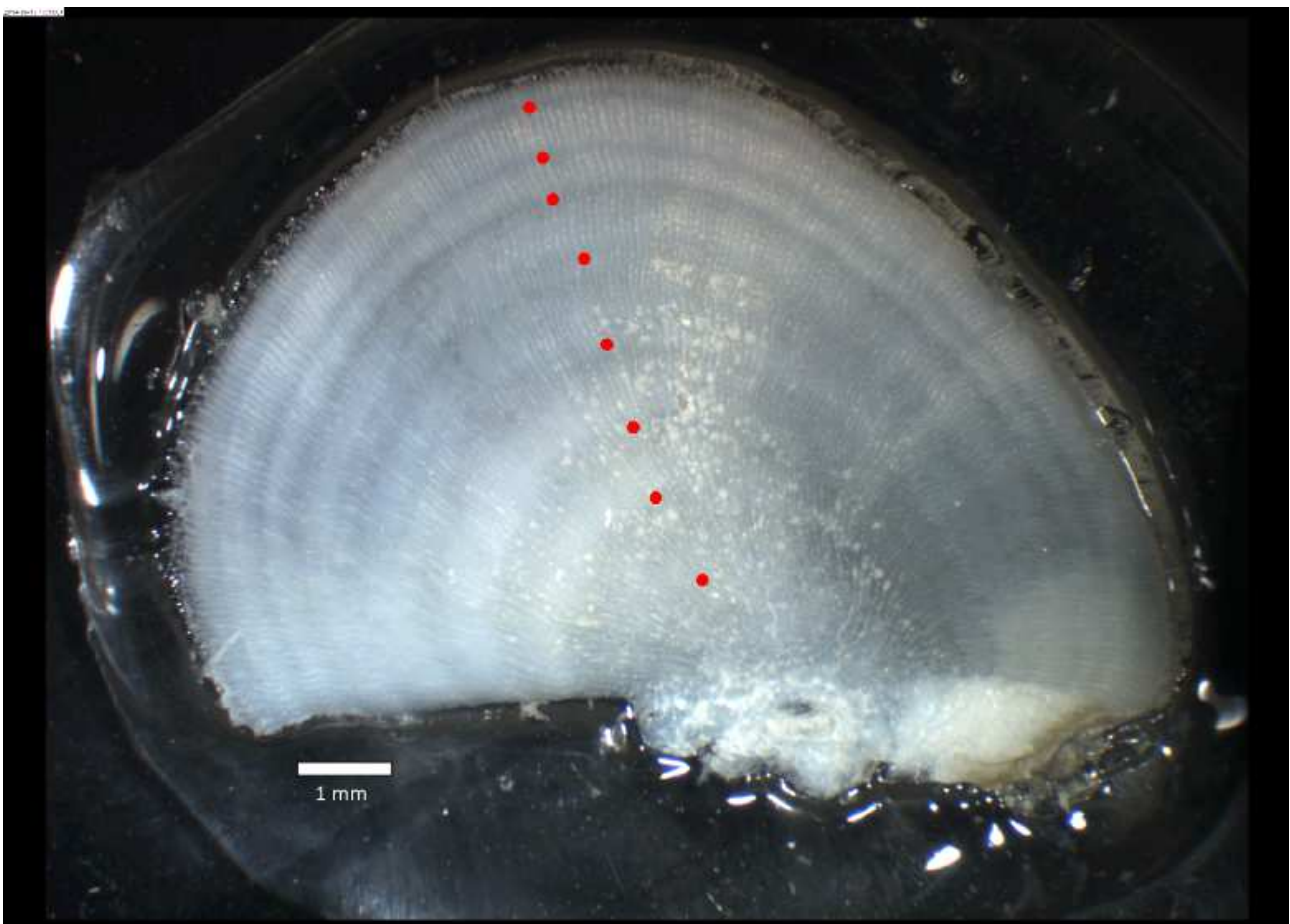


Figure 3 Swordfish #148 (female, 195 cm OFL, October) fin ray prepared for annual ageing with the outer edge of translucent zones indicated by red dots.

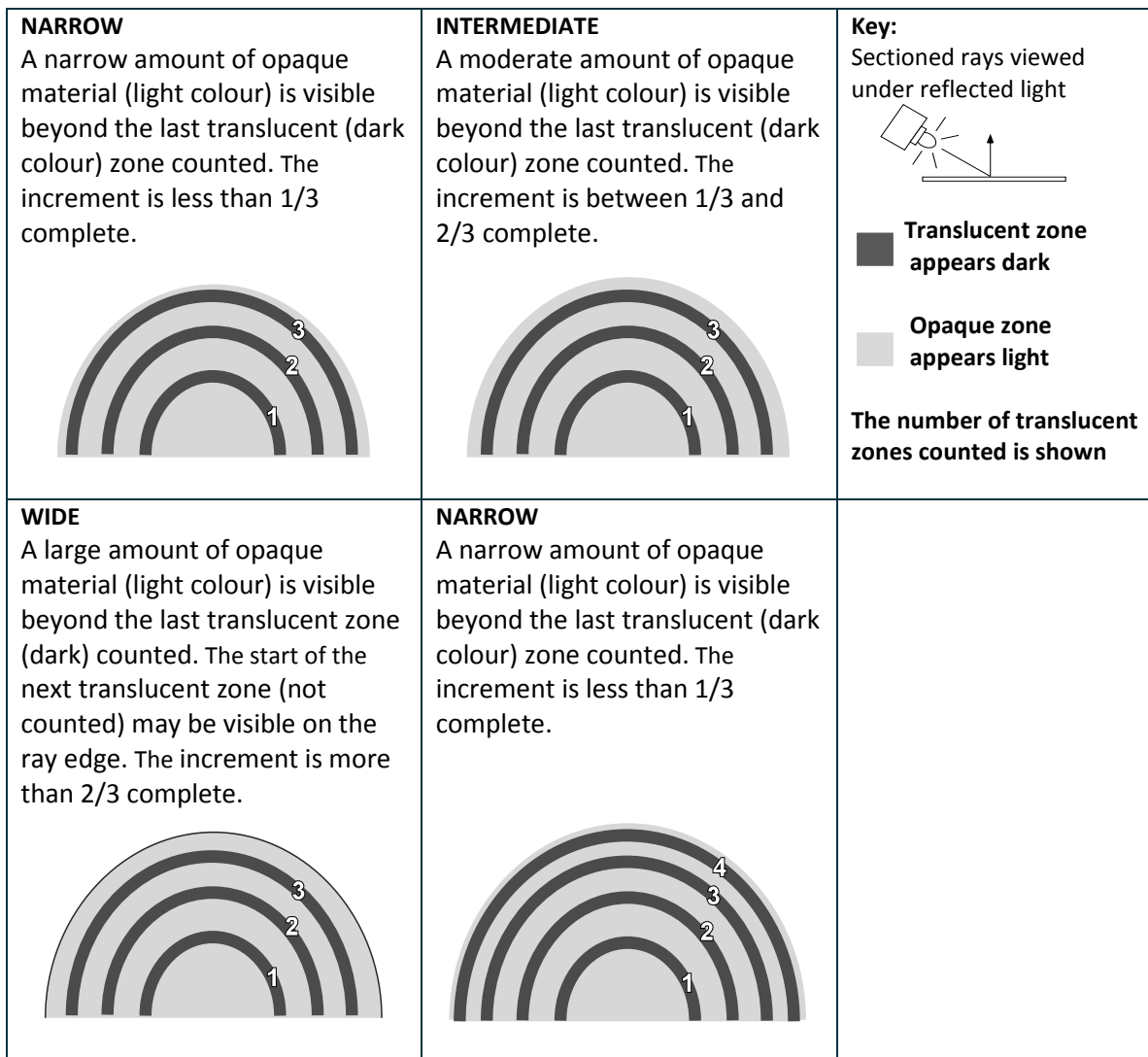


Figure 4 The cycle of edge classifications used for swordfish rays.

5.2.3 Otoliths

Initial investigation

For most fish with otoliths collected, the three structures (sagittae, lapilli and asteriscus; Figure 5) were usually present. Being the largest of the three structures, the sagittae is the only otolith that has been used previously for investigating the age of swordfish.

Ten samples that contained the left and the right sagittae plus at least one of the lapilli were selected for initial investigation. Otoliths were selected from four small fish between 80 and 137 cm OFL and six larger fish between 157 and 230 cm OFL. This initial investigation was aimed at determining the most appropriate structure and preparation method for both daily and annual age estimation. Since the asterisci was not always collected, this structure was not considered for further analysis in the current study.

Firstly we compared the lapilli and sagittae from two of the smaller samples for daily analysis. The otoliths were initially prepared by polishing the distal surface of both structures with P800 and P1200 wet/dry sand paper and finally with 3µm lapping film. Preparations of the dorsal lobe (ground distally) of the sagittae often removed the primordial, which resulted in only one sample

clear enough to read. In the prepared lapilli the daily growth zones (DGZ) were relatively clear around the primordia and mid-section regions; however in all of the preparations, the outer edges showed irregular growth planes which made interpretation of the DGZs very difficult, particularly after approximately after 100 zones. For the one sample that both otoliths were prepared successfully, counts of DGZs were made from both preparations and compared. While the DGZ count was comparable between the two structures, we decided not to continue with the lapilli due to the fragile outer area and the multiple planes of growth. The otolith preparations of one lapilli (distally ground) and both sagittae (both distally ground and transversely ground) from the same specimen is shown in Appendix A.

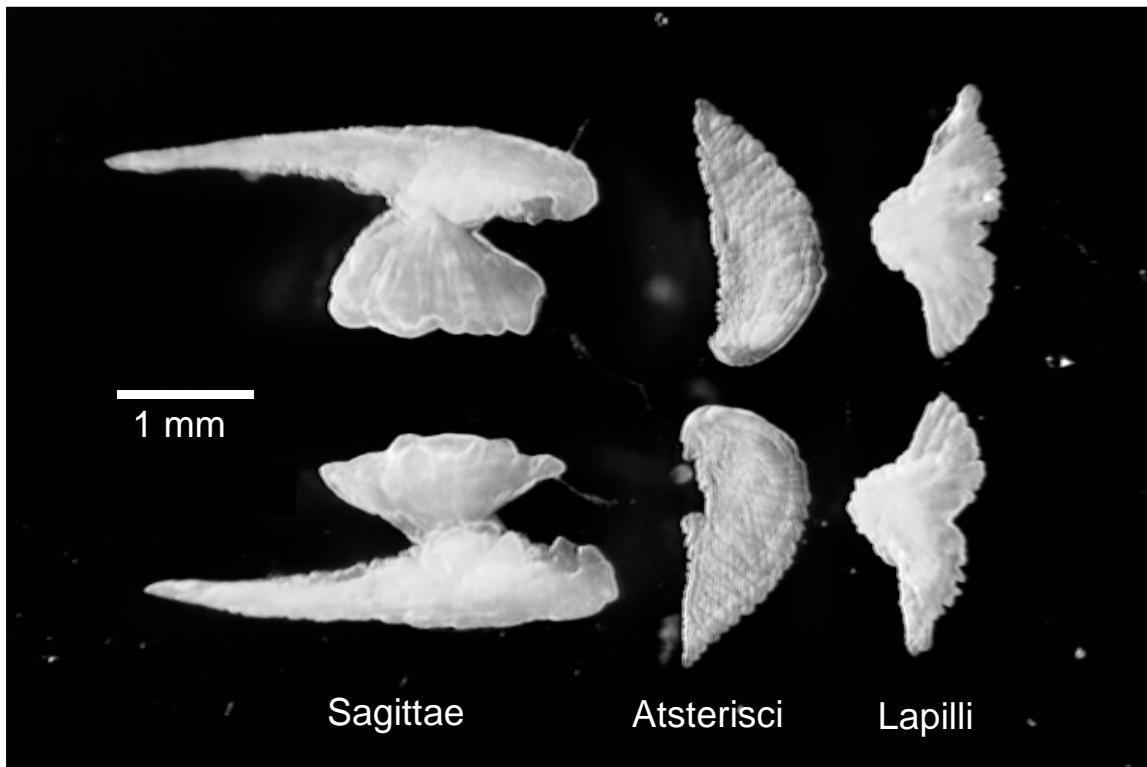


Figure 5 The three different otolith structures of swordfish, indicating their size and shape.

Since both distal (DeMartini et al. 2007) and transverse (Nishimoto et al. 2006) preparations of the sagittae had been used previously to provide counts of daily age, we compared the counts of DGZ from one sample (fish) in which one of the sagittae was prepared in the distal plane and the other in the transverse plane. Similar counts were recorded for both preparation methods (Appendix A).

To prepare thin transverse sections of the sagittae for DGZ examination the otoliths were ground down in a four-step process. First, the otolith was fixed on the edge (end) of a slide using thermoplastic mounting media (crystalbond 509) with the anterior side of the otolith hanging over the edge. Care was taken to ensure that the primordium was just on the inside of the glass edge (approximately 50 μm). Second, the otolith was ground down to the edge using 400 and 800 grit wet and dry paper. Third, the slide was reheated and the otolith was removed and placed (ground side down) on another slide and the crystalbond was allowed to cool. Fourth, once cooled the otolith section was ground horizontally to the grinding surface using varying grades (800 & 1200 grit) of wet and dry sandpaper and finally 3 μm lapping film. During this process the otolith preparation was continuously checked and where necessary flipped to ensure that the

recommended section thickness (50-80 μm) was reached and that the remaining section still contained the primordium (Figure 6).

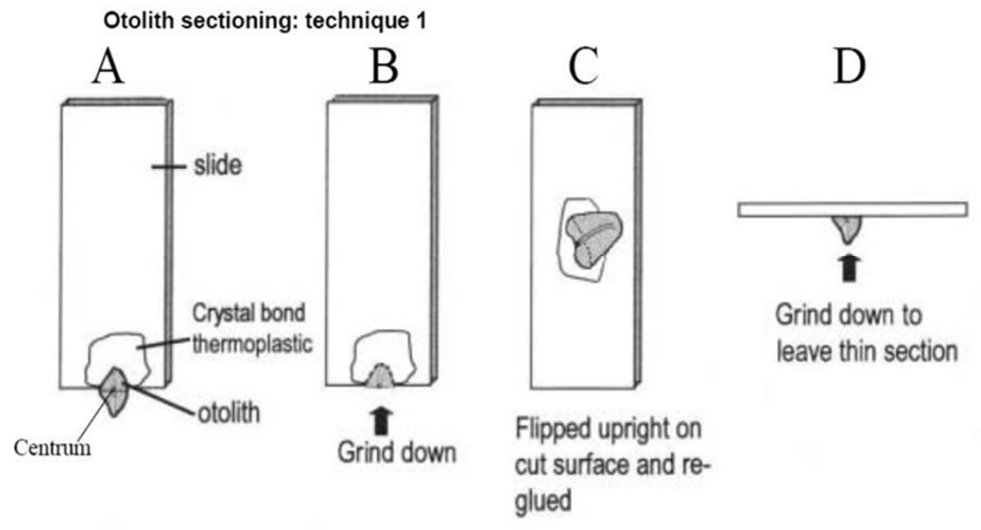


Figure 6 Illustration of the individual grinding process for preparation transverse otolith thin sections (Source: Robbins & Choat 2002).

As one of our aims was to directly compare daily counts with annual counts, both sagittae from each sample in the remaining investigation set were prepared; one otolith for daily reading and one otolith for annual reading. The preparation of the otoliths for annual estimation followed the same procedure as described for daily preparation, however in the first step the primordia was aligned approximately 100-150 μm in from the edge of the slides and in the fourth step the thickness of the section was measured continuously with a digital calliper until the desired thickness was reached (250-300 μm). The preliminary preparations of the otoliths from the larger samples showed a reasonably clear pattern of alternating opaque and translucent zones (Figure 7).

Our trial work and reservations about using the counts of "ridges" on the distal and proximal surface of the dorsal lobe (DeMartini et al. 2007 and Uchiyama et al. 1998), combined with the positive results achieved by Nishimoto et al. (2006) through the use of thin transverse sections for annual ageing indicated that transverse sections of the sagittal otolith were most promising for both daily and annual age estimation. We did also attempt to prepare one sagittal otolith in the longitudinal plain, however lining up the primordium and the rostrum along a straight line was difficult and the rostrum itself proved too brittle to allow further preparation.

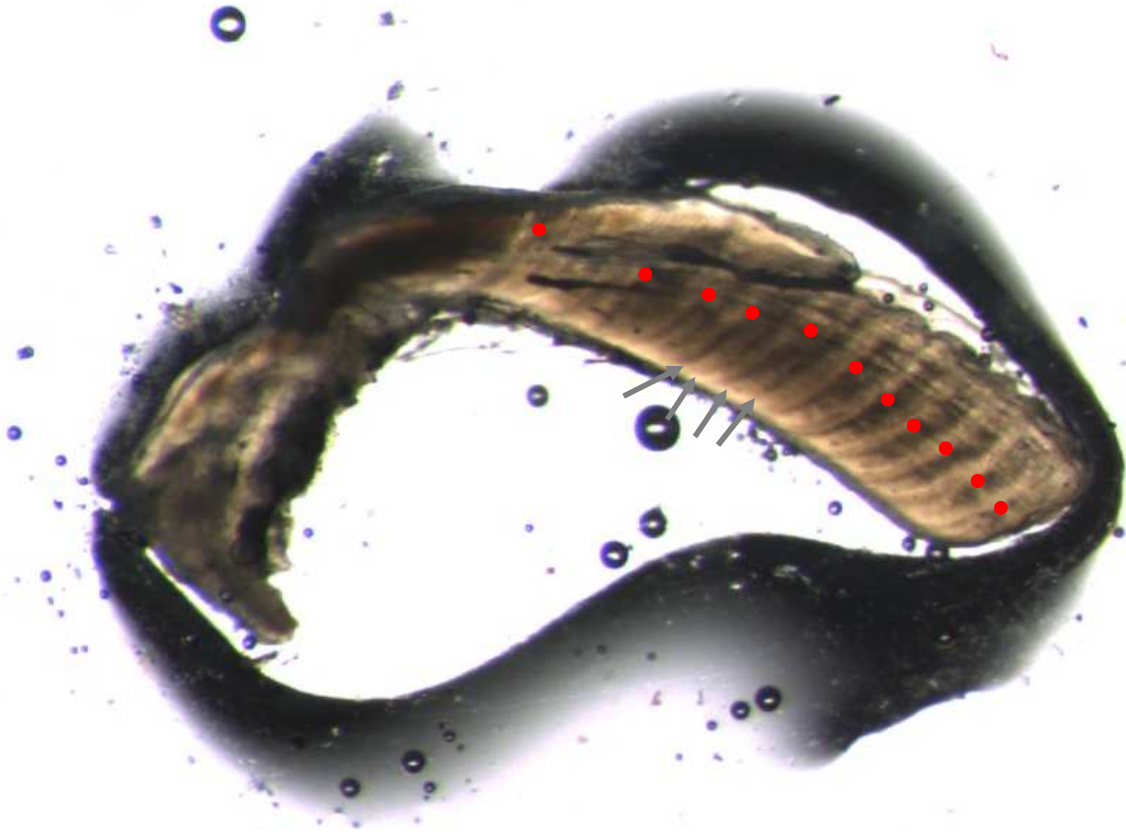


Figure 7 Transverse preparation of a swordfish sagittae (#224) prepared for annual reading showing the reasonably clear alternating opaque and translucent zones with the outer edge of translucent zones (or start of the opaque zones) indicated by red dots. Note the double banding (grey arrows) in the opaque zones in the first 5 or 6 assumed annual increments.

Daily ageing

A further 33 sagittae (herein referred to as otoliths) from the smallest fish were selected for daily ageing, and one otolith from each pair was prepared as a thin transverse section. The remaining otolith was retained for annual ageing.

To improve the clarity of the preparations, before examination the prepared side of the otolith was covered with non-drying immersion oil for microscopy (Cargill[®]). The transverse sections were examined at 640 and 1000x magnification with transmitted light. Daily growth zones were counted by reader 3 (R3; primary otolith reader) on the dorsal lobe along the clearest path out to the otolith edge. The DGZs have been previously described in detail by Sun et al. (2002) and Megalofonou et al. (1995). In the few swordfish otoliths trailed for daily analysis, it was evident that there was a transition point in the otolith microstructure approximately 500µm out from the primordia (Figure 8). For future reference and to potentially aid the annual estimation process, measurements were taken from the primordia to the start of the transition (measurement A), from the primordia to the proximal edge of the otolith along the same path at measurement A (measurement B) and thirdly from the primordia to the distal inflection and the inflection to the proximal tip (measurement C) (Figure 9).



Figure 8 Example of assumed daily increments in a transverse sectioned otolith and also the approximate position (white arrow) where there is a noticeable change in the pattern and clarity of the DGZs.

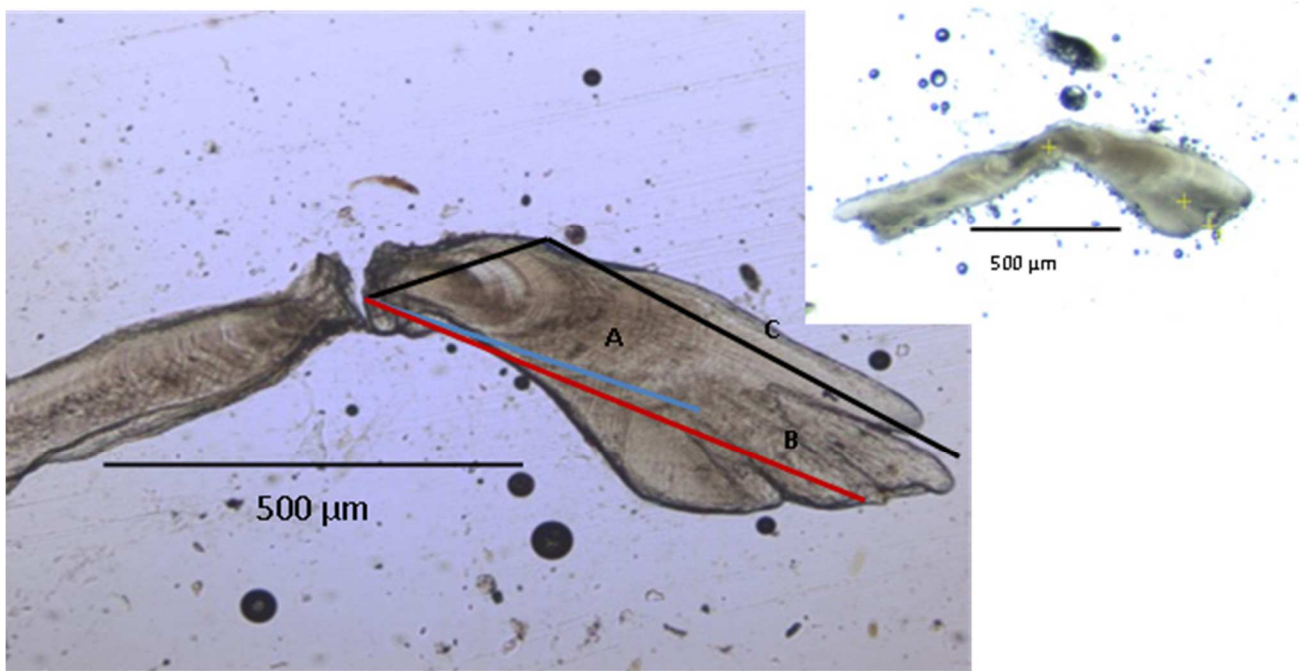


Figure 9 Transverse section of an otolith indicating the locations of measurements taken. Blue line measurement A, red line measurement B and black line measurement C. The transverse section prepared for annual age estimation is also shown for comparison (right). The yellow crosses indicate the primordium, the first assumed opaque zone and the otolith edge.

Annual ageing

One otolith from all the available samples were prepared as thin transverse sections according to the methods described previously. The otolith sections were read by reader 3 (R3) without reference to size of fish or capture date. All preparations were illuminated with transmitted light and the whole set was viewed once before any attempt was made at age estimation.

Several sections, which showed these clear inner zones, were selected and the distance between the primordium and the start of the first and second opaque zone was measured. Figure 10 to Figure 12 show examples of sectioned otoliths with presumed annual opaque zones indicated. These proxy measurements were used in the ageing process to help locate the first two opaque zones.

An image analysis system was used to age sectioned otoliths and to capture images each section. This system counts and measures the distance of each manually marked increment from the primordium and collects an annotated image from each sample aged. The start of each opaque zone was marked and distance from the primordium to each marked opaque zone and to the otolith edge was collected. Opaque zones at the terminal edge of the otolith were counted only if some translucent material was evident after the opaque zone.

The otolith edge was classified as new opaque, narrow translucent or wide translucent following the criteria shown in Figure 13, and each reading was assigned a confidence score of 0-5 (poor-good). A digital image was captured of each section indicating the position of each opaque zone counted.

To examine precision, the otoliths were read by two additional readers (R1 and R2) using the protocols described above. However, R1 and R2 read the otoliths twice and each assigned a final count and confidence score. The coefficient of variation (CV) was used to assess the precision of readings (Chang 1982), while age-bias plots (Campana et al. 1995) and mean difference was used to detect systematic disagreement between age estimates obtained from otoliths and fin rays.

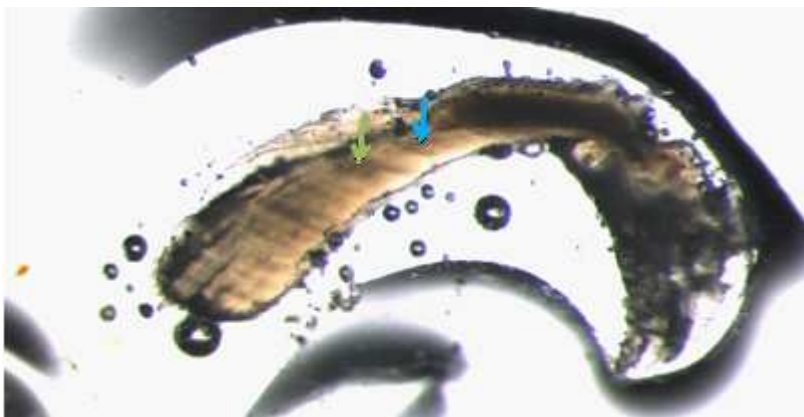


Figure 10 Swordfish otolith (#228; 230 cm OFL, female) prepared for annual ageing with two presumed annual opaque zones indicated by arrows. The blue arrow is at 0.550 mm and the green arrow at 0.750 mm from the primordium.

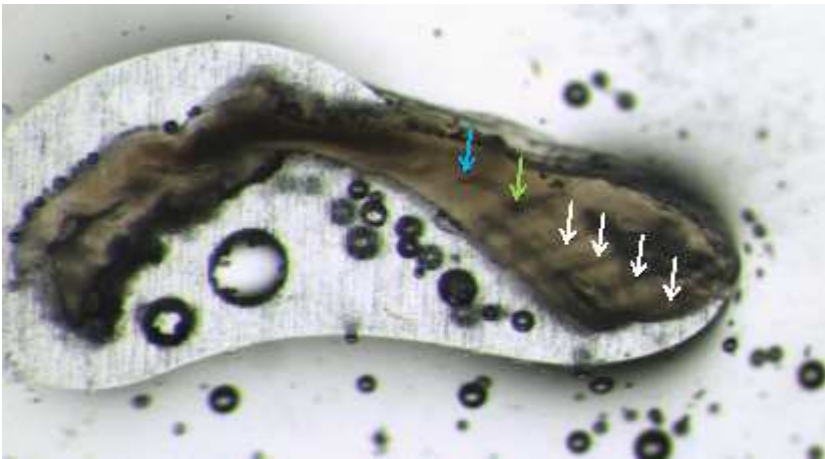


Figure 11 Swordfish otolith (#589, 161 cm OFL, male) prepared for annual ageing with presumed annual opaque zones indicated by arrows. The blue arrow is at 0.612 mm. The green and subsequent white arrows indicate the presumed 2nd to 6th opaque zones.



Figure 12 Swordfish otolith (#196, 257 cm OFL, female) otolith prepared for annual ageing with presumed annual opaque zones indicated by crosses. The primordial and edge are also marked with a cross.

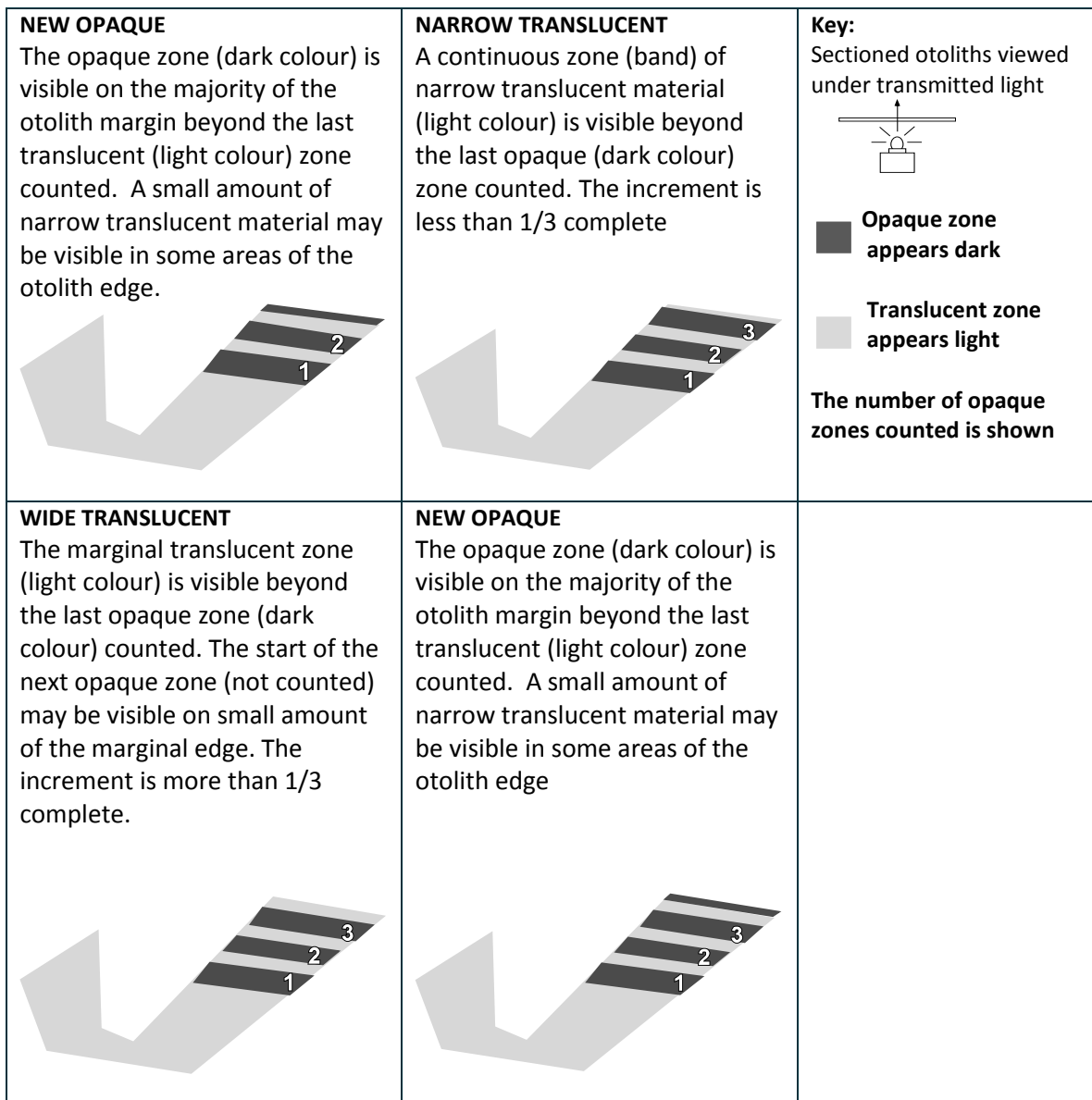


Figure 13 Cycle of edge classifications used for swordfish otoliths.

5.2.4 Growth analysis

We fitted the von Bertalanffy growth model (VBGM) (von Bertalanffy 1938) to the length-at-age data from both rays (R1 estimates) and otoliths (R3 estimates):

$$L_t = L_\infty (1 - e^{-k(t-t_0)})$$

where L_t is the fork length at age t , L_∞ is the mean asymptotic length, k is a relative growth rate parameter (year^{-1}), and t_0 is the age at which fish have a theoretical length of zero. We used maximum likelihood estimation assuming a Gaussian error structure with mean 0 and variance σ^2 . The optim function in R (R Core Team 2013) was used to minimize the log likelihood. Standard errors were calculated for the parameter estimates using the inverse Hessian, which is an output of the optim function.

5.3 Results and Discussion

5.3.1 Hardparts

Fin ray diameter increased linearly with increasing fish size for both male and female swordfish (Figure 14A). Similarly, otolith weight and transverse section length increased with fish size, and the goodness of fit of the power curves was relatively high (Figure 14B, C) despite some variability in otolith morphology among individuals (Appendix B). This shows that rays and otoliths continue to grow during the life of the fish.

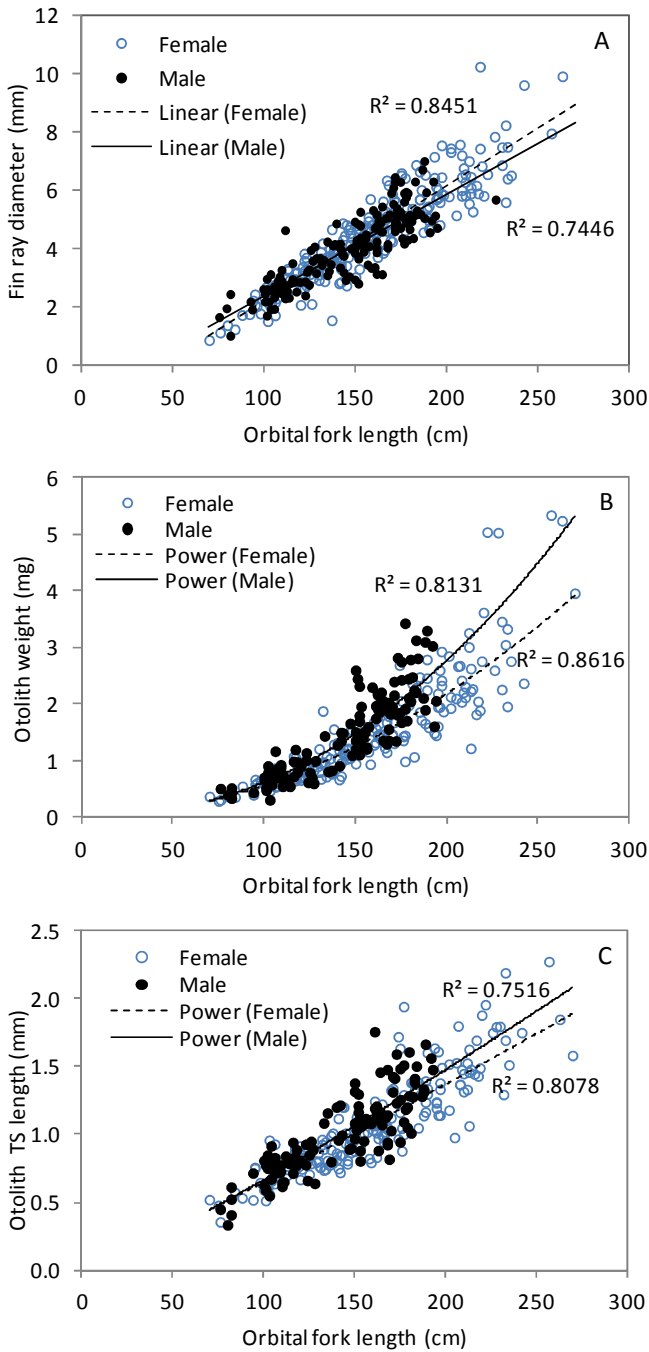


Figure 14 Relationship between fish size and: fin ray diameter (n=390) (A), otolith weight (n=305) (B) and otolith transverse section (TS) length (n=296) (C) for male and female swordfish.

5.3.2 Fin rays

Annual age estimates (counts of translucent zones) were obtained for 368 of the 423 rays examined. The other 55 (13.0%) were considered unreadable. Of the 368 rays, 106 were assessed to have between one to three missing translucent zones due to vascularisation of the core. Age estimates ranged from 0-10 years for males and 0-14 years for females, although the majority were <8 years (Table 3). The average confidence scores were 2.50 and 2.46 for females and males respectively. The average confidence scores did not vary noticeably with age, although the sample sizes were small for fish ≥ 9 years.

The mean radius of each translucent zone by age class is shown in Table 4. The average radius of the first increment (all age classes combined) was 1.40 mm and 1.39 mm for male and females respectively. This distance is similar to that obtained for swordfish caught around Taiwan (1.49 mm and 1.34 mm for males and females) (Sun et al. 2002). A direct comparison could not be made with swordfish caught around Hawaii because a different ray sectioning location was used (DeMartini et al. 2000).

Table 3 Number of age estimates obtained from rays and otoliths by age class and by sex.

Age (years)	Ray-based age		Otolith-based age	
	Female (n)	Male (n)	Female (n)	Male (n)
0	3	4	1	3
1	18	16	14	14
2	37	24	33	18
3	30	20	36	14
4	35	35	18	15
5	18	17	20	14
6	20	16	11	14
7	22	10	12	8
8	15	7	8	7
9	6	1	8	
10	3	2	7	6
11	4		4	1
12	1		3	
13	2		2	1
14	1		3	
15				1
16			1	
17				1
18				
19				
20			1	
21			2	
Total	215	152	184	117

Table 4 Mean radius of the distal edge of each translucent zone in rays for male and female swordfish caught in the ETBF. SD = standard deviation. Increment = increase in the mean radii from the preceding increment.

Age class (yr)	Sample size	Mean radius (mm) to each translucent zone													
		1	2	3	4	5	6	7	8	9	10	11	12	13	14
FEMALES															
0	3														
1	18	1.45													
2	37	1.45	2.30	2.61											
3	30	1.27	2.23	3.01	3.82										
4	35	1.34	2.44	3.39	4.13										
5	18	1.42	2.41	3.21	4.02	4.66									
6	20	1.47	2.38	3.22	3.93	4.57	5.05								
7	22	1.49	2.49	3.34	4.19	4.94	5.50	5.97							
8	15	1.25	2.20	3.13	3.90	4.65	5.25	5.78	6.22						
9	6		2.51	3.31	3.91	4.44	4.93	5.42	5.80	6.23					
10	3		1.86	2.80	3.67	4.38	4.91	5.36	5.67	5.94	6.17				
11	4		2.86	3.72	4.46	5.13	5.71	6.26	6.75	7.11	7.44	7.69			
12	1			3.00	3.76	4.38	4.89	5.38	5.89	6.46	6.74	7.05	7.39		
13	2	1.51	2.15	3.19	3.69	4.30	4.75	5.19	5.65	5.95	6.26	6.64	6.97	7.17	
14	1		1.97	2.97	3.77	4.14	4.44	4.65	4.90	5.03	5.16	5.35	5.48	5.55	5.69
Mean		1.40	2.35	3.22	4.04	4.69	5.23	5.78	6.06	6.30	6.61	7.06	6.70	6.63	5.69
SD		0.38	0.40	0.49	0.58	0.71	0.84	0.97	0.92	0.85	1.11	1.19	0.90	1.04	0.38
Increment			0.95	0.87	0.82	0.65	0.55	0.55	0.28	0.24	0.31	0.45	-0.36	-0.07	-0.94
MALES															
0	6														
1	16	1.61													
2	24	1.33	2.29												
3	20	1.47	2.44	3.11											
4	35	1.38	2.32	3.21	3.88	3.80									
5	18	1.28	2.31	3.06	3.70	4.16									
6	16	1.29	2.24	3.10	3.88	4.43	4.86								
7	10	1.00	2.21	3.15	3.95	4.49	4.94	5.32							
8	7	0.98	2.06	3.26	3.97	4.48	4.70	5.18	5.46						
9	1			3.54	4.55	5.18	5.72	6.10	6.51	6.74					
10	2	1.17	2.04	2.67	3.14	3.66	4.17	4.53	4.90	5.23	5.50				
Mean		1.39	2.31	3.14	3.85	4.33	4.84	5.21	5.45	5.73	5.50				
SD		0.31	0.33	0.37	0.48	0.50	0.51	0.66	0.66	0.91	0.35				
Increment			0.92	0.83	0.71	0.48	0.51	0.38	0.24	0.28	-0.23				

5.3.3 Otoliths

Daily ageing

Transversely ground sagittae display relatively clear and uniform DGZs for the first 150-170 zones. In most of the otoliths examined, at approximately a count of 150, a transition area in the otolith morphology was observed. This transition point was characterised by a relatively diffuse area where the DGZs change in pattern and optical clarity (Figure 15; Figure 16). The zones that followed the transition point were difficult to interpret and the pattern of zone deposition far less concentric than the zones prior to the transition point (Figure 15; Figure 16).

Of the 43 otoliths prepared for daily age estimation, we were able to provide total counts for 36 of the samples (Appendix C). In four of the seven unreadable samples, counts were made out to at least the transition point and the distances referred to as A, B and C (see Figure 9) were still measured. Total counts ranged from 146 in a 75 cm fish to 512 in a 230 cm fish. In larger fish (≥ 120 cm OFL), counts appear to underestimate daily age when compared to counts of annual zones (Figure 17; Appendix C), and the difference increased with increasing (annual) age. The oldest daily age estimate obtained was 512 days from a fish aged as 11 years from annual ageing. Appendix D shows examples of otoliths from the same fish prepared for annual and daily examination.

The number of DGZs counted to the transition point ranged from 124 to 227 (mean = 168.56 ± 22.10 SD; $n=103$). This variation is consistent with the peak spawning duration and the relative hatch date of each sample (see section 6.2.1). This assumes that the transition point occurs at a similar time of the year in the fish and is not influenced by spatial and temporal effects. The mean distance to the transition point (measurement A) was 0.540 mm (± 0.055 SD) ($n=36$). The distance to the proximal edge (measurement B) ranged from 0.497 mm for the smallest sample that could be measured (80 cm OFL) to 0.998 mm for the largest sample (113 cm OFL).

The daily counts appear to slightly underestimate age relative to counts obtained by Young & Drake (2004) for swordfish sampled in the ETBF (Figure 18). Young & Drake (2004), however, estimated the number of increments in “indistinct areas” using the density of increments before and after the regions (which we assume included the transition area), and could account for the smaller lengths at age obtained. The comparison of DGZ counts suggests that the indistinct regions have lower densities of increments relative to the preceding and following regions.

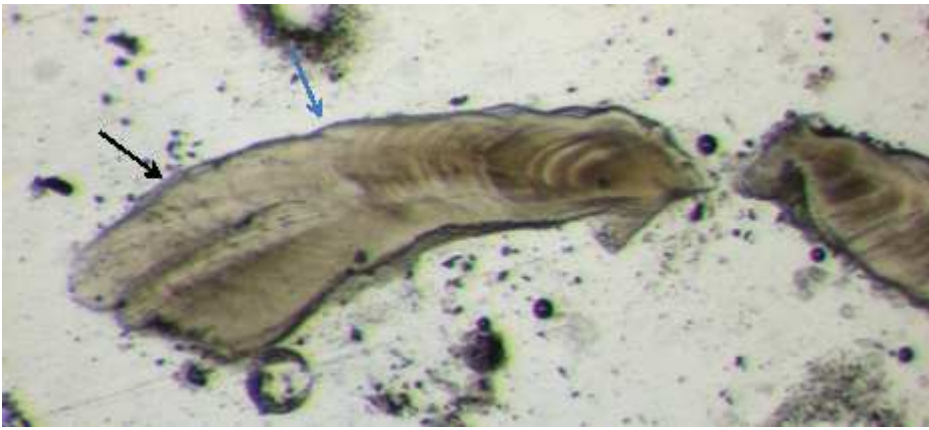


Figure 15 Transverse section of an otolith (108 cm OFL). Blue arrow indicates 100 increments and the black arrow indicates 150 increments. The total count was 299 increments.

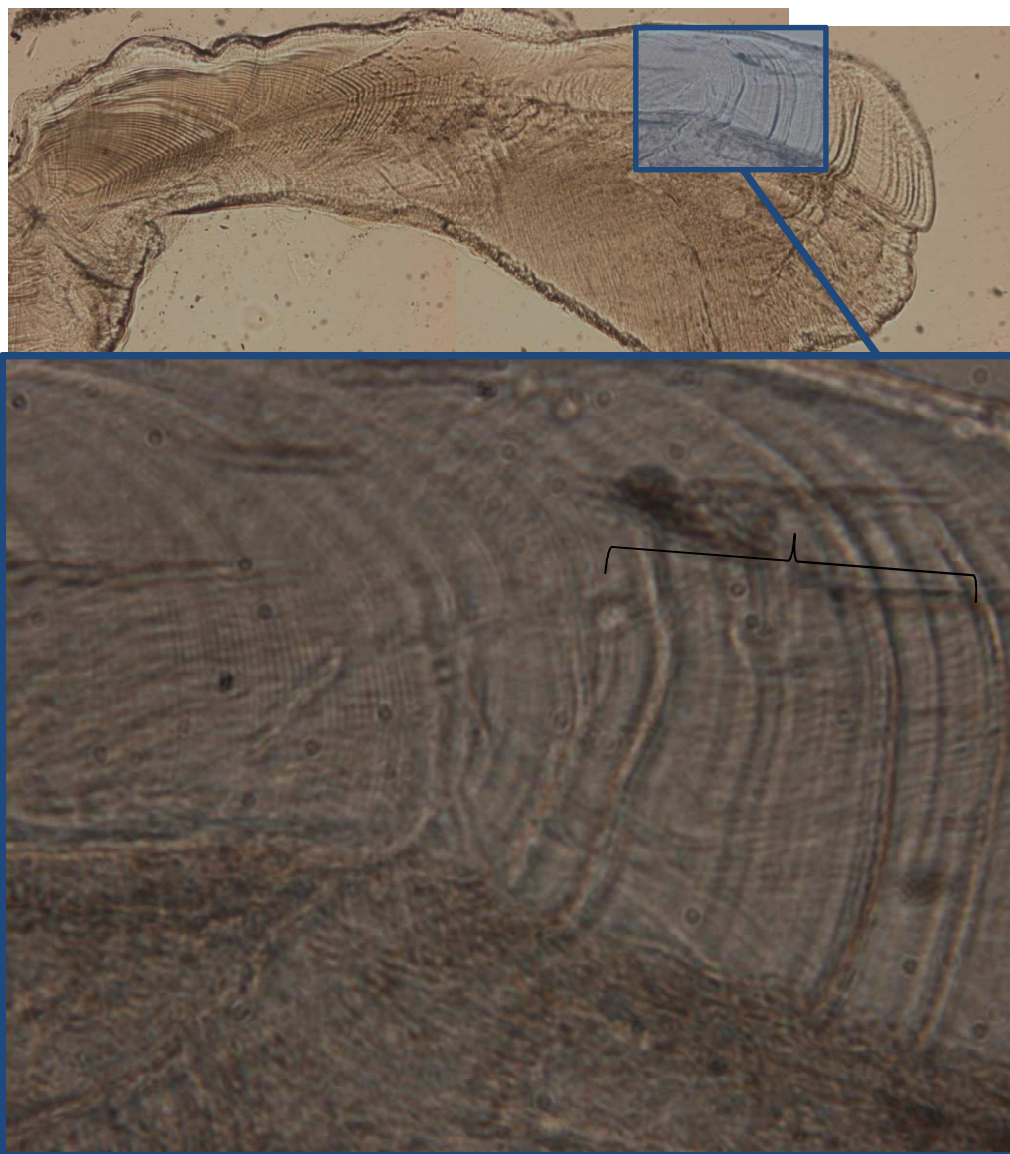


Figure 16 Highlighted area under higher magnification (100x) of the transition point in the otolith (other examples are shown in Appendix E).

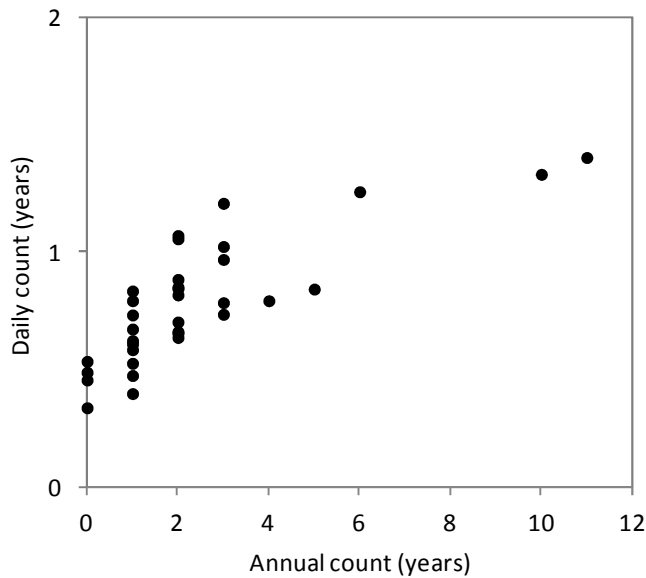


Figure 17 Comparison of daily and annual counts from transverse sectioned otoliths sampled from the same fish.

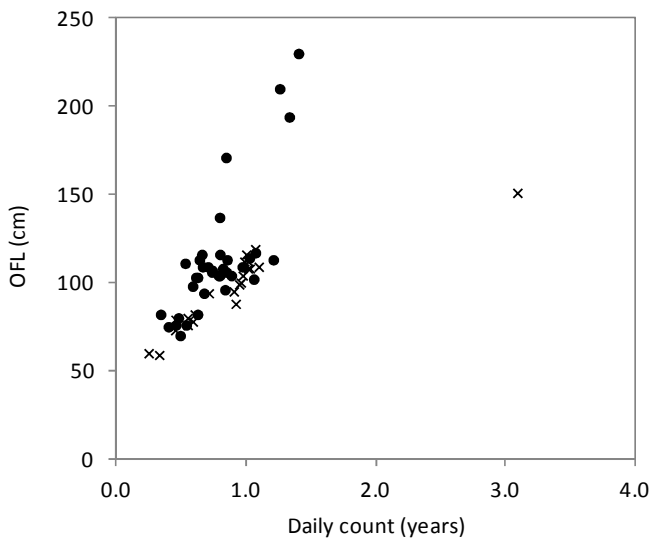


Figure 18 Relationship between orbital fork length (OFL, cm) and daily counts from transverse sectioned otoliths obtained in the current study (•) and the study by Young & Drake (2004) (x) for fish sampled in the SW Pacific.

Annual ageing

Age estimates (counts of opaque zones) were achieved for 301 of the 307 otoliths prepared for annual ageing. Of the unread otoliths, three were not successfully prepared and the other four were considered unreadable. The percent of otoliths found to be unreadable (1.3%) was lower than for rays (12.3%). Age estimates ranged from 0-17 years for males and 0-21 years for females (Table 3). No difference was observed in the difficulty of reading otoliths between sexes, and the average confidence scores were 2.87 and 2.83 for females and males respectively. The relationship between otolith weight and estimated age was linear with an R^2 value of 0.77 (Figure 19).

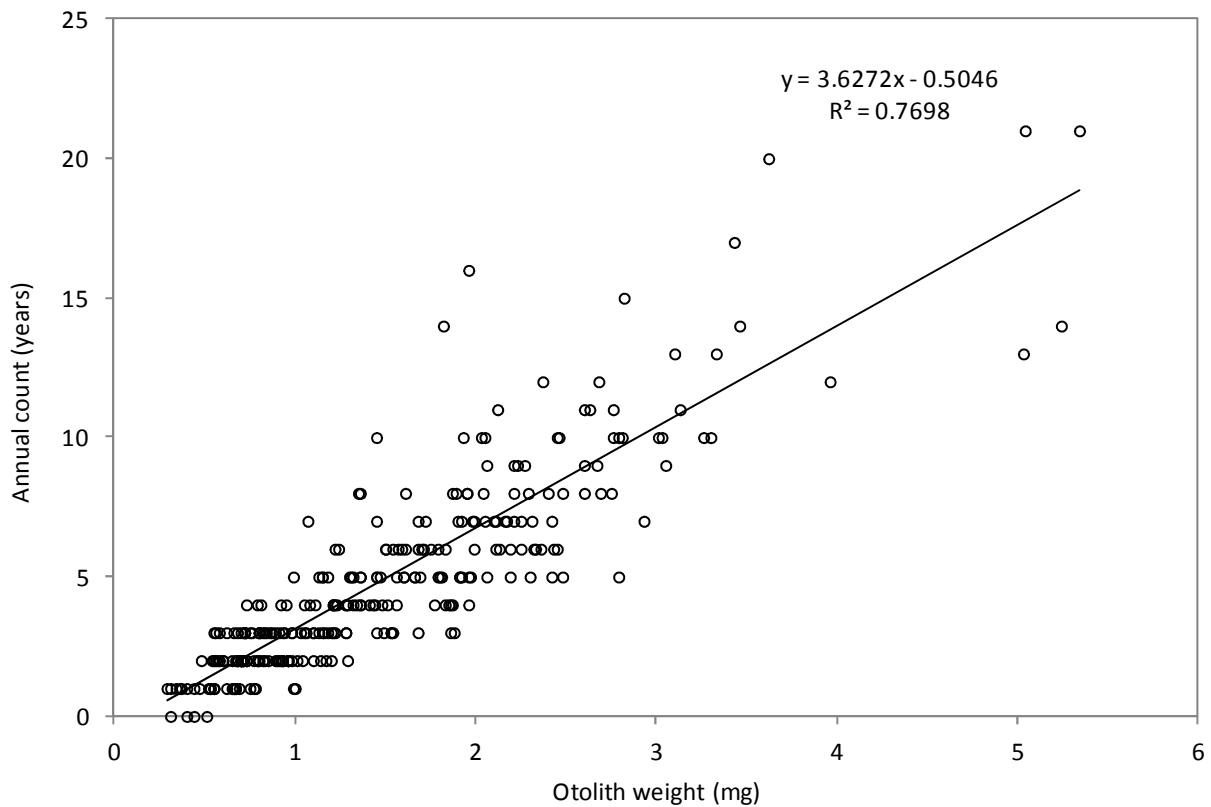


Figure 19 The relationship between otolith weight and annual age for swordfish in the SW Pacific (n=290). $R^2 = 0.7698$.

5.3.4 Precision and bias among readers

The precision of age estimates varied between readers (Table 5). For fin rays, R1 and R2 assigned similar ages on average, with a CV of 15.1 and mean difference of 0.03 years (Table 5). No clear evidence of bias was detected between these readers (Appendix F, Figure F.1). Comparisons of age estimates by R1 and R2 with Young & Drake (2004) (reader 4; R4), however, indicated a bias (Appendix F, Figure F.2). Counts by R4 were higher on average than R1 and R2, and CVs were 30.7 and 30.6 respectively (Table 5). Given that R1 and R2 used the same ray reading methods as DeMartini et al (2007), these results suggests that methodological differences did exist between the studies of Young & Drake (2004) and DeMartini et al. (2007), which could account for the different growth rates obtained in those studies.

For otoliths, the CV among readers ranged from 9.8 to 12.8 (Table 5). A slight positive bias was detected between R1 vs R3 and R2 vs R3 for ages >7 years, and a slight negative bias between R2 and R3 for ages 3 to 13 years (Appendix F, Figure F.3). However, these differences appear to have little effect on estimated von Bertalanffy growth curves (Appendix G).

Table 5 Precision for age estimates (counts) between readers and hardparts.

HARDPART	SEX	READER	COUNT	CV	MEAN DIFFERENCE (YRS)
Rays	Combined	R1 vs R2	253	15.1	0.03
Rays	Combined	R1 vs R4	255	30.7	1.48
Rays	Combined	R2 vs R4	270	30.6	1.40
Otoliths	Combined	R1 vs R2	250	12.8	0.32
Otoliths	Combined	R1 vs R3	255	9.80	0.23
Otoliths	Combined	R2 vs R3	255	11.6	-0.13
Otoliths vs Rays	Female	R3 vs R1	156	16.9	-0.50
Otoliths vs Rays	Male	R3 vs R1	93	25.5	-0.73

5.3.5 Age validation

Location of the first two opaque zone in otoliths

The mean distance from the primordia to the start of the first opaque zone in otoliths was 0.517 mm (± 0.078), which was consistent with the distance recorded to the transition zone (measurement A; at approximately 150 days) in the otoliths prepared for daily age estimation (see above). This suggests that the first opaque zone starts to form at around 150 days. The mean distance to the start of the second opaque zone was 0.718 mm (± 0.097).

Marginal increment analysis (indirect validation)

Given the small number of rays and otoliths analysed, it was necessary to combine the marginal increment ratio (MIR) data across age classes to determine the relative state of completion of the most distal increments. For rays, there appears to be a seasonal cycle in mean MIR for males with the highest values in July to November and lowest values in March to May suggesting that one translucent zone forms annually between November and April (Figure 20). This is consistent with previous studies of swordfish in the Pacific which found that the annulus (translucent zone) is completed by late summer (Sun et al. 2002; DeMartini et al. 2007). The pattern was similar but not as clear for females as relatively low mean MIR values were also present in October-November. This may be due to the higher proportion of older (slower growing) females in the sample. MIR analysis is only suitable for “fast growing and/or young fish” and requires sample sizes >100 (Campana 2001).

For otoliths, the precise time that increments are deposited in otoliths could not be determined from MIR analysis. This was partly due to insufficient sample sizes for many months, which made interpretation difficult (Figure 21), but may also be due in part to inaccurate otolith measurements. Given the very small size of swordfish otoliths, problems occur when trying to precisely locate and measure the increments (Campana 2001; Farley et al. 2006).

For both hardparts examined, pooling the data across year classes also meant that it was not possible to indirectly validate the periodicity of increment formation across the full age range - particularly for older fish where the divergence in age between rays and otoliths was observed.

Appendix H provides examples of the marginal stage of otoliths and rays.

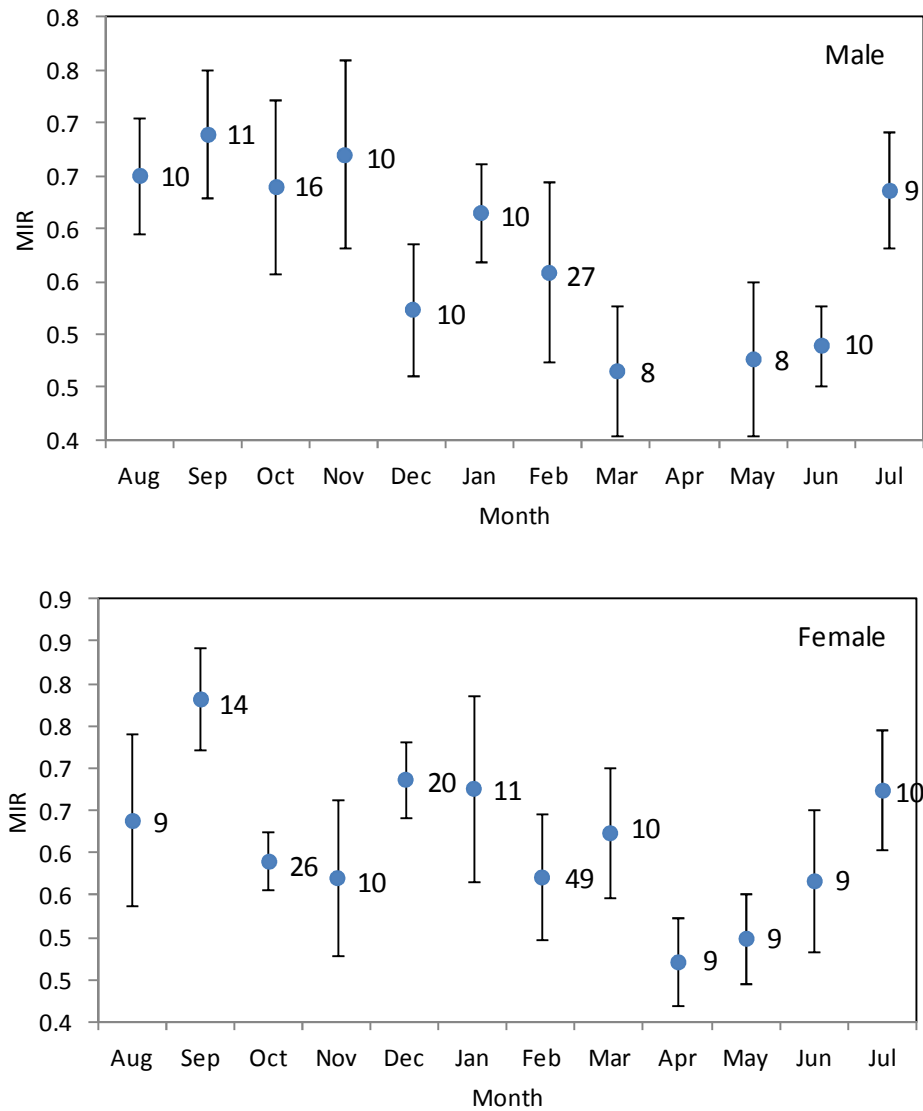


Figure 20 Mean (+/- SE) monthly ray marginal increment ratio (MIR) for male and female swordfish (n = 318). Sample size is shown next to the mean; only months where n ≥ 5 are shown.

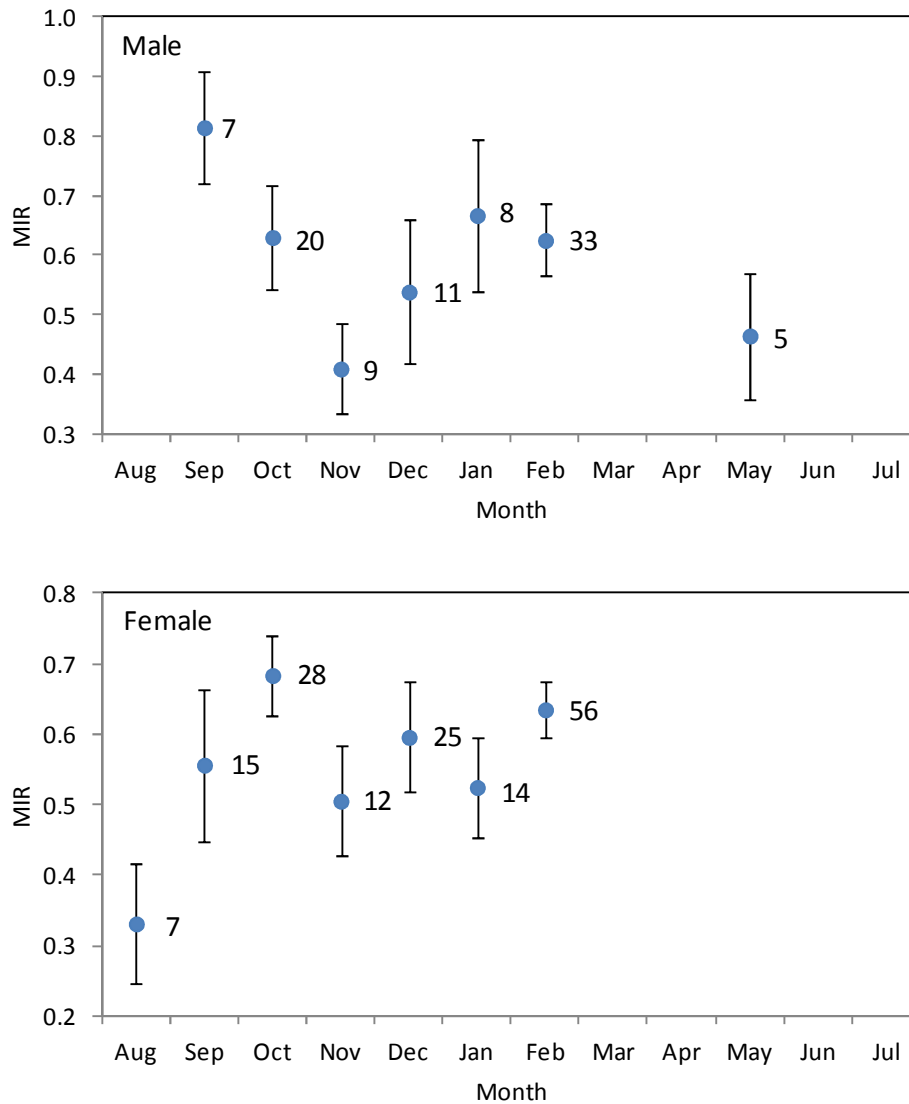


Figure 21 Mean (+/- SE) monthly otolith marginal increment ratio (MIR) for male and female swordfish (m = 263). Sample size is shown next to the mean; only months where n ≥ 5 are shown.

Comparison of structures

The precision of age estimates varied between the hardparts examined. The CV of age estimates obtained from rays (R1) and otoliths (R3) from the same fish were relatively high at 16.9 and 25.5 for female and male fish respectively (Table 5). Figure 22 indicates substantial bias for both males and females. Ray-based counts were similar on average to otolith-based counts in the youngest age classes, however, a bias was evident in age classes >7 years for females and >4 years for males, where ray counts were lower on average compared to otolith counts (Figure 22). Paired t-tests confirmed the bias for these age classes. No significant difference was detected among age estimates from otoliths and rays for ages 1-7 for females and 0-4 for males (Table 6).

For females, the bias in age begins well after age at 50% maturity (~4.4 years) and closer to age at 100% maturity (see section 6.3.3 below). It is not surprising, therefore, that the bias starts at a

younger age for males since males mature at a younger age. Length at 50% maturity is around 102 cm (1 year) (DeMartini et al. 2007; Young & Drake 2002).

Table 6 Summary table of paired t-test results for age estimates obtained from otoliths and rays from the same fish. The results are shown by sex and otolith-age. Significant differences among ages are indicated by *.

Otolith age (years)	Females		Males	
	d.f.	P	d.f.	P
0	0	NA	1	0.423
1	13	0.336	10	0.219
2	25	0.294	15	0.164
3	31	0.525	10	0.465
4	13	0.793	11	0.862
5	15	0.618	11	0.001*
6	9	0.798	6	0.084
7	9	0.434	7	0.014*
8	8	0.018*	6	0.005*
9	8	0.017*		
10+	23	<0.001*	4	0.026*
All	155	0.001*	93	<0.001*

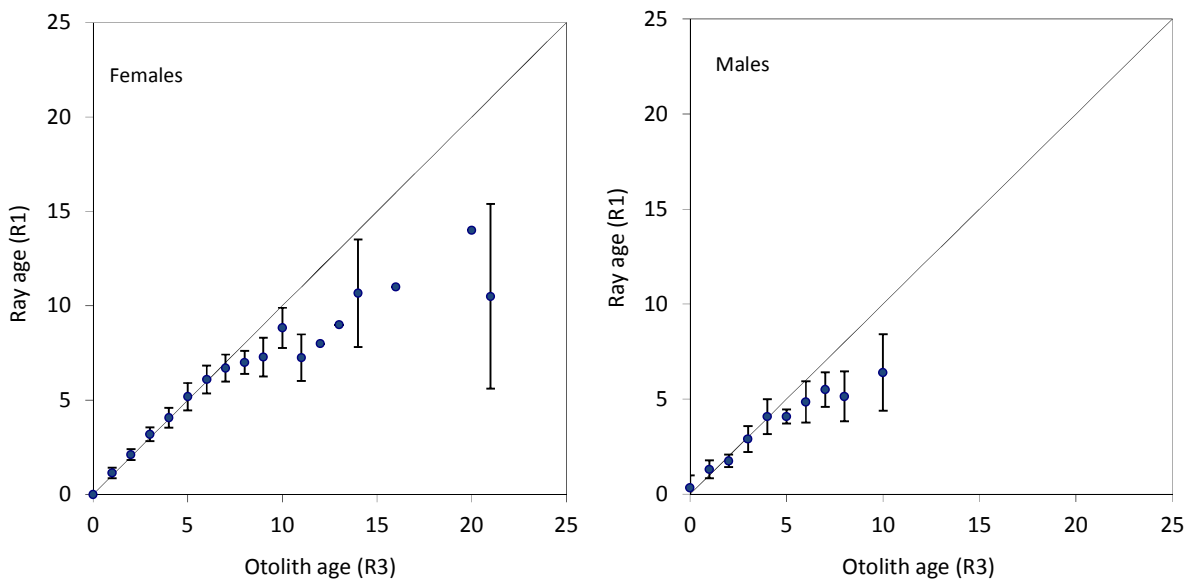


Figure 22 Age bias plots by sex comparing final age estimates from otoliths and rays from the same fish. R1 = reader 1, R3 = reader 3.

Four possible explanations for the divergence of age counts between otoliths and fin rays are:

1. More than one increment is deposited annually on otoliths after a certain age,
2. Increments are not deposited on fin rays after a certain age,
3. Increments are deposited so close together on the margin of fin rays as the fish gets older that readers cannot differentiate/resolve them,
4. Vascularisation at the core and bone remodelling on the surface of fin rays obscures increments.

In previous studies where ages from swordfish otoliths and other hard parts from the same fish have been compared, there was close agreement between ages estimated from small fish (Wilson & Dean 1983; Castro-Longoria & Sosa-Nishizaki 1998). In studies where higher numbers of larger fish were examined, counts obtained from otoliths were higher than for fin rays and vertebrae, and consequentially, otoliths were considered unreliable and their use for age and growth studies was discouraged (Uchiyama et al. 1986; Nishimoto et al. 2006).

A similar result was found in Atlantic bluefin tuna (*Thunnus thynnus*) (Lee et al. 1983) where, after around 10 years, ages from otoliths were higher than those from vertebrae from the same fish. To account for this, Lee et al. (1983) developed a “revised otolith method”, for which they assumed two increments were deposited per year after age 10 on otoliths. An equivalent situation was found in southern bluefin tuna (*Thunnus maccoyii*) where vertebral counts matched otolith counts until around 10 years of age, after which otolith counts were higher (Gunn et al. 2008). However, this study included a direct validation of age estimates from otoliths and showed that each increment on the otoliths represented a year’s growth and that vertebrae underestimated the true age. Higher age estimates from otoliths compared to rays from the same fish have been reported in other billfish and tunas (e.g., Atlantic sailfish, Prince et al. 1986; Atlantic bluefin tuna, Rodríguez-Marín et al. 2007; South Pacific albacore tuna, Farley et al. 2013a). In each case apart from Atlantic bluefin tuna, otoliths were the preferred structure to estimate age across the full size range. For eastern Atlantic bluefin tuna, otoliths are not available for all fisheries so rays are commonly used for ageing, although they are difficult to interpret after age 10 years (Rodríguez-Marín et al. 2007). Otoliths are the preferred structure to directly age western Atlantic bluefin, and recent work has validated the annual periodicity of the opaque zones counted (Neilson & Campana 2008; Restrepo et al. 2010; Siskey et al. 2015).

In ageing studies of albacore tuna using rays, two translucent bands per year were reported and referred to as doublets (Bard & Compean-Jimenez 1980). Gonzales-Garces & Farina-Perwz (1983) saw similar patterns in rays and counted the doublets as 1 year, for the first year of life. Megalofonou (2000) also noted the appearance of “doublets” in rays, and counted them as one year, but set rules about when to count these translucent bands as one year or two. In the current study of swordfish we saw doublets and even “triplets” in the fin ray sections and developed protocols (adapted from Megalofonou 2000) for determining if they were counted as one or more year’s growth; these included assessing the amount of space between translucent zones and whether or not the translucent zones coalesced at the core.

From our examination of fin rays and otoliths from the same fish, it seems unlikely that two increments are deposited annually in otoliths. Some fish deposit a spawning check in addition to an annual increment (Geffen et al. 2002). However, this appears unlikely in swordfish as the

divergence in counts between rays and otoliths occurred well after maturation in females, suggesting that spawning does not interrupt growth during the spawning season. We also noted that the discrepancy between age counts in rays and otoliths does not occur in all cases. In some older fish, fin ray counts were the same or higher than those for otoliths (e.g., Figure 23). This supports the current theory that underpins fish ageing studies, that increments are deposited throughout the life of the fish on both structures (Campana 1999). These results also suggest that even in some older age classes, it is possible to resolve increments on the margins of some fin rays.

Loss of increments on fin rays due to vascularisation and bone remodelling may provide the best explanation for the discrepancies between the two structures. These processes occur only in the fin rays, not otoliths, and this difference is due to the structure, arrangement and function of the two hardparts. Otoliths are composed largely of calcium carbonate, in the form of aragonite, whereas fin rays are hydroxyapatite, and form part of the bony skeleton of a fish. In both otoliths and fin rays, calcium is a major element: about 40% in the aragonite matrix of otoliths and 23% in the hydroxyapatite matrix of fin rays and scales (Clarke et al. 2007). The structures perform very different functions however both grow by accretion on to the marginal surface.

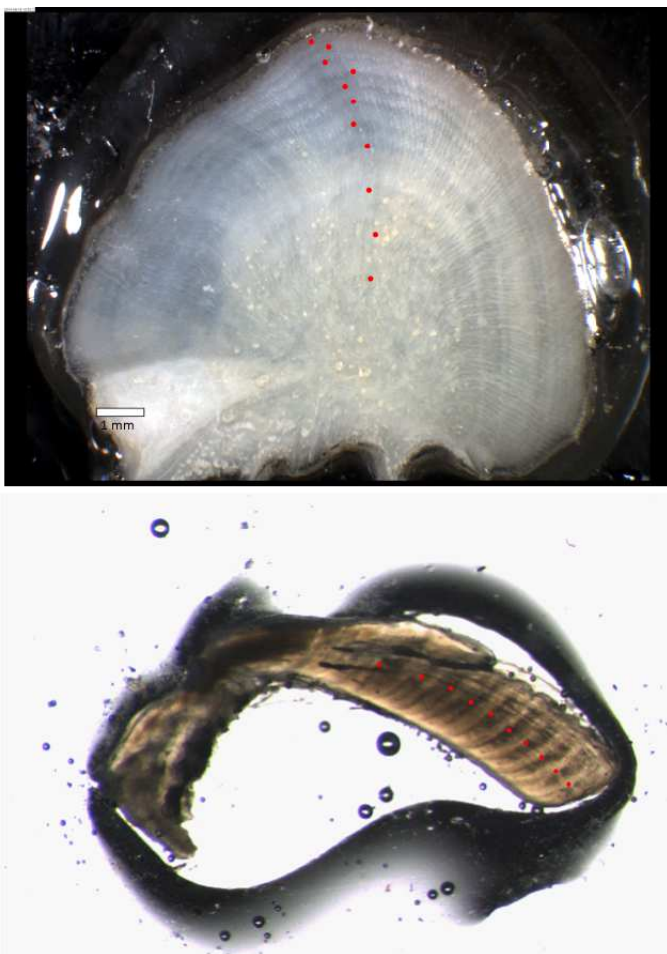


Figure 23 Swordfish #224 (female, 219 cm OFL) fin ray and otolith prepared for annual ageing. The red dots indicate the outer edge of the translucent zones counted, giving a slightly higher age from the ray (11 years) compared to the otolith (10 years).

Fin rays

Growth in fin rays, as in other bone, begins when osteoblasts synthesize protein macromolecules (collagen) on the surface of the fin ray. These are progressively surrounded by the organic matrix and mineralisation occurs, subsequently forming cellular bone or osteocytes. When osteoblasts are relatively numerous on the external surface of a bone, they form a membrane, the periosteum (Francillon-Vieillor et al. 1990).

This process produces primary bone that can last for the life of the fish. However, it can be partially destroyed, and replaced by new bone. When a fish is undergoing physiological demand, resorption of the contents of the bone can occur by erosion of the bone surface. Osteoclasts destroy bony tissue by forming a depression on the fin ray surface. When osteoclasts merge they create cavities that then fill with “secondary” bone. The process of erosion and reconstruction is called bone remodelling. Remodelling of bone can contribute to the disappearance of increments and thus lead to underestimates of age (Wright et al. 2002). In addition, primary and adjacent secondary bone is separated by cementing or resorption lines, creating a discontinuity within the bone tissue, adding to the complexity of the appearance of fin ray sections (Meunier 2002).

Tuna and related species, such as swordfish, undergo abundant remodelling of their skeleton. However, it occurs more frequently in the axial skeleton and less so in superficial bone such as fin rays (Meunier and Panfili 2002).

Remodelling of fin rays can occur not only on the outer surface but also in the core, and this is part of the process known as vascularisation. Fin rays include spaces that house blood vessels, adipose cells and fibrocytes (connective and nerve tissue), which provide metabolites to surrounding bony tissue. Primary vascular canals form at the same time as the fin ray and are obvious in the core of fin rays. In fish species where metabolic activity is high, such as swordfish, vascular canals are more developed (Amprino & Godina 1956). Osteoclasts are active in vascular canals and perform resorption activity, forming tunnels-shaped cavities that are invaded by vessels as the fish grows. Osteoblasts then deposit new bone on the walls of these tunnels. As a fish and the fin ray grows, the area taken up by vascular canals increases and, in some cases, increments closest to the core of the fin ray, those deposited early in life, are obscured.

Otoliths

Otoliths are located in otic sacs within the semicircular canals and their main function is maintaining equilibrium. Otoliths grow throughout the life of a fish but, unlike fin rays, they are not vascularised, and once crystallized from surrounding endolymph, otoliths are not subject to resorption (Mugiya & Uchimura 1989).

Otoliths are precipitated from the fluid of the endolymphatic sacs and grow in size by accretion on the outer surface. Calcium carbonate is the major component of otoliths but they also contain a soluble, protein matrix. Growth occurs by addition of concentric layers of proteins and calcium carbonate. In otolith studies, these two layers are referred to as the D-zone, the mineral deficient zone that is higher in organic proteins; and the L-zone that is rich in calcium carbonate. The two layers have different opacities, width and size of aragonite crystals. A D-zone and L-zone together combine to form microincrements which, in some species, have been validated as forming daily (Meunier 2002)

The ratio of constituents and their arrangement in the matrix of the otoliths also changes seasonally to form cyclic patterns of increments that can be counted. In some species, increment deposition can be directly influenced by temperature, seasonality in somatic growth and environmental activity or, in other species, less directly as a physiological response to environmental variation. The timing and appearance of increments in otoliths can change throughout the life of a fish due to factors such as reproductive activity, age, sex, geographical distribution, food availability and nutrient content of prey (Wright et al. 2002, Morales-Nin & Panfili 2002).

5.3.6 Growth analysis

Age estimates (counts) from otoliths and fin rays produce different growth curves for both males and females (Table 7; Figure 24). Both hardparts indicate that early growth in swordfish much be rapid in order to reach the sizes at age 1 observed. This initial fast growth is reflected in the negative t_0 values estimated. The otolith-based growth curves then indicate slower growth and a higher maximum age for males and females compared to the ray-based growth curves. Both hardparts show that length-at-age is greater for females than males after age 3-4 years (Figure 25).

Otoliths are generally considered to be the more accurate structure to age fish (Campana et al. 1995), and validated annual age estimates using otoliths have been obtained for Atlantic sailfish (Prince et al. 1986) as well as several tuna species including Atlantic bluefin, southern bluefin, bigeye (*Thunnus obesus*), albacore and longtail (*Thunnus tonggol*) (Clear et al. 2000; Farley et al. 2006; 2013a; Neilson & Campana 2008; Griffiths et al. 2009; Shimose et al. 2009). The highest estimated age for swordfish from count of opaque bands in sectioned otoliths is 23 years (Nishimoto et al. 2006).

Figure 26 shows the growth curves obtained for swordfish in the current study compared to the previous studies in Hawaii (DeMartini et al. 2007) and the SW Pacific (Young & Drake 2004). The early growth of swordfish estimated in the current study is faster than obtained by Young & Drake (2004) for both sexes and hardparts analysed, but is slightly slower than the ray-based growth rates estimated by DeMartini et al. (2007).

Table 7 Sex-specific VB growth parameters estimated using otolith and ray count data, with standard errors in parentheses.

DATA SOURCE	SEX	L_{∞}	k	t_0	σ
Ray	F	279.6 (16.0)	0.123 (0.017)	-2.55 (0.34)	14.9 (0.72)
Otolith	F	249.6 (7.6)	0.157 (0.016)	-2.13 (0.30)	15.2 (0.79)
Ray	M	213.8 (10.5)	0.197 (0.031)	-2.28 (0.36)	12.8 (0.74)
Otolith	M	191.9 (6.0)	0.235 (0.022)	-2.10 (0.35)	13.6 (0.90)

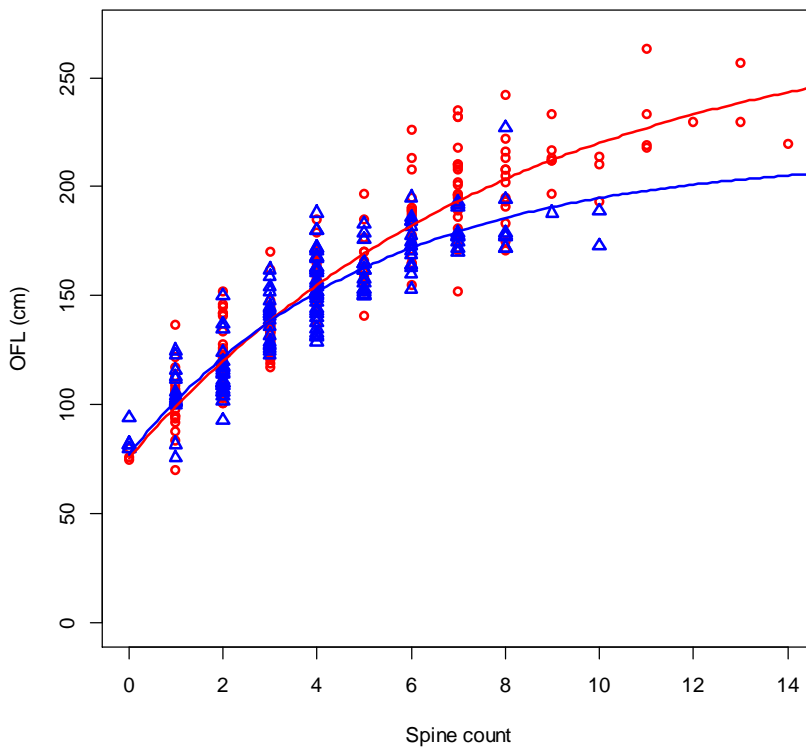
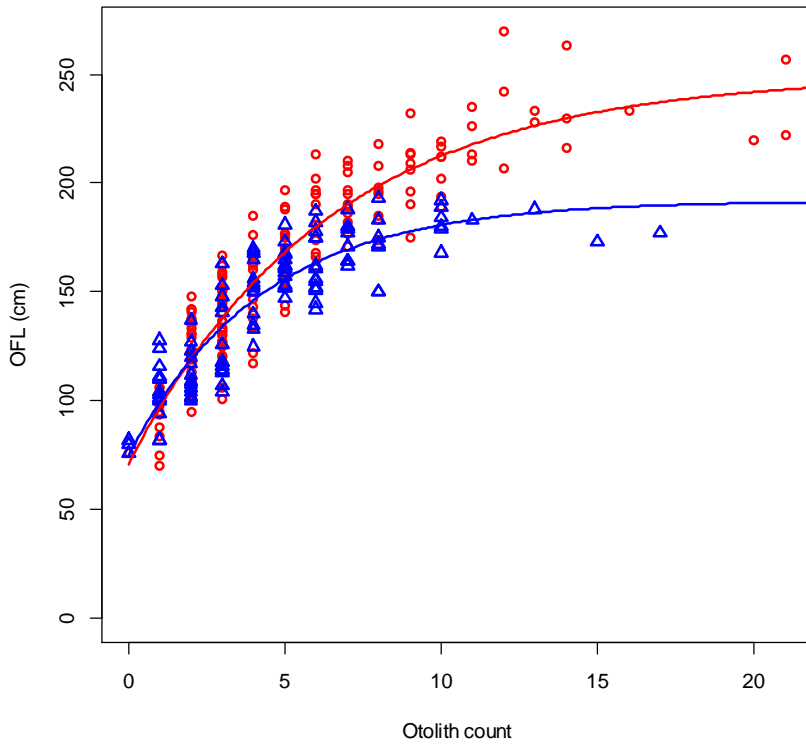


Figure 24 von Bertalanffy growth curves fitted to length at age (count) from otoliths (top) and rays (i.e., spines) (bottom) by sex (○= females; △ = males).

VB growth curves for SWO

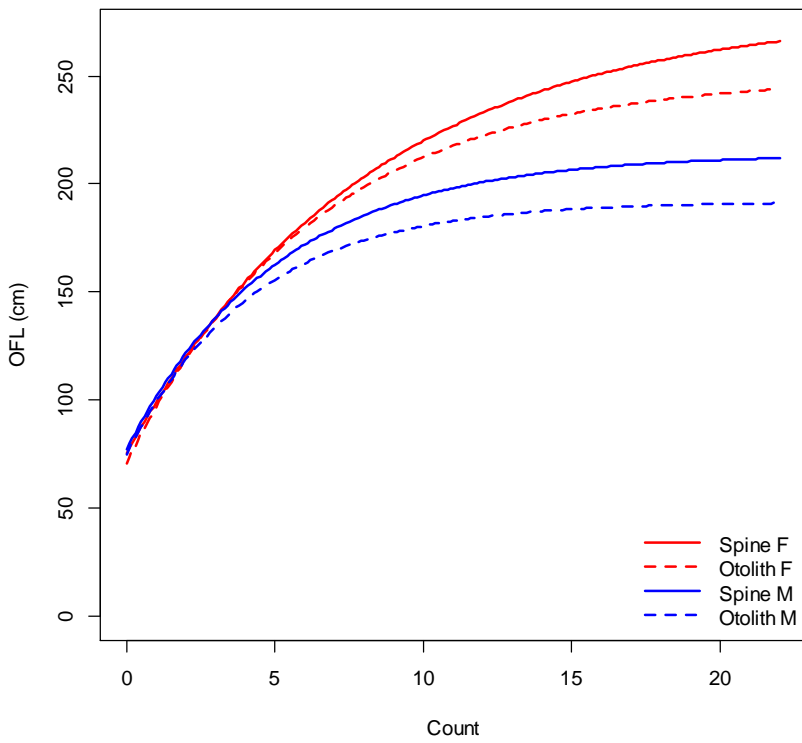


Figure 25 Comparison of sex-specific VB growth curves estimated using otolith and ray (i.e., spine) count data.

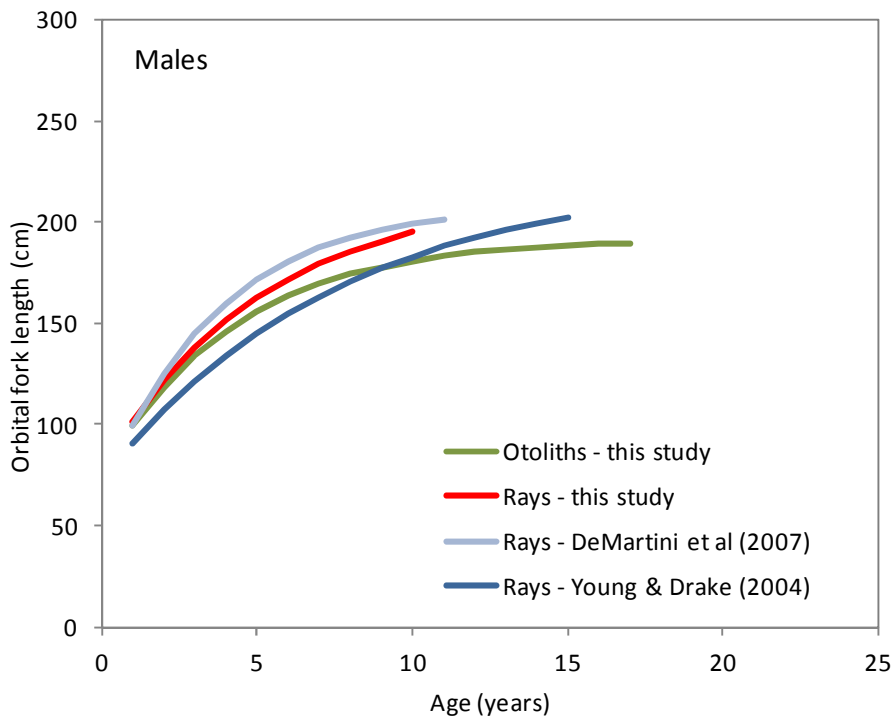
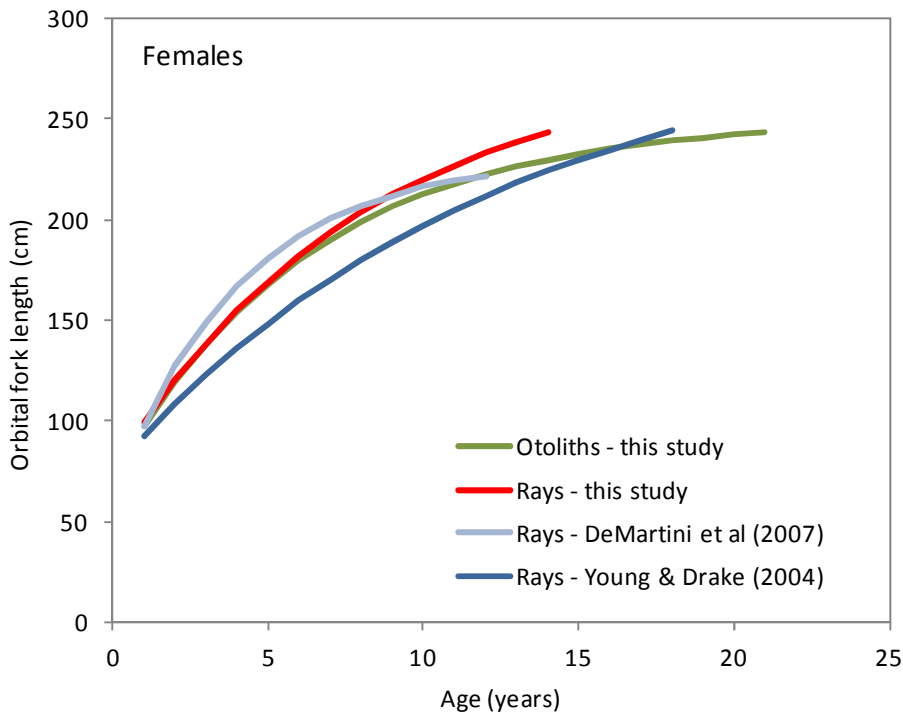


Figure 26 von Bertalanffy growth curves estimated by sex for swordfish in the current study compared to previous studies by DeMartini et al. (2007) and (Young & Drake 2004). The curves only cover the age range of the data.

5.4 Conclusions

Age estimates obtained from fin rays and otoliths appear to be precise and reproducible. Marginal increment ratio (MIR) analysis suggests that one translucent zone is formed annually in the fin rays, but there was insufficient data to examine the monthly MIR for otoliths. Campana (1991)

noted that the MIR method is only suitable for “fast growing and/or young fish” and requires sample sizes >100. For the MIR method to be useful for otoliths, additional samples would be required for all months and/or age classes. While not definitive, the similarity of ray and otolith-based age estimates for the first few years (7 for females and 4 for males) provides independent corroboration of the early growth rates obtained.

In larger/older fish, research indicates that age estimates from otoliths are likely to be more reliable for swordfish because fin rays are subject to remodelling and resorption. Fin rays are rarely used in fish ageing studies because of this vascularisation (Morales-Nin & Panfili 2002). However, due to the precision required when sampling and sectioning swordfish otoliths, rays may be the more practical structure for ageing small fish up to approximately 170 cm OFL for females and 120 cm for males. These lengths correspond to the ages up to which otoliths and rays give similar results.

Direct validation of the accuracy of the ageing methods used (for otoliths or rays) was not possible in the current project, and has not been undertaken for swordfish in any ocean. Without direct age validation it is impossible to determine which structure provides accurate age estimates for the largest fish. Bomb radiocarbon analysis of swordfish vertebrae sampled in Hawaii was difficult due to the resorption and reworking of vertebral material, although age estimates of around 30 years were obtained for the largest fish (Kalish & DeMartini 1993).

6 Maturity of swordfish in the SW Pacific

6.1 Introduction

Mean length at maturity has been estimated for swordfish in the Pacific, Indian and Atlantic Oceans and in the Mediterranean Sea. The techniques used to determine the maturity status of individual fish varied among studies, some using histological assessment (Taylor & Murphy 1992; DeMartini et al. 2000; Young & Drake 2002; Wang et al. 2003) and others using gonad index analysis, oocyte size distribution and/or macroscopic staging of ovaries (De la Serna et al. 1996; Arocha 1997; Hazin et al. 2002; Arocha 2007; Poisson & Fauvel 2009; Varghese et al. 2013; Mejuto & Garcia-Cortés 2014). Although expensive, histological analysis is considered the most precise technique to determine ovary development stage (West 1990). Using histology, females are typically classified as mature if their ovaries contain advanced yolked oocytes (tertiary vitellogenic, migratory nucleus or hydrated) or early-stage atresia of yolked oocytes (alpha and beta). Females without these follicles are assumed to be either immature (virgin) or of uncertain maturity because the ovaries of mature-regenerating females are histologically similar to immature ovaries. If using this classification scheme to estimate a maturity ogive, it is often recommended that ovaries are sampled just prior to or during the early part of the spawning period to reduce the chance of misclassifying regenerating females as immature (Hunter & Macewicz 2003; Murua et al. 2003). Some swordfish studies, however, were able to use ovaries collected year-round by using the presence of late-stage atresia (gamma and delta) to identify regenerating females (DeMartini et al. 2000; Wang et al. 2003).

Young & Drake (2002) did not use late stage atresia to identify regenerating females in the SW Pacific, possibly due to the difficulty of distinguishing these features in frozen-fixed ovary material. Recent work on albacore tuna, however, has provided additional histological criteria to distinguish regenerating from immature females when using frozen-fixed ovary material (Farley et al. 2013b).

In this study, we aim to investigate additional histological criteria ('maturity markers') in swordfish ovaries sampled by Young et al. (2003) and determine the type and number of maturity markers required to identify regenerating females, and to provide an unbiased maturity ogive for swordfish in the SW Pacific.

6.2 Methods

6.2.1 Study material

Young et al. (2003) collected gonads from swordfish caught by Australian, New Zealand and New Caledonian longline fisheries between 1998 and 2001 (Figure 27). Most fish were caught in Australia's Eastern Tuna and Billfish Fishery between 25-30°S and east to 165°E. The gonads were frozen on board and sent to the laboratory where they were defrosted, weighed to the nearest 1 g (if whole), and a subsample fixed in 10% neutral buffered formalin. A subsample was taken from 27 ovaries prior to freezing. Standard histological sections (cut to 6 µm and stained with Harris'

haematoxylin and eosin) were prepared and the maturity status was obtained for 768 females (Young et al. 2003). Differences in histological classification of ovaries were not detected between frozen- and fresh-fixed ovaries (Young et al. 2003).

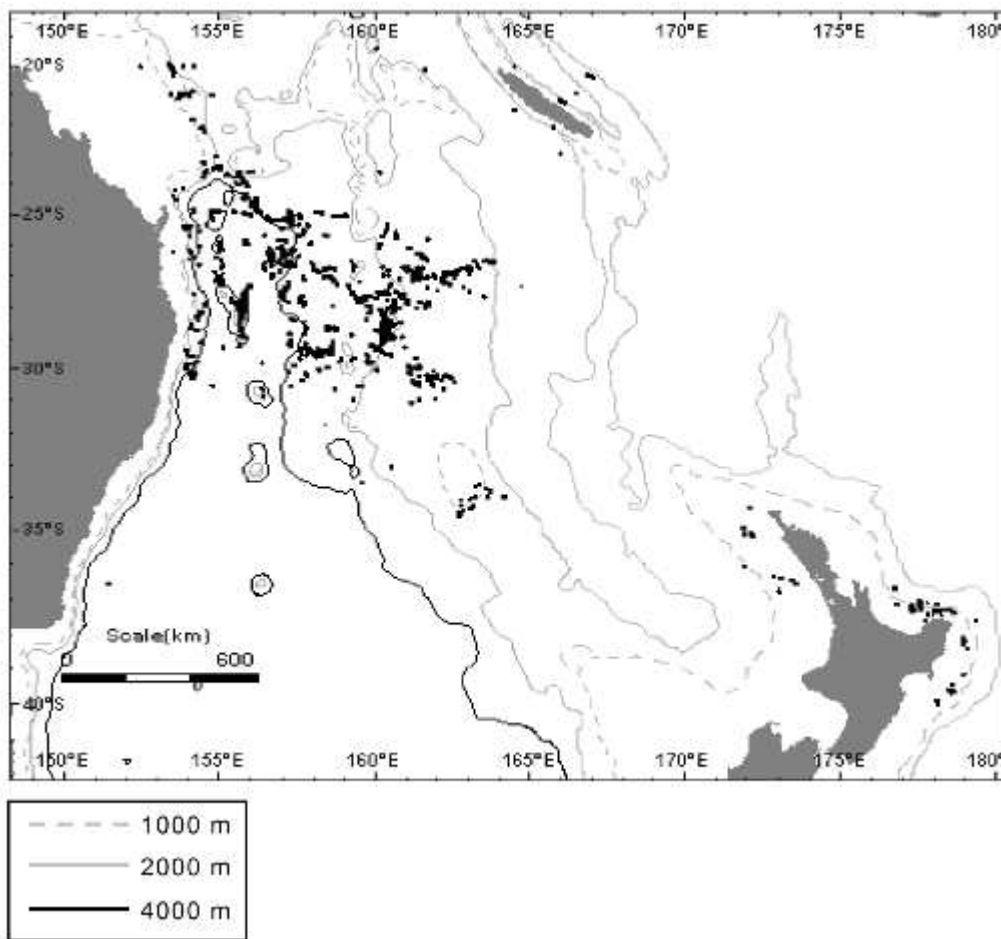


Figure 27 Map indicating the capture locations of swordfish sampled for gonads (from Young & Drake 2002).

6.2.2 Re-examination of ovary histology

Of the histology prepared by Young et al. (2003), 685 ovary sections were deemed suitable for re-analysis as the material was in good condition and of sufficient size for reading, and catch data were present (i.e., OFL, capture date and location). Gonad weight was obtained for 658 females and a gonadosomatic index (GSI) was calculated following Hinton et al. (1997).

The histological sections were read using standardised terminology (Brown-Peterson et al. 2011) and classification criteria for large pelagic tuna species (e.g., Schaefer 2001; Farley et al. 2013b). The most advanced group of oocytes (MAGO) was staged into one of 5 classes: unyolked (primary growth and cortical alveolar), early yolked (primary and secondary vitellogenic), advanced yolked (tertiary vitellogenic), migratory nucleus (germinal vesicle migration) or hydrated (Figure 28). Each ovary was also scored according to the presence or absence of postovulatory follicles (POFs) (Figure 29), advanced yolked oocytes undergoing alpha (α) or beta (β) atresia (Figure 30) and maturity markers (Figure 31). The maturity markers considered were well defined muscle bundles,

numerous “brown bodies” and residual yolked oocytes, which are considered signs of prior reproductive activity. Muscle bundles are distinct structures of remnant muscle and connective tissue surrounding blood vessels and are an indicator of previous spawning (Shapiro et al. 1993; Brown-Peterson 2011; Lowerre-Barbieri et al. 2011) (Figure 31). Brown bodies are aggregates of yellow-brown pigment which may be remnant atretic oocytes (e.g., delta and gamma atresia; Hunter and Macewicz 1985) or structures similar to melano-macrophage centres/aggregates (Blazer 2002) which are linked to post-spawning activity in the gonad (Figure 31B-D). Residual yolked oocytes occurred in the ovary lumen as single or ‘clumps’ of hydrated oocytes (Figure 31E-F) or as unovulated follicles within the connective tissue of the ovary.

Ovary wall thickness and circumnuclear oil droplets in primary growth (PG) oocytes were not used as an indicator of maturity because the ovary wall was not often present in the histological sections, and cell lysis was apparent in some sections (due to the freezing of the tissue prior to fixation) reducing the ability to resolve and quantify cellular structure in some PG oocytes.

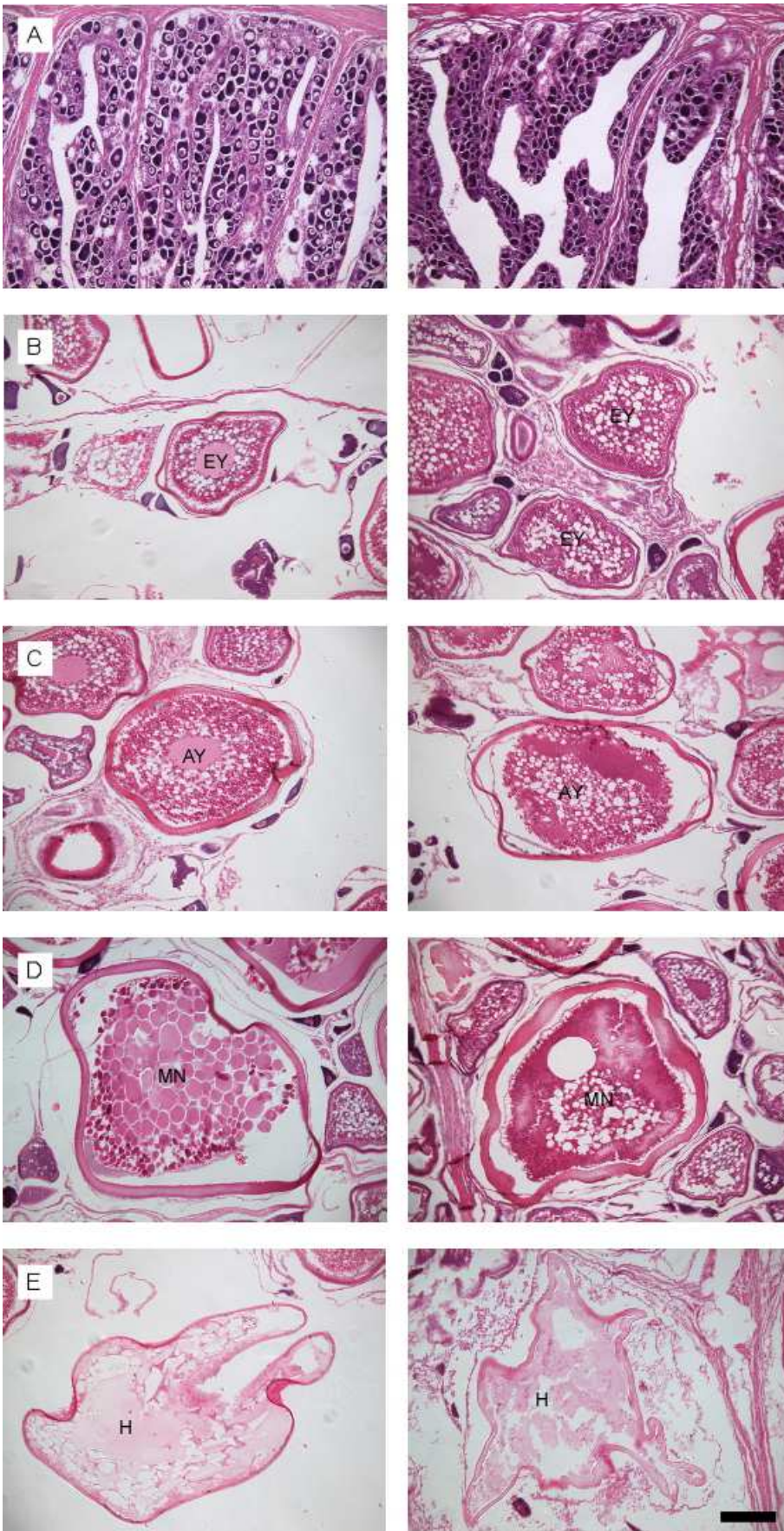


Figure 28 Oocyte development classes in fresh (left) and frozen (right) fixed swordfish ovaries. A: unyolked (UY). B: early yolked (EY). C: advanced yolked (AY). D: migratory nucleus (MN). E: Hydrated. Bar equals 500 μ m.

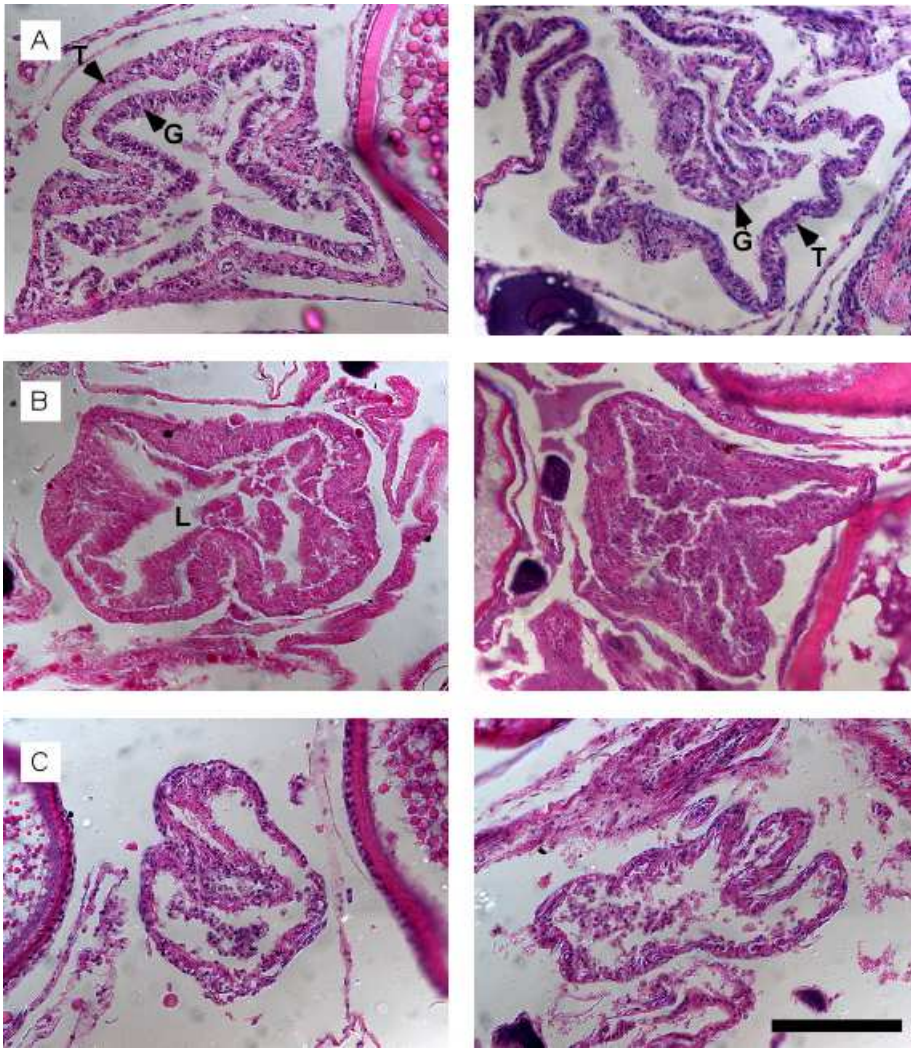


Figure 29 Postovulatory follicles degeneration in fresh (left) and frozen (right) fixed swordfish ovaries. **A:** Early stage POF which has a clear convoluted shape and two distinct layers (T = thecal; G = granulosa). **B:** later stage POF which has a smaller lumen (L) and the thickness of the thecal and granulosa layers has increased. **C:** old POF where the folds have shrunk and convoluted shape is disappearing. Bar equals 100 μm .

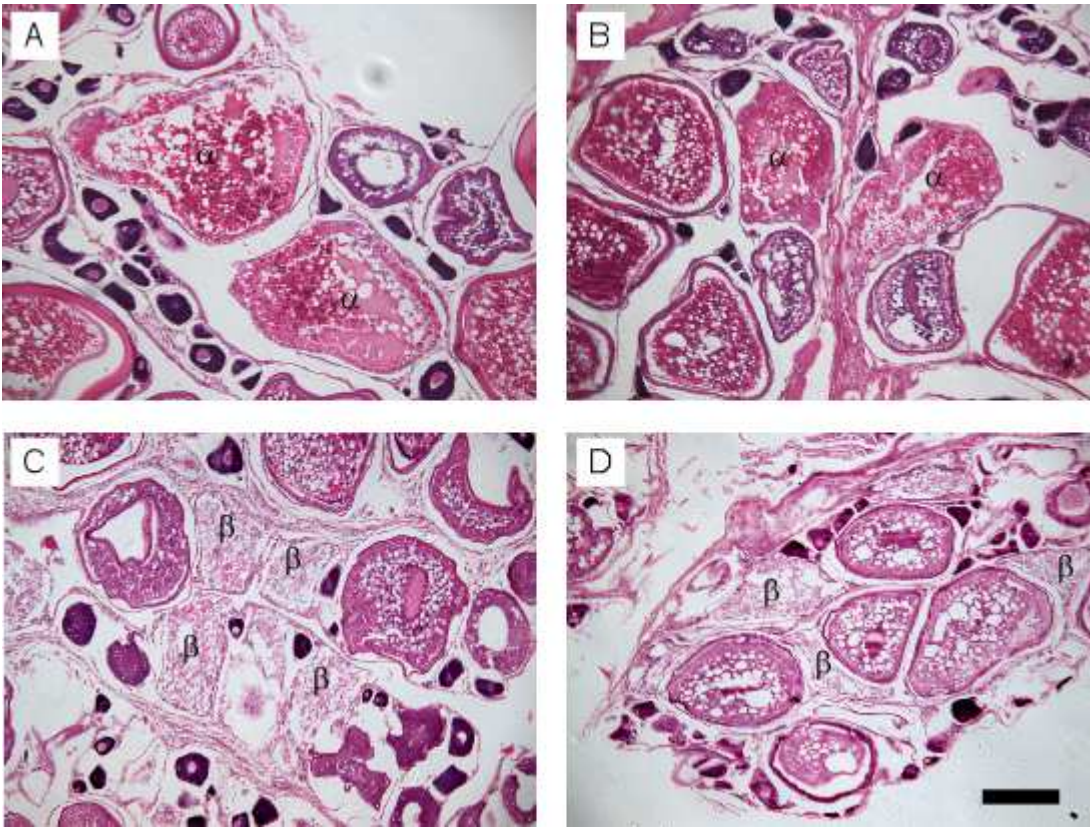


Figure 30 Atresia of advance yolked oocytes in fresh- (left) and frozen (right) fixed swordfish ovaries. A-B: Late stage alpha (α) with some yolk granules remaining. C-D: Beta (β). Bar equals 200 μ m.

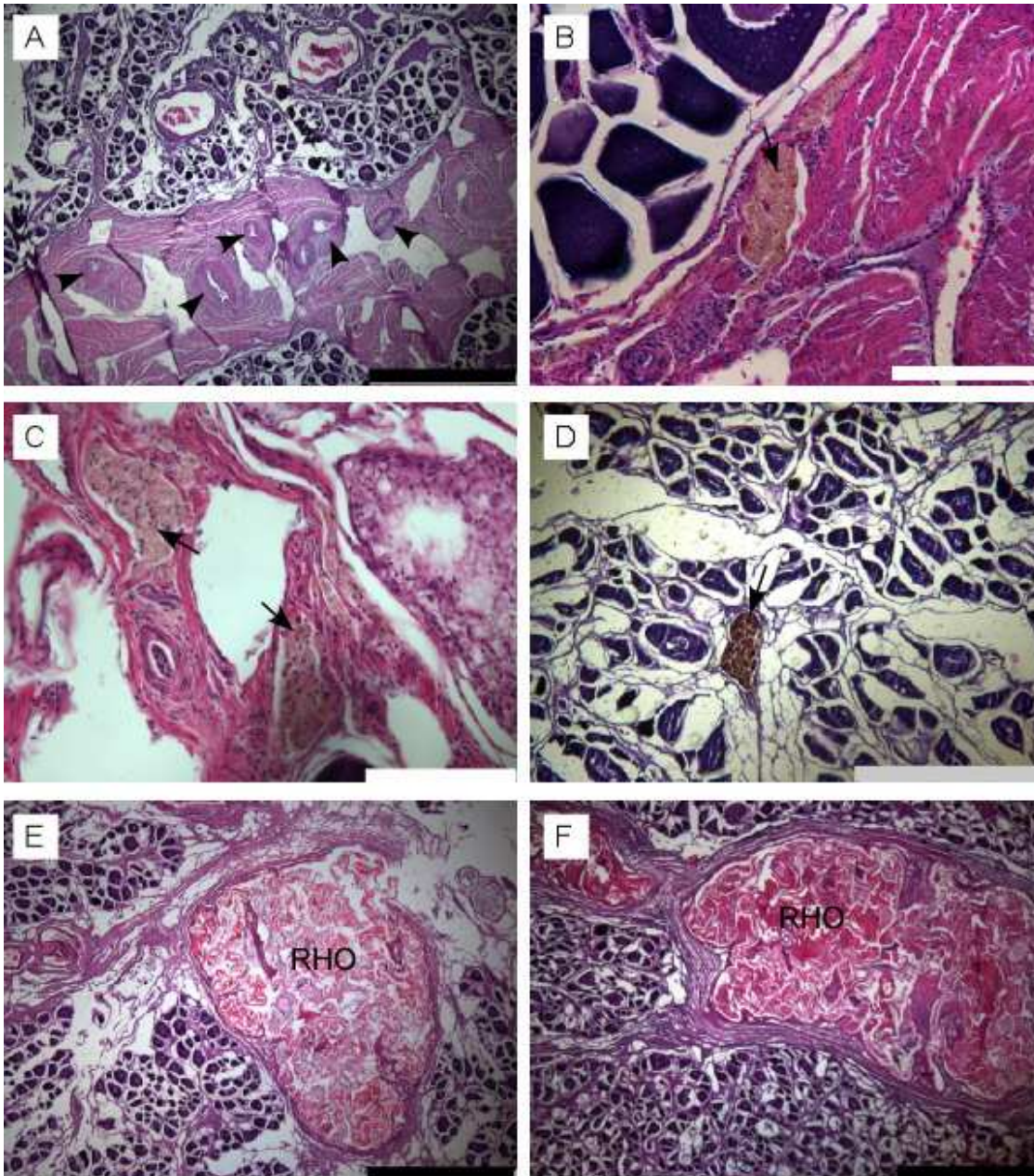


Figure 31 Histological sections of ovaries containing maturity markers considered in this study including (A) well defined muscle bundles (black arrows), (B-D) “brown bodies” (black arrows), and (E-F) clumps of residual hydrated oocytes (RHO). Black bar equals 1000 μm , grey bar equals 500 μm white bar equals 100 μm .

6.2.3 Fitting maturity curves

The proportion of mature females, p , was modelled as a function of OFL using a binomial generalized linear model with link function $g(\cdot)$:

$$g(p) = \alpha + \beta x$$

where x is either OFL in cm or age in years.

Three different link functions were tried:

1. logit: $g(p) = \log\left(\frac{p}{1-p}\right)$
2. probit: $g(p) = \Phi^{-1}(p)$ where Φ is the cumulative standard normal distribution function
3. complementary log-log: $g(p) = \log(-\log(1-p))$

The models were fit using the glm function in R (R Core Team 2013). The predict.glm function was used to obtain the fitted values on the response scale (i.e., $\hat{p} = g^{-1}(\hat{p})$), and also to estimate the standard error of the fitted values. Akaike's information criterion (AIC) (Akaike 1974) was used to select the best-fitting model. Estimates of L_{50} or A_{50} were compared between models.

In the maturity at age models, age was estimated from length using two alternative von Bertalanffy growth curves for females: one derived using age estimates from rays and one derived using age estimates from otoliths (see section 5).

6.3 Results and Discussion

6.3.1 Reproductive classification

Females were classified into reproductive phases and subphases depending on the MAGO, POFs, atresia and maturity markers present in the ovary (Table 8) using criteria similar to that developed for albacore tuna (Farley et al. 2013b). The maturity status of swordfish was determined from this classification. Ovaries containing advance yolked, migratory nucleus or hydrated oocytes and/or POFs were classed as mature, as were ovaries with unyolked or early yolked oocytes as the MAGO but with maturity markers present. Ovaries containing unyolked or early yolked oocytes as the MAGO but no POFs, atresia or maturity markers were classified as immature (Table 8).

The maturity markers considered useful for swordfish were well defined muscle bundles and numerous brown bodies. Although subjective, small muscle bundles and/or rare brown bodies in ovaries were not considered signs of previous reproductive activity as these structures also occurred in small numbers in immature ovaries. Residual yolked oocytes were also not considered to be useful maturity markers for swordfish as many relatively small fish (i.e., 42.3% of fish <125 cm OFL) contained these structures (Figure 32) but had no other maturity markers to indicate prior reproductive activity (e.g., muscle bundles or brown bodies). Some females appear to have developed a batch of hydrated oocytes but did not release the oocytes and did not contribute to egg production (e.g., Figure 32A, B). There is evidence of abortive spawning in all size classes of swordfish, as characterised by mass atresia of hydrated oocytes in the lumen. Mass atretic hydrated oocytes have also been documented in blue marlin *Makaira nigricans* (Brown-Peterson et al. 2008).

Table 8 Number of swordfish by histological classification. MAGO = most advanced group of oocytes, POF = postovulatory follicle.

MATURITY STATUS	PHASE	SUB-PHASE	MAGO AND POF STAGE	ATRESIA OF ADVANCED YOLKED OOCYTES	MATURITY MARKERS ²	COUNT
Immature	Immature		Unyolked, no POFs	Absent	Absent	279
Immature	Developing		Early yolked, no POFs	Absent	Absent	2
Mature	Spawning capable	Non-spawning	Advanced yolked, no POFs	α and β atresia may be present	Possible	36
Mature	Spawning capable	Actively spawning	Migratory nucleus or hydrated and/or POF's	α and β atresia may be present	Possible	45
Mature	Regressing		Unyolked or early yolked, no POFs	All yolked oocytes are in the α or β stages of atresia	Possible	43
Mature	Regenerating ¹		Unyolked or early yolked, no POFs	Absent	Present	280
Total						685

¹ Regenerating is equivalent to mature-resting.

² Maturity markers were well defined muscle bundles and numerous brown bodies.

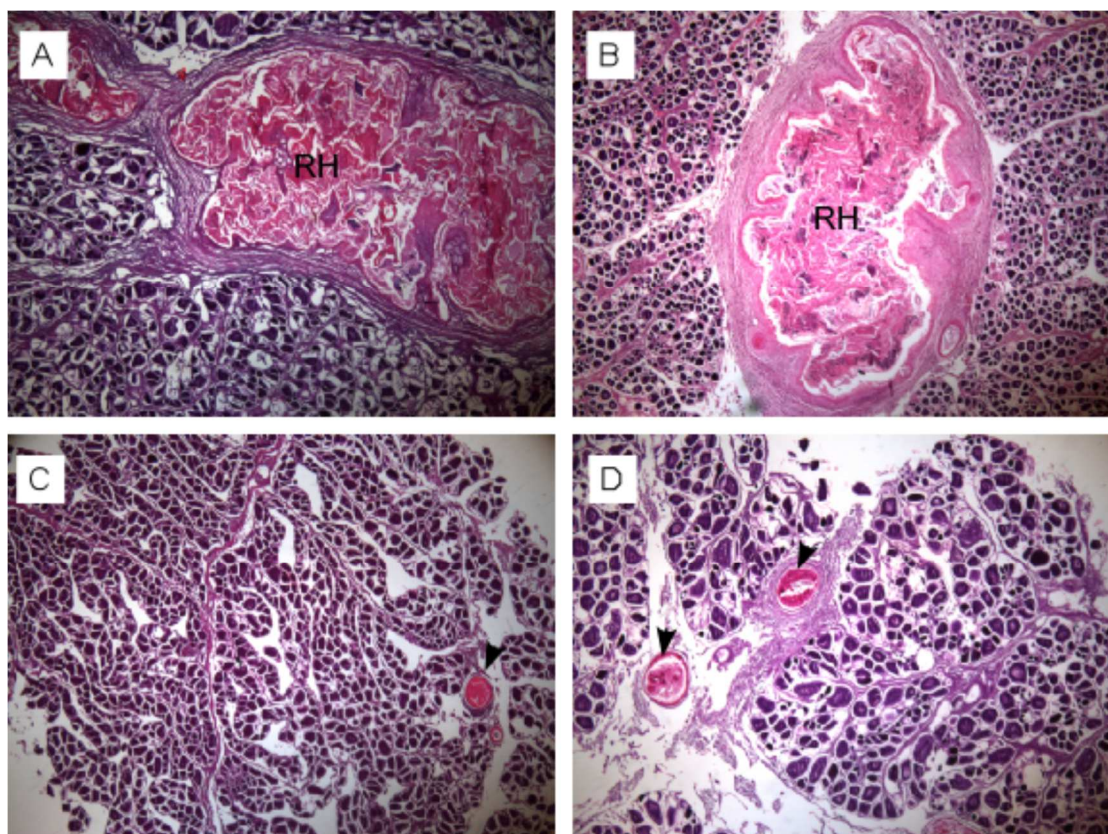


Figure 32 Examples of residual hydrated oocytes (RH, black arrows) in the ovary lumen (A, B) and connective tissue (C, D) of swordfish <125 cm OFL. A = 121 cm OFL, B = 97 cm, C = 111 cm, B = 80 cm.

Based on our classification system, female swordfish in our samples were immature (41.0%), spawning capable (11.8%), regressing (6.3%) or regenerating (40.9%) (Table 8). The relative number of immature and regenerating females combined (81.6%) was consistent with the results of Young et al. (2003) who classified 80.1% of females as immature/resting. The seasonal

spawning pattern observed was also consistent with that reported in Young et al. (2003). Spawning capable females were present from August to May, but their relative abundance peaked in December and January (Figure 33). Regressed females increased in relative abundance from November until April as females completed spawning, and then declined from May to October as the relative abundance of regenerating fish increased (Figure 33). As expected, GSI peaked in December and January when spawning activity was at its highest (Figure 34).

The histological classification scheme presented here is slightly different to that used by DeMartini et al. (2000). We differentiated regenerating (mature-resting) from immature females using two specific maturity markers, while DeMartini et al. (2000) used late stage atresia. This difference was necessary because the majority of ovary material analysed was frozen before being fixed in formalin, resulting in poorer quality histological sections. As noted in section 4, it was agreed that the histological classification system used in this study was appropriate and was successfully identifying mature and immature female swordfish.

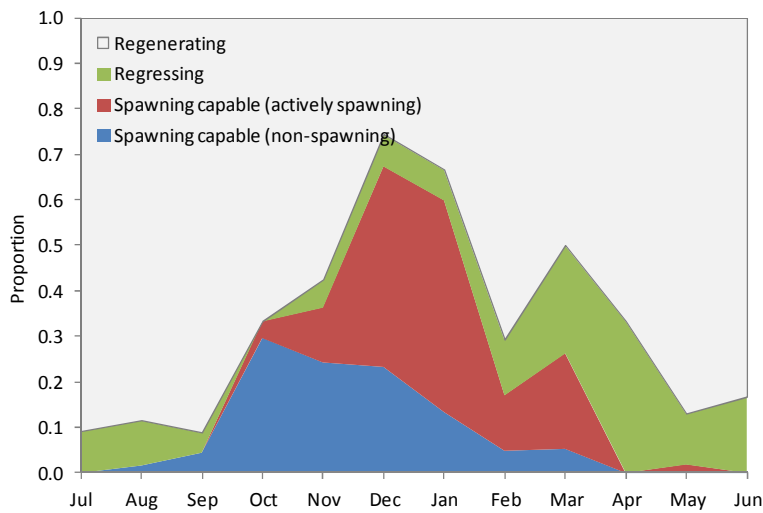


Figure 33 Proportion of mature female swordfish by reproductive phases sampled by month (n=432).

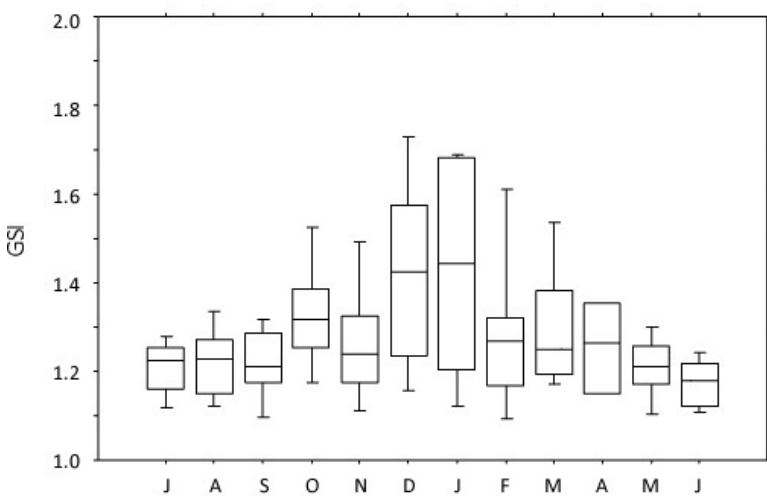


Figure 34 Box plot of gonadosomatic index (GSI) by month for female swordfish. The horizontal line through a box indicates the median, the length of a box represents the inter-quartile range, and the vertical lines extend to the 10th and 90th percentiles.

6.3.2 Verifying maturity status

Distinguishing immature from mature-regenerating females is difficult for species with indeterminate annual fecundity because the spawning season is usually long and determining the reproductive history of an individual is potentially difficult (Rideout & Tomkiewicz 2011). As detailed above, we considered the occurrence of maturity markers as evidence of prior reproductive activity and sexual maturity, which permitted the identification of both immature and regenerating females in this study.

For maturity markers to be useful, however, it is important to know length of time they remain visible in ovaries. Direct validation of their duration was not possible; however, there are indirect ways to verify the classification scheme used. Firstly, regressing fish were caught almost year-round with the lowest relative abundance at the beginning of the spawning season and highest abundance immediately after the spawning season (Figure 33). This annual cycle suggest that maturity markers persist in ovaries after spawning until the at least the start of the following spawning season, and that the low number of regenerating females caught in September to December is due to fish progressing into the spawning capable phase by that time. To corroborate this, we compared maturity at length using all data and data for September to December only. The results are provided in section 6.3.3 below; the estimated L_{50} was very similar (0.8 cm difference), suggesting that the criteria for identifying mature and immature females are precise enough for year-round sampling.

A comparison of ovary weight at length by reproductive phase also suggests that the classification scheme used in the current study is appropriate (Figure 33). For example, most small females (<150 cm OFL) classed as regenerating had ovaries weighing more than those classed as immature. The smallest mature fish was 102 cm OFL (regenerating) but as total gonad weight was not available this fish does not appear in Figure 35. However, one of its ovary lobes was large, weighing 532 g, which is consistent with the fish being in a mature-regenerating phase. Immature fish of similar size (100-104 cm OFL) had a mean ovary weight of 98 g (n=9). The smallest fish classed as spawning capable was 154 cm OFL.

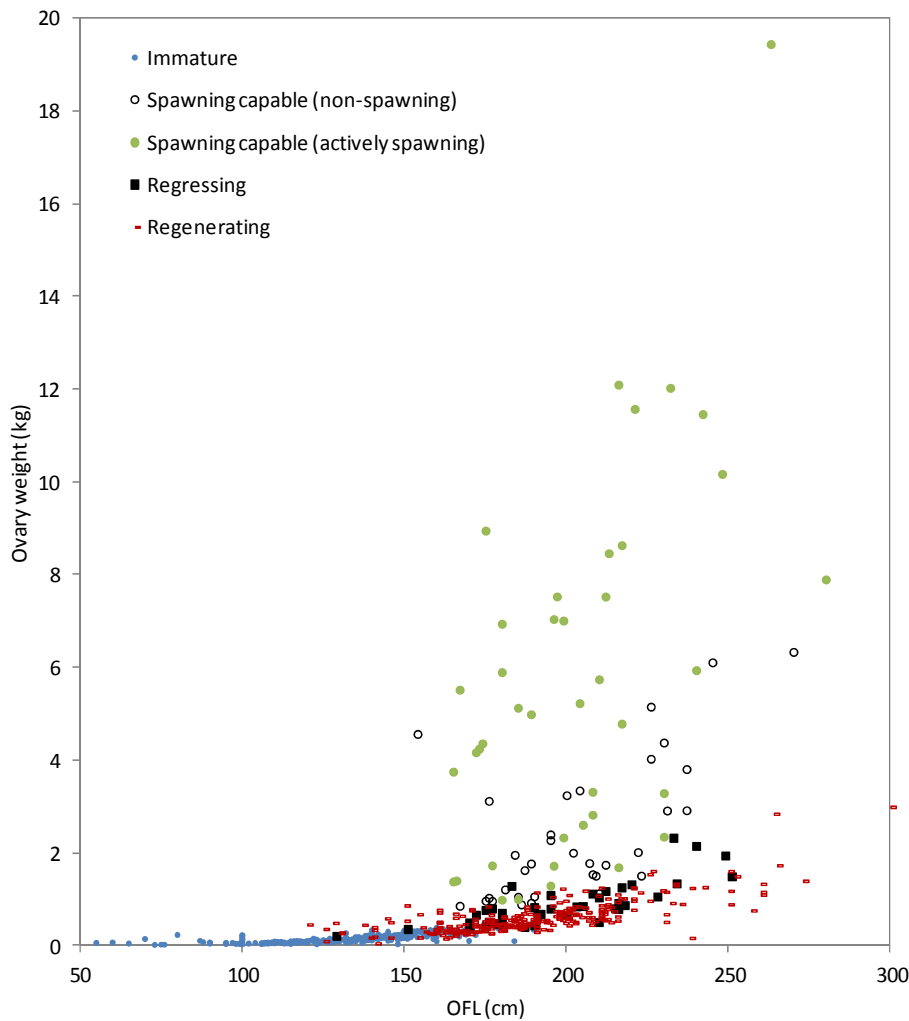


Figure 35 Observed ovary weight at orbital fork length (OFL) for female swordfish (n=656).

6.3.3 Maturity ogive estimation

Maturity at length

The model with a complementary log-log link function fit the maturity at length data best according to AIC (Table 9). Although the fitted maturity curves are similar for all three link functions (Figure 36), unlike the logit and probit, the complementary log-log function is asymmetric and therefore better able to capture the quicker transition to maturity for larger fish (150-200 cm OFL) than smaller fish (100-150 cm OFL). The estimate of L_{50} from the complementary log-log model is 161.5 cm OFL, which is over 2 cm larger than the estimates using the logit and probit links (Figure 35). The estimated proportions mature at length from the complementary log-log model have reasonably high precision (Figure 37). The approximate 95% confidence interval for the proportion mature at L_{50} (161.5 cm OFL) is 0.50 ± 0.060 .

When the data were restricted to the early part of the spawning season (September to December), the estimate of L_{50} from the best fitting model (complementary log-log) is 160.7 cm OFL, only 0.8 cm lower than when all data were analysed.

Table 9 Comparison of maturity at length model results using the logit, probit and complementary log-log (cloglog) link functions. L_{50} denotes the length at which 50% of females are estimated to be mature.

LINK	α	β	AIC	L_{50} (CM)
Logit	-16.7	0.105	370.7	159.0
Probit	-8.9	0.056	376.0	158.2
cloglog	-11.6	0.070	362.1	161.5

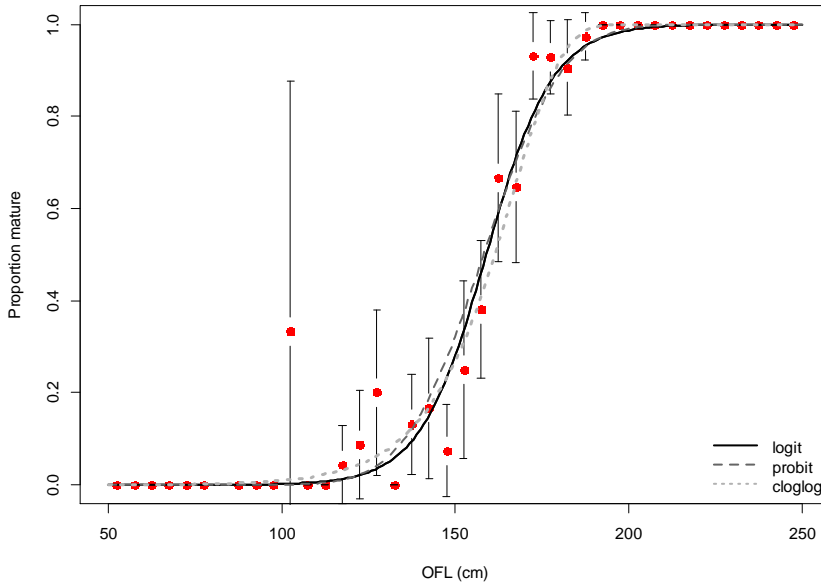


Figure 36 Comparison of maturity curves estimated using three different link functions (cloglog = complementary log-log). Also shown is the observed proportion of mature females in each 5-cm length class (filled red circles) ± 2 standard errors.

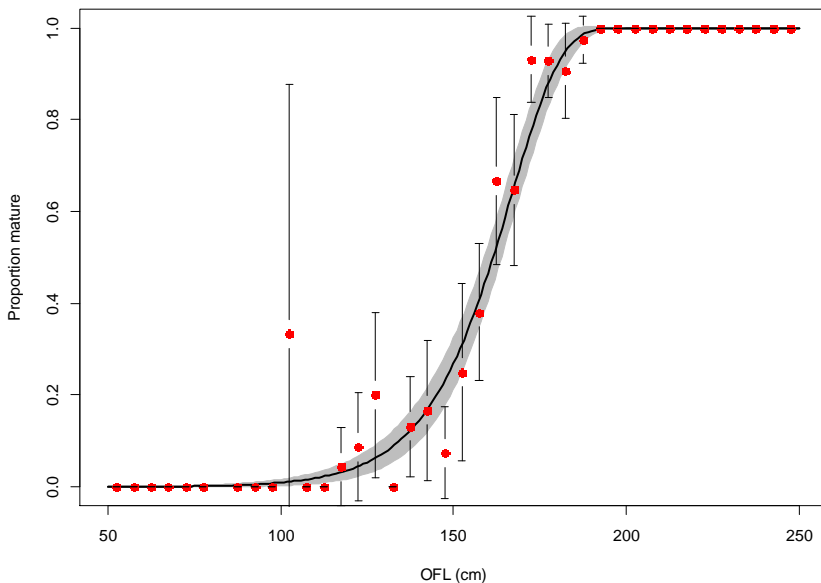


Figure 37 The fitted maturity curve from the best-fitting complementary log-log model (solid black line) with approximate 95% confidence region (grey shaded region), calculated as the estimated proportion mature ± 2 standard errors. Also shown is the observed proportion of mature females in each 5-cm length class (filled red circles) ± 2 standard errors.

Maturity at age

In the case of maturity at age, the model with a logit link function fit both the ray-based and otolith-based data best according to AIC (Table 10). As for maturity at length, the fitted maturity at age curves were very similar for all three link functions, particularly the logit and probit links, and this was true for both types of age data, so only the best fitting logit curves are shown (Figure 38 and Figure 39). The estimate of A_{50} from the logit model is 4.34 years using ray-based age data, and 4.42 years using otolith-based age data (Table 10). The approximate 95% confidence interval for the proportion mature at A_{50} is 0.50 ± 0.067 for both the ray-based and otolith-based logit models. The similarity of A_{50} estimates from ray and otolith data are not surprising given the similar growth rates obtained using these structures for females aged 0-7 years (see section 5).

Table 10 Comparison of maturity at age model results using the logit, probit and complementary log-log (cloglog) link functions. Age was estimated from length using the female VB growth curve derived from ray and otolith data.

LINK	RAY				OTOLITH			
	α	β	AIC	A_{50} (CM)	α	β	AIC	A_{50} (CM)
Logit	-6.8	1.57	363.2	4.34	-6.6	1.50	361.6	4.42
Probit	-3.7	0.86	366.8	4.31	-3.6	0.82	365.0	4.40
cloglog	-4.9	1.00	364.1	4.52	-4.7	0.94	365.8	4.62

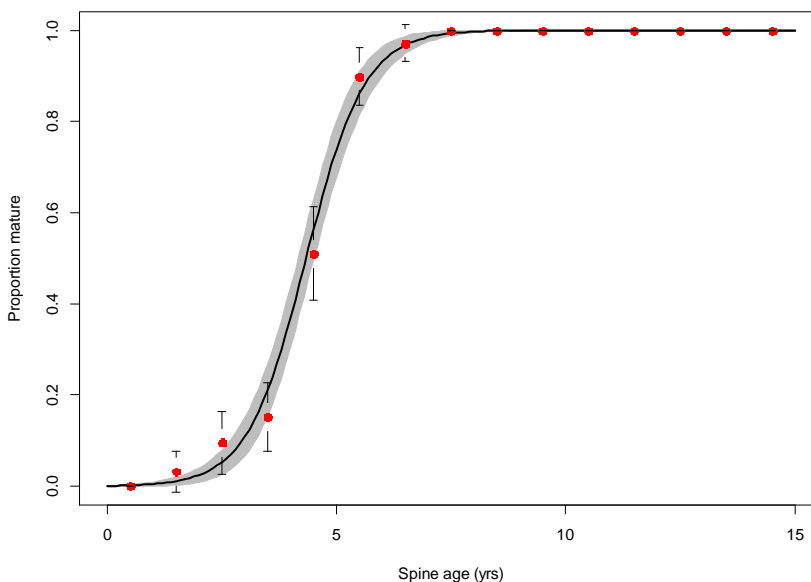


Figure 38 The fitted maturity at age curve from the best-fitting logit model (solid black line), where age was estimated from length using the female VB growth curve derived from ray (i.e., spine) data. The grey shaded region is the approximate 95% confidence region, calculated as the estimated proportion mature ± 2 standard errors. Also shown is the observed proportion of mature females in each age class (filled red circles) ± 2 standard deviations.

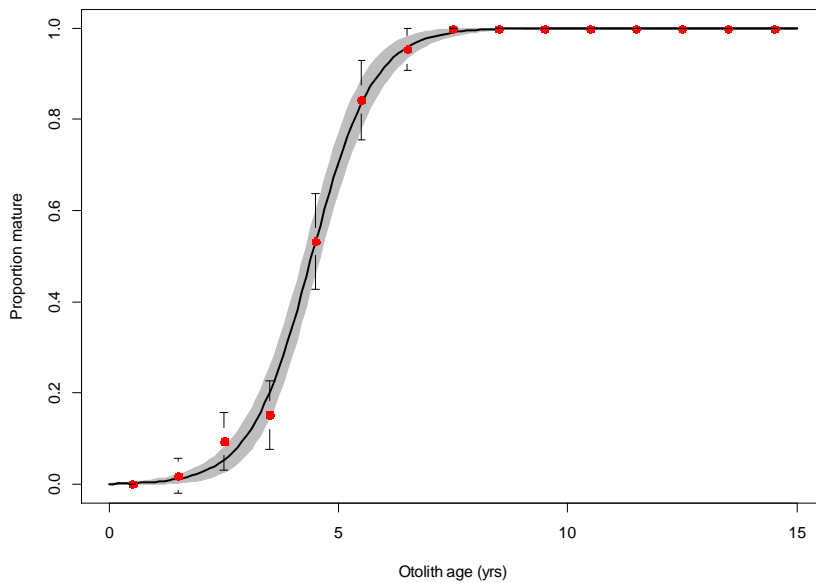


Figure 39 The fitted maturity at age curve from the best-fitting logit model (solid black line), where age was estimated from length using the female VB growth curve derived from otolith data. The grey shaded region is the approximate 95% confidence region, calculated as the estimated proportion mature ± 2 standard errors. Also shown is the observed proportion of mature females in each age class (filled red circles) ± 2 standard deviations.

Comparison with previous studies

Young et al. (2003) did not distinguish mature-resting (regenerating) from immature females noting that after spawning, females absorb all their yolked eggs and appear histologically similar to immature females. Young & Drake (2002) limited their maturity analysis to the spawning months of September to March to reduce the likelihood that regenerating females would be present. However, our results show that regenerating females are present in all months of the year, including the months of September to March (Figure 33), thus limiting the data to the spawning months was not useful. By not specifically identifying mature but regenerating females, Young & Drake (2002) overestimated L_{50} relative to the current study and that of DeMartini et al. (2000) (Table 11).

The new estimate of L_{50} for swordfish in the SW Pacific (161.5 cm OFL or 181.5 cm lower jaw fork length) is higher than obtained by DeMartini et al. (2000) and Wang et al. (2003) for fish around Hawaii and Taiwan respectively, but within the range of values for swordfish worldwide (Table 11).

Table 11 Estimated length at 50% maturity (L_{50}) for female swordfish. The estimate for the current study and DeMartini are shown in OFL and lower jaw fork length (LJFL) for comparison with other studies.

OCEAN	REGION	L_{50} (OFL CM)	L_{50} (LJFL CM)	METHOD	STUDY
Pacific	Southwest	161.5	181.5	Histology	Current study
	Southwest	193.6 – 199.8	216.6 – 222.9	Histology	Young & Drake (2002)
	Central North	143.6	161.9	Histology	DeMartini et al. (2000)
	Northwest		168.2	Histology	Wang et al. (2003)
Mediterranean	Western		142.2	Gonad index	De la Serna et al. (1996)
Atlantic	Western North		178.7	Gonad index & oocyte diameter	Arocha (1997)
	Western North		182.0	Histology	Taylor & Murphy (1992)
	Western tropical		156.0	Macroscopic & histology	Hazin et al. (2002)
	Western tropical		146.5	Macroscopic & gonad index	Mejuto & Garcia-Cortés (2014)
	South		156.0	Gonad index & oocyte diameter	Arocha (2007)
Indian	North		164.0	Macroscopic & microscopic	Varghese et al. (2013)
	Southwest		170.4	Gonad index	Poisson & Fauvel (2009)

6.4 Conclusions

Estimating a maturity schedule for swordfish is difficult as it requires precise interpretation of gonad development and maturity stages to discriminate immature (virgin) from regenerating (mature-resting) females. This study has shown that it is possible to differentiate between the two stages based on the presence of maturity markers in histological sections of ovaries. By re-classifying all female swordfish samples in the SW Pacific, we found that a large proportion of fish classified as immature by Young & Drake (2002) were in a regenerating state. The new estimate of L_{50} for females is 161.5 cm OFL, which is substantially lower than the preliminary estimate obtained by Young & Drake (2002) (193.6 to 199.8 cm OFL) but is reasonably similar to the DeMartini et al. (2000) estimate. The new estimate of age at 50% maturity swordfish in the SW Pacific is 4.34 years and 4.42 years using ray- and otolith based ages respectively.

7 Implications of new growth, maturity and natural mortality estimates for the stock assessment

7.1 Introduction

The most recent SW Pacific swordfish stock assessment is described in Davies et al. (2013). Key features include:

- Multifan-CL was used as the parameter estimation software.
- The spatial domain included the entire WCPFC convention area south of the equator.
- The model was iterated quarterly 1952-2011.
- The population was age-structured, sex-aggregated, and divided spatially with a longitudinal split in the Tasman Sea (165°E). A single spawning stock was assumed.
- Fourteen fisheries were defined, partitioned by gear, nation, the east-west population boundaries and additional northern, central and southern regions.
- The model was fit to observations of total catch, standardized catch rates and size composition with a negative-log-likelihood-based objective function that also includes priors and penalties.
- Key estimated parameters included virgin recruitment, stationary selectivity, stationary catchability (for fleets with informative CPUE series) and annual region-specific recruitment deviations.
- Fixed inputs included movement rates (derived from external analyses), Beverton-Holt stock recruit relationship, growth, maturity, and natural mortality.
- Detailed results were presented for a reference case, while stock status inferences were synthesized across a range of 561 model specifications (15 additional models failed to converge to plausible results). These models included different combinations of assumptions across 5 main uncertainty axes, including:
 - 8 combinations of growth, maturity and natural mortality (M)
 - 3 stock recruit steepness options
 - 4 movement rates
 - 3 CPUE options
 - 2 size data weighting options
- Stock status reference points were generally optimistic ($B_{current}/B_{MSY} > 1.0$; $F_{current}/F_{MSY} < 1.0$) with the fast growth, high M , early maturity life history combinations, while the slow

growth, low M , late maturity assumptions were more likely to estimate recent over-exploitation ($F_{current}/F_{MSY} > 1.0$).

In this section we evaluate the stock assessment implications of the new growth and maturity estimates in relation to a small subset of the configurations used in the 2013 assessment. The results are indicative of how the last assessment would have been affected by the new biological parameters, however, we emphasize that this is a simple substitution analysis that does not constitute a revised assessment (i.e., model diagnostics were not examined, except for the overall objective function value and maximum gradient at the minimum).

7.2 Methods

The 2013 assessment data, configuration files, bash script and Multifan-CL software (64-bit windows executable released March 2013) were obtained from the authors. We refit the reference case model to confirm that the specification was correct. Results were extremely similar, but not identical. It remains unclear whether the minor discrepancy is related to the convergence criteria (maximum iteration setting), operating system (windows vs linux, 32 bit vs 64 bit), software version or something else. However, it appears that the discrepancy is trivial in terms of the stock status inferences, and the results of these sensitivity tests should be strongly indicative of differences due to the alternative life history assumptions.

The 2013 assessment used a sex-aggregated configuration, with the length-at-age relationship derived from the mean of male and female growth curves, assuming that the combined relationship would be approximately normally-distributed with the variance on length-at-age estimated to encompass both sexes. The orbital fork length (OFL) units, used elsewhere in this report, were converted to lower jaw fork length (LJFL) units to be consistent with the assessment via the relationship used in Davies et al. (2013): $LJFL = 1.0753(OFL + 6.898)$. Multifan-CL parameterizes the von Bertalanffy growth curve in terms of the length of the youngest and oldest ages (provided in Table 12). Figure 40A compares the mean sex-aggregated LJFL growth curves derived from this study with those used in the 2013 assessment.

The standard deviations (SDs) of the sex-aggregated length-at-age relationships were calculated to be larger than the SDs of the sex-specific relationships, with a substantial increase with age (as expected, given that the sexes diverge). Figure 41 illustrates age-specific length distributions from the dimorphic otolith-based growth curves (equal numbers of males and females), and from a sex-aggregated curve (representing the mean of males and females and the variance of the pooled distribution). The distributions are very similar at age 5, begin to diverge appreciably by age 10, and the bimodal distribution evident by age 15 is poorly described.

The reference case assessment model specification had an upper bound on the estimated SD of length-at-age of 20cm (and converged to the bound). This bound is probably reasonable for ages up to ~10, but low for older ages. However, for this sensitivity test, we retained the original SD parameter specifications noting that there are measures taken to ensure that the size composition data are not overly influential in the assessment (e.g., the assumed effective sample sizes are generally much smaller than the real values, the normal distribution is heavy-tailed relative to the bimodal distribution (Figure 41), and the size composition likelihood term is designed to be robust to outliers). The question of how best to represent length-at-age variance is beyond the scope of

this study. A simple option would be to retain the sex aggregation, but aggregate a large “plus”-bin to encompass the ages where sexes are strongly divergent. This should remove biases due to the compromise representation of sex dimorphism, but discards information about older ages. Alternatively, disaggregating the sexes within the model has obvious potential to extract information from older ages and reduce biases in catch-at-length fitting due to sex-dimorphism. However, without additional knowledge about sex-specific M and selectivity, it is not certain that the latter approach would improve the assessment. For this study, we are only attempting to examine alternative biological assumptions, not restructure the whole assessment.

The maturity estimates from the 2013 assessment and this study are compared in Figure 40B. We adopted the *logit* option for both the otolith-based and ray-based maturity estimates for the assessment modelling exercise. The new estimates are negligibly different from one another, very similar to the Hawaiian estimates used in 2013 from DeMartini et al. (2007), and much younger than the Australian estimates used in 2013 from Young & Drake (2002).

While this project focuses on assessment uncertainties related to growth and maturity, it is important to note that natural mortality (M) assumptions are also uncertain and were directly linked to the growth and maturity assumptions. The M assumptions in Davies et al. (2013, adopted from Kolody et al. 2008) attempted to represent substantial uncertainty in terms of both the magnitude of M , and the functional form of M by age. A total of 8 M vectors were considered equally plausible in the assessment uncertainty grid (Figure 42), however, the M vectors were specific to the growth/maturity assumptions, with the two sets of growth/maturity representing two very different life histories. Eight analogous M vectors, corresponding to the otolith-based and ray-based growth curves from this study are also presented in Figure 42 (four for each of the otolith-based and ray-based growth curves). The vectors of M at age (a) are derived from the same ad hoc approach:

$$M'_a = 0.1 + \left(\frac{L_\infty}{L_a}\right)^\alpha + \beta(\text{Maturity}_a), \text{ and}$$

$$M_a = \left(\frac{M'_a}{\sum_1^{15} M'_a}\right) \cdot f(L_\infty, K, T)$$

where:

L_∞, K = von Bertalanffy growth parameters for the sex-aggregated, LJFL growth curve (parameterized in the classical way),

α = a length-based effect, estimated such that $\max(M_a) / \min(M_a) = 1.5$ for $1 \leq a \leq 15$.

β = a spawning-related effect (0 or 1), and

$$f(L_\infty, K, T) = \exp(-0.0066 - 0.279 \log(L_\infty) + 0.6543 \log(K) + 0.4634 * \log(T))$$

is the relationship from the Pauly (1980) meta-analysis describing M as a function of temperature preferences (T) and growth-related parameters. In this case, the upper and lower temperature preferences (14.57, 22.83°C) reported for swordfish in Boyce et al. (2008) were adopted as the basis for the high (H, HS), and low (L, LS) M vectors. The four different M vectors are summarized in Table 13. There is no claim either here or in the assessment that this is a particularly good approach for representing M , but it at least attempts to admit several features commonly assumed for M in tuna and tuna-like species, i.e., i) M is likely size-dependent within a species, ii) spawning-related stress may increase M , iii) larger species tend to live longer than smaller species,

iv) species located in colder waters tend to live longer than those in warmer water, and v) M is highly uncertain for most tuna and billfish species. One obvious and dubious feature in the approach above is the low M for young ages in the spawning-related mortality scenarios (HS, LS) for all life histories except for the Australian estimates derived from Young & Drake (2002; 2004) (slow growth, late maturity) (for which it was originally derived).

Other than growth, maturity and M , all of the other assessment assumptions were identical to the reference case model (GHMHS; fast growth, 4+ maturity, relatively high M with spawning effect) from the 2013 assessment. This includes the 5 other elements of the uncertainty grid (i.e., stock recruit steepness, movement rate, CPUE series and relative weighting of the size composition data; see Davies et al. 2013).

Table 14 describes the growth, maturity and M assumptions and key stock assessment model outputs from two contrasting models from the 2013 assessment, two corresponding sets of model results that would have been obtained if the growth, maturity and M options had been replaced by the otolith- or ray-derived results of this study, 6 additional models that recombine the 2013 assessment assumptions (in unrealistic ways) to explore the relative importance of the three life history parameters, and 6 additional models that examine the effects of the alternative M assumptions in relation to the new growth and maturity estimates.

Table 12 Multifan-CL growth parameters for the sex-aggregated growth curves derived from this study.

GROWTH CURVE	$L_{0=0}$	$L_{0=19}$	K
Otolith-based	86.1	238.9	0.186
Ray-based	87.2	259.9	0.152

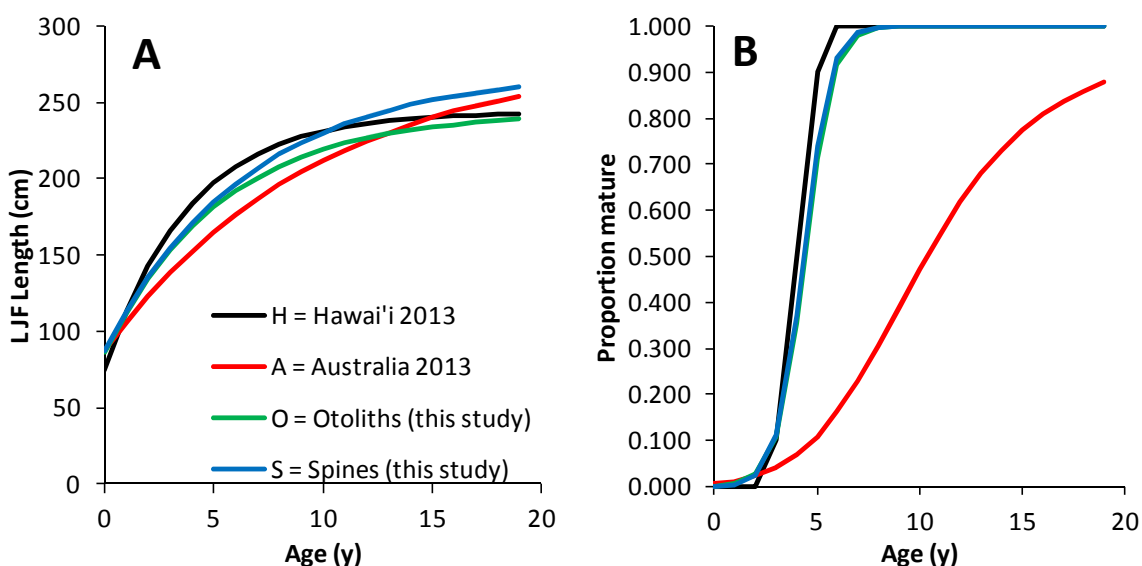


Figure 40 Sex-aggregated growth curves (A) and female maturity ogives (B) used in the Davies et al. (2013) assessment, and the otolith-derived and spine-derived age estimates from this study, used for evaluating stock assessment implications. Note that the term spine is used here rather than ray.

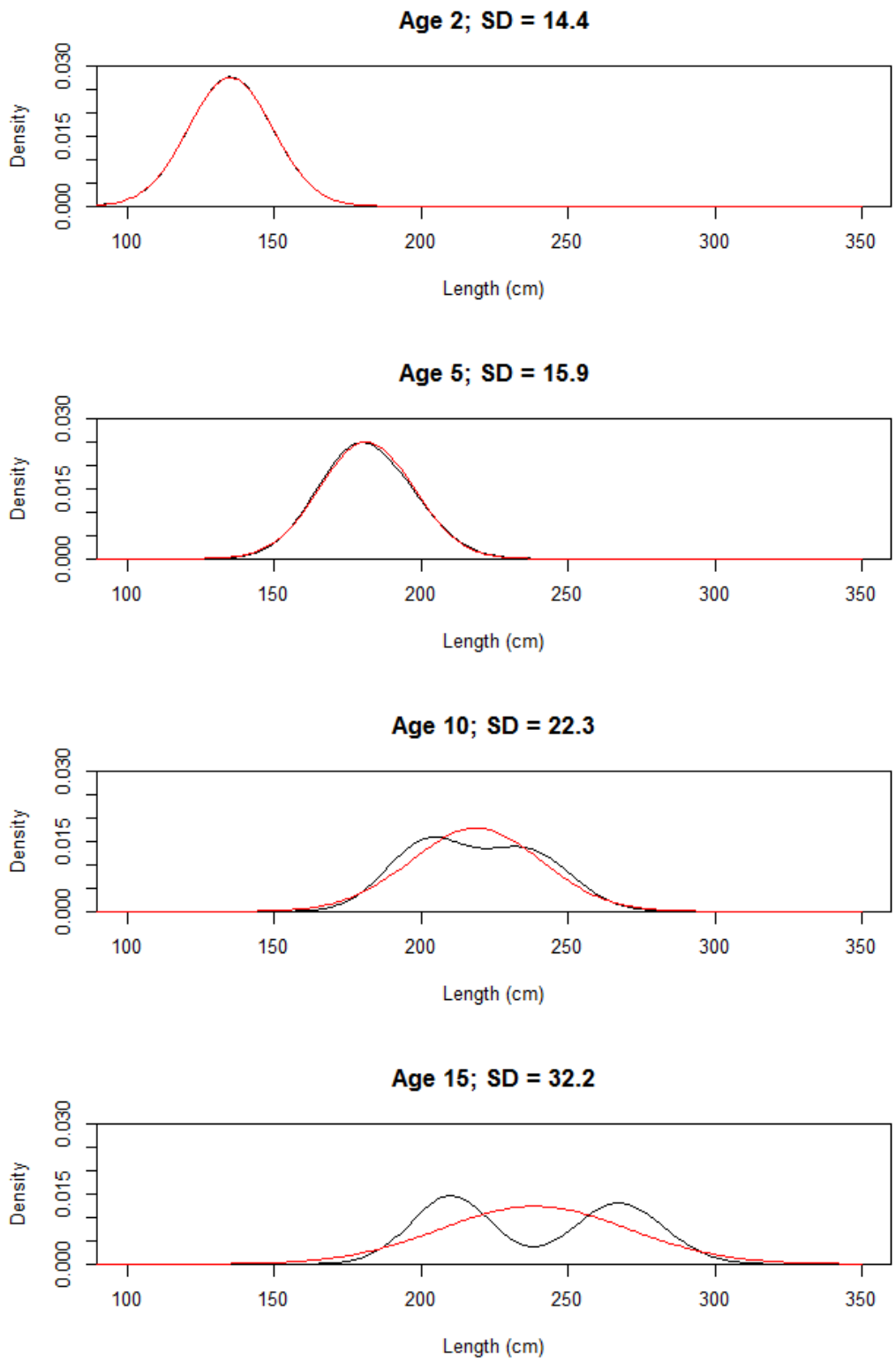


Figure 41 Comparison of age-specific length frequency distributions assuming equal numbers of males and females using the otolith-based LJFL growth curves from this study (black line), and the combined sex-aggregated approach (red line). The indicated SD applies to both distributions within each age class.

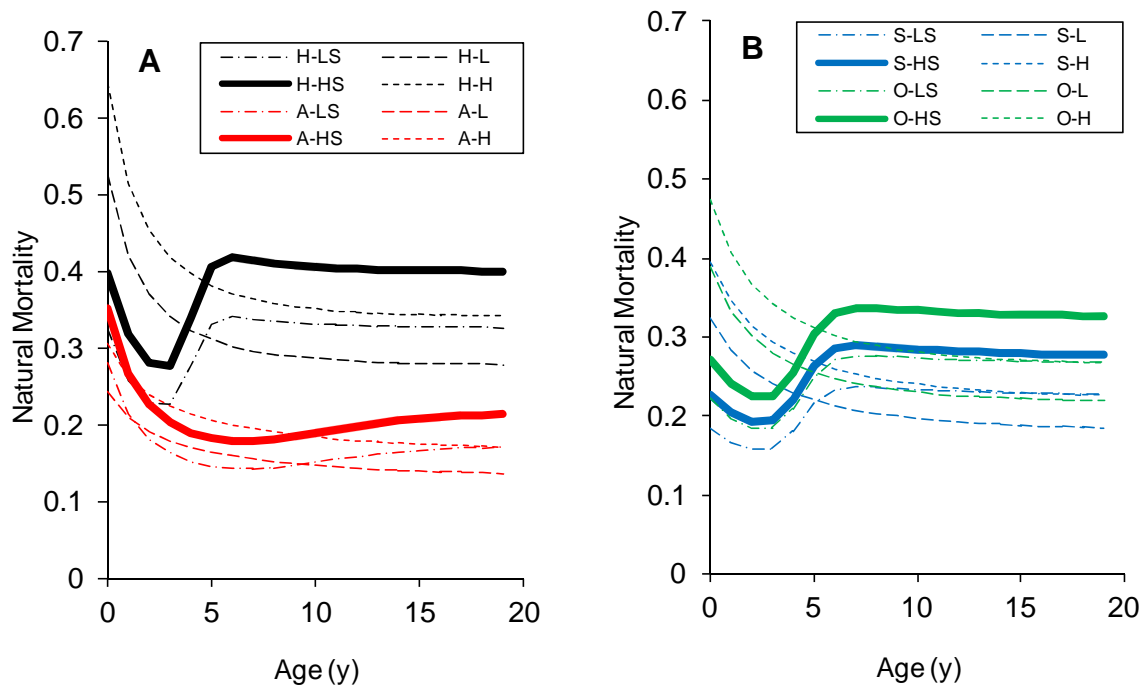


Figure 42 The eight natural mortality (M) vectors explored in the Davies et al. (2013) assessment (A) and analogous M vectors derived from otolith-based and spine-based growth/maturity estimates from this study (B). Scenario H-HS represents the reference case mortality assumption from the 2013 assessment (relatively high M , with a spawning-related component, derived for the Hawaiian growth and maturity estimates from DeMartini et al (2000; 2007), referred to as GHMHS in Davies et al. 2013); A-HS is the analogous model from the 2013 assessment based on the Australian growth and maturity estimates from Young & Drake (2002; 2004) (GAMHS in Davies et al. 2013); S-HS (spine-based) and O-HS (otolith-based) represent the analogous M assumptions derived from this study. M abbreviations are explained in Table 13 and Table 14. Note that the term spine is used here rather than ray.

Table 13 *M* vectors (instantaneous annual) analogous to those used in 2008 and 2013 assessments, derived from the otolith-based and spine-based growth and maturity estimates in this study (shown in Figure 42). Note that the term spine is used here rather than ray.

<i>M</i> LABEL	S-LS	S-L	S-HS	S-H	O-LS	O-L	O-HS	O-H
Ageing method	Spines	Spines	Spines	Spines	Otoliths	Otoliths	Otoliths	Otoliths
Temp. preference	Lower	Lower	Higher	Higher	Lower	Lower	Lower	Higher
Spawning effect	Yes	No	Yes	No	Yes	No	Yes	No
Age	<i>M</i>							
0	0.184	0.324	0.226	0.395	0.222	0.388	0.271	0.474
1	0.166	0.283	0.204	0.346	0.197	0.333	0.241	0.407
2	0.157	0.258	0.193	0.315	0.185	0.301	0.225	0.367
3	0.159	0.241	0.194	0.294	0.185	0.280	0.226	0.342
4	0.181	0.229	0.222	0.280	0.209	0.266	0.255	0.324
5	0.217	0.220	0.264	0.269	0.249	0.255	0.304	0.312
6	0.234	0.213	0.285	0.260	0.271	0.248	0.331	0.302
7	0.237	0.208	0.289	0.253	0.277	0.242	0.337	0.295
8	0.236	0.203	0.288	0.248	0.276	0.237	0.337	0.289
9	0.235	0.200	0.286	0.244	0.275	0.233	0.335	0.285
10	0.233	0.197	0.284	0.240	0.273	0.230	0.333	0.281
11	0.232	0.195	0.283	0.237	0.272	0.228	0.332	0.278
12	0.231	0.193	0.282	0.235	0.271	0.226	0.331	0.276
13	0.231	0.191	0.281	0.233	0.270	0.224	0.330	0.274
14	0.230	0.190	0.280	0.231	0.270	0.223	0.329	0.272
15	0.229	0.188	0.279	0.230	0.269	0.222	0.328	0.271
16	0.229	0.187	0.279	0.229	0.269	0.221	0.328	0.270
17	0.228	0.187	0.278	0.228	0.268	0.221	0.327	0.269
18	0.228	0.186	0.278	0.227	0.268	0.220	0.327	0.269
19	0.228	0.185	0.277	0.226	0.268	0.220	0.327	0.268

Table 14 Suite of MFCL assessment models exploring the implications of a range of growth, maturity and *M* assumptions, including the reference case model defined in Davies et al. (2013) with Hawaiian-based life history assumptions from DeMartini et al. (2000; 2007), the analogous model with the Australian life history assumptions from Young & Drake (2002; 2004), analogous models with the new otolith-based and spine-based growth and maturity estimates from this study (3-4), intermediate model configurations that partition the relative effects of growth, maturity and *M* from the 2013 assessment (models 5-10), and a suite of models using the growth and maturity estimates from this study and spanning the range of *M* uncertainty from the assessment (i.e., using *M* vectors analogous to those used in the assessment, but derived for the growth and maturity estimates from this study) (models 11-16). Assessment assumptions other than growth, maturity and *M* correspond to the reference case from the 2013 assessment. A = Australian studies (Young & Drake 2002, 2004), H = Hawaiian studies (DeMartini et al. 2000, 2007), O = this study Otoliths, S = this study Spines; *M* definitions are explained in the text and shown in Figure 42. Note that the term spine is used here rather than ray.

MODEL NUMBER AND LABEL	GROWTH	MATURITY	<i>M</i>	NOTES
1. HHH-HS	H	H	H-HS	Reference case from the 2013 assessment, including the Hawaiian life history assumptions (labelled GHMHS in the assessment).
2. AAA-HS	A	A	A-HS	2013 assessment model analogous to the reference case, except with Australian life history assumptions (labelled GAMHS in the assessment)
3. OOO-HS	O	O	O-HS	New model, analogous to the reference case, with otolith-derived life history assumptions from this study
4. SSS-HS	S	S	S-HS	New model, analogous to the reference case, with spine-derived life history assumptions from this study
5. HHA-HS	H	H	A-HS	Suite of models combining 2013 growth, maturity and <i>M</i> in different (and NOT recommended) ways, to partition relative effects of the three assumptions.
6. HAH-HS	H	A	H-HS	
7. AHH-HS	A	H	H-HS	
8. HAA-HS	H	A	A-HS	
9. AHA-HS	A	H	A-HS	
10. AAH-HS	A	A	H-HS	
11. OOO-H	O	O	O-H	Suite of models based on the otolith-based and spine-based growth and maturity estimates from this study, combined with different <i>M</i> vectors analogous to the range represented in the 2013 assessment
12. OOO-LS	O	O	O-LS	
13. OOO-L	O	O	O-L	
14. SSS-H	S	S	S-H	
15. SSS-LS	S	S	S-LS	
16. SSS-L	S	S	S-L	

7.3 Results and Discussion

Table 15 lists key model summary statistics for the 16 assessment models defined in Table 14, from which we note the following:

- All of the models appeared to converge acceptably (model 7 is probably marginal, but the estimates are qualitatively consistent with what we would expect on the basis of the other models).

- In comparing the 2013 growth and maturity assumptions with this study (for the HS M assumptions) (models 1-4), the stock status uncertainty does not appear to be meaningfully reduced. As further emphasized in Figure 43, the new otolith-based growth/maturity yields SSB/SSB_{MSY} and F/F_{MSY} estimates very similar to those of the 2013 Hawaiian life history assumptions from DeMartini et al. (2000; 2007), while the new ray-based stock status estimates are very similar to the 2013 Australian life history assumptions from Young & Drake (2002 2004). This is a curious result given that the new growth estimates (and M assumptions) are more similar to each other (at least to age 8 for growth), and intermediate to the HHH-HS and AAA-HS models from 2013. Assessment dynamics can be strongly influenced by uncertain growth at older ages (e.g., see Kolody et al. 2015), which might be the key point of similarity between the old and new assumptions. Alternatively, the similarity may be largely a coincidence, such that the old and new life history assumptions might have divergent stock status implications as data accumulate in future assessments.
- The results from models 1-2 and 5-10 attempt to partition how the Hawaiian and Australian life history assumptions from 2013 interact to produce the stock status uncertainty observed in the assessment. This is emphasized in Figure 44, which suggests that i) maturity has a lower effect on stock status than growth and M , and ii) the mixed (and probably unrealistic) combinations of growth and M result in considerably more extreme levels of stock status uncertainty. Australian growth combined with Hawaiian M yields the most optimistic outcome, while Hawaiian growth with Australian M is the most pessimistic. The pessimistic combinations also represent the best overall fit to the objective function.
- Models 5 and 8 represent the best fit in terms of the objective function. However, since these models both represent an internally inconsistent mix of Hawaiian and Australian life history characteristics, we do not consider them to be realistic. However, they do illustrate the risk of interpreting these sorts of model likelihoods too literally (i.e., for model selection purposes). Presumably the model likelihood is deceptive because of structural problems, e.g., failure to recognize sex dimorphism, non-homogeneous fishery definitions leading to non-stationary selectivity, biased sampling, etc.
- Comparison of stock status from models 3-4, 11-16 (shown in Figure 45) show the stock status uncertainty corresponding to the new otolith-based and ray-based growth and maturity, combined with the eight M assumptions of Table 13 (four for each of the new age estimation methods conditional on all other reference case assumptions). These results indicate that the reference case M assumptions (HS) are the most optimistic of the M assumptions. Furthermore, in terms of relative order, the ray-based growth and maturity estimates are all more pessimistic than the otolith-based estimates, irrespective of M . All of the new ray-based models suggest $F/F_{MSY} > 1.0$ for several recent years. One of the otolith-based models (OOO-LS) is almost as pessimistic as the most optimistic ray-based model.

7.4 Conclusions

This study has provided increased confidence in the swordfish growth and maturity estimates for (at least the western part of) the SW Pacific stock assessment region. However, it appears that considerable stock status uncertainty remains in relation to the choice of age estimation method, and M assumptions. Only a subset of eight models analogous to the 2013 assessment are

presented for the new life history parameters, but as shown in Figure 45 five of these models (all ray-based and one otolith-based scenario) suggest that overfishing has occurred in at least some recent years ($F > F_{MSY}$). We are inclined to weight the reliability of the otolith estimates higher than the ray-based estimates for the reasons discussed in section 5. However, in the absence of direct validation studies and a broad consensus within the swordfish ageing community, it might be premature to entirely dismiss ray-based estimates.

Table 15 Convergence and stock status statistics from the suite of MFCL assessment defined in Table 14. The negative log-likelihood-based objective function has been rescaled relative to the lowest (best fit) value. A = Australian studies (Young & Drake 2002, 2004), H = Hawaiian studies (DeMartini et al. 2000, 2007), O = this study Otoliths, S = this study Ray/Spines; M definitions are described in the text and shown in Figure 42.

MODEL NUMBER AND NAME	GROWTH	MATURITY	M	OBJECTIVE FUNCTION	MAX. GRADIENT	SSB_{2011}/SSB_{MSY}	SSB_{2011}/SSB_{1952}	F_{2011}/F_{MSY}
1. HHH-HS	H	H	H-HS	42.444	0.298	1.881	0.459	0.617
2. AAA-HS	A	A	A-HS	20.192	0.063	1.226	0.273	1.179
3. OOO-HS	O	O	O-HS	50.418	0.002	1.937	0.456	0.526
4. SSS-HS	S	S	S-HS	26.053	0.001	1.427	0.397	0.994
5. HHA-HS	H	H	A-HS	0.017	0.482	0.836	0.241	1.599
6. HAH-HS	H	A	H-HS	42.411	0.319	1.958	0.425	0.664
7. AHH-HS	A	H	H-HS	26.838	1.855	2.564	0.572	0.278
8. HAA-HS	H	A	A-HS	0.000	0.407	0.767	0.189	1.848
9. AHA-HS	A	H	A-HS	20.167	0.107	1.273	0.334	0.995
10. AAH-HS	A	A	H-HS	43.798	0.869	2.993	0.549	0.257
11. OOO-H	O	O	O-H	47.229	0.203	2.012	0.435	0.525
12. OOO-LS	O	O	O-LS	25.132	0.001	1.536	0.415	0.908
13. OOO-L	O	O	O-L	43.441	0.136	1.608	0.371	0.734
14. SSS-H	S	S	S-H	16.183	0.001	1.463	0.365	0.959
15. SSS-LS	S	S	S-LS	17.696	0.001	1.237	0.360	1.180
16. SSS-L	S	S	S-L	14.811	0.001	1.168	0.312	1.233

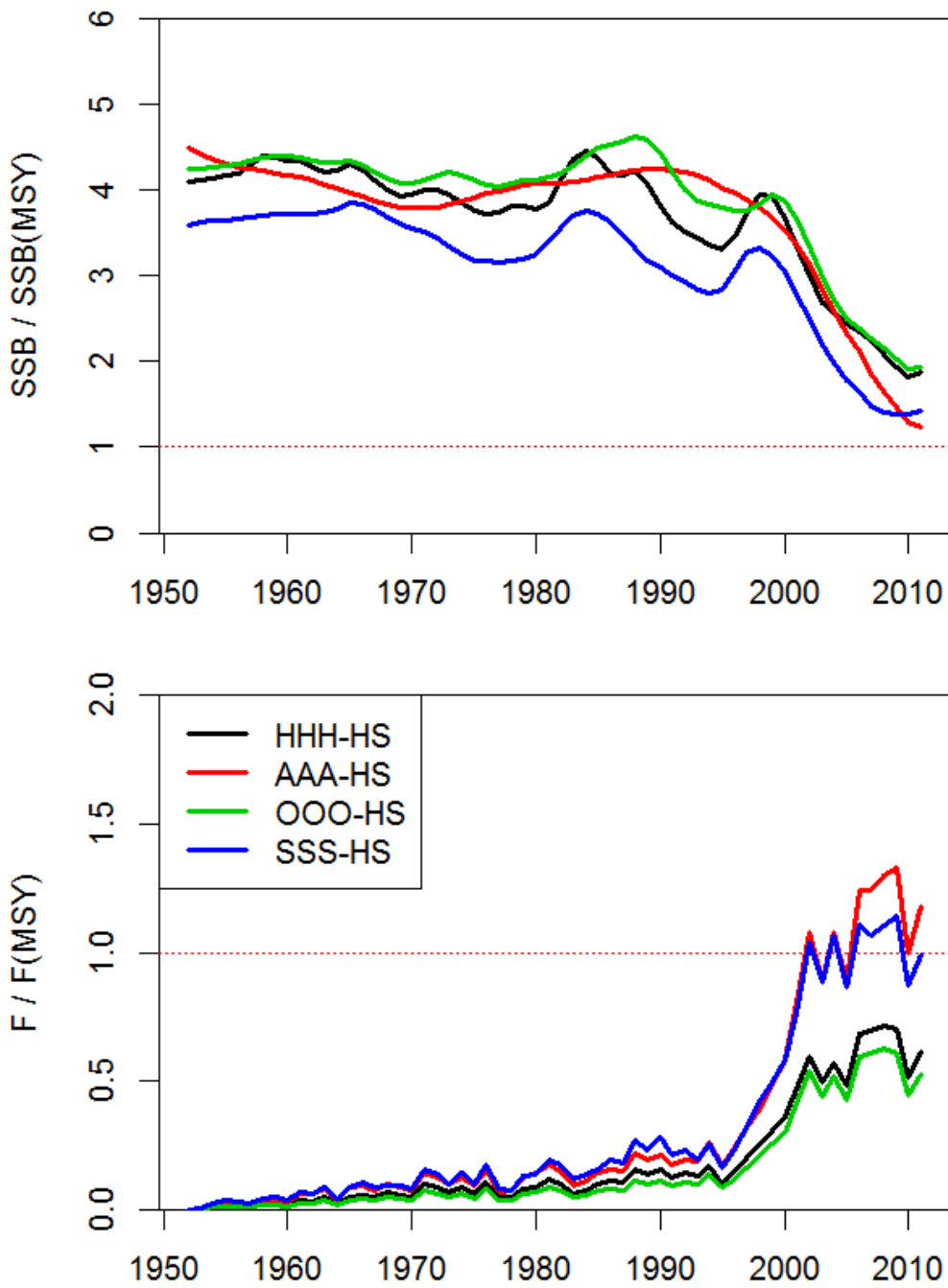


Figure 43 Time series of estimated stock status reference points for the Davies et al. (2013) reference model (derived from the Hawaiian life history parameters HHH-HS), and the analogous models (in terms of M) derived from the Australian life history parameters in 2013 (AAA-HS), the otolith-based (OOO-HS) parameters from this study, and the ray/spine-based (SSS-HS) parameters from this study. Model abbreviations are explained in Table 13 and Table 14.

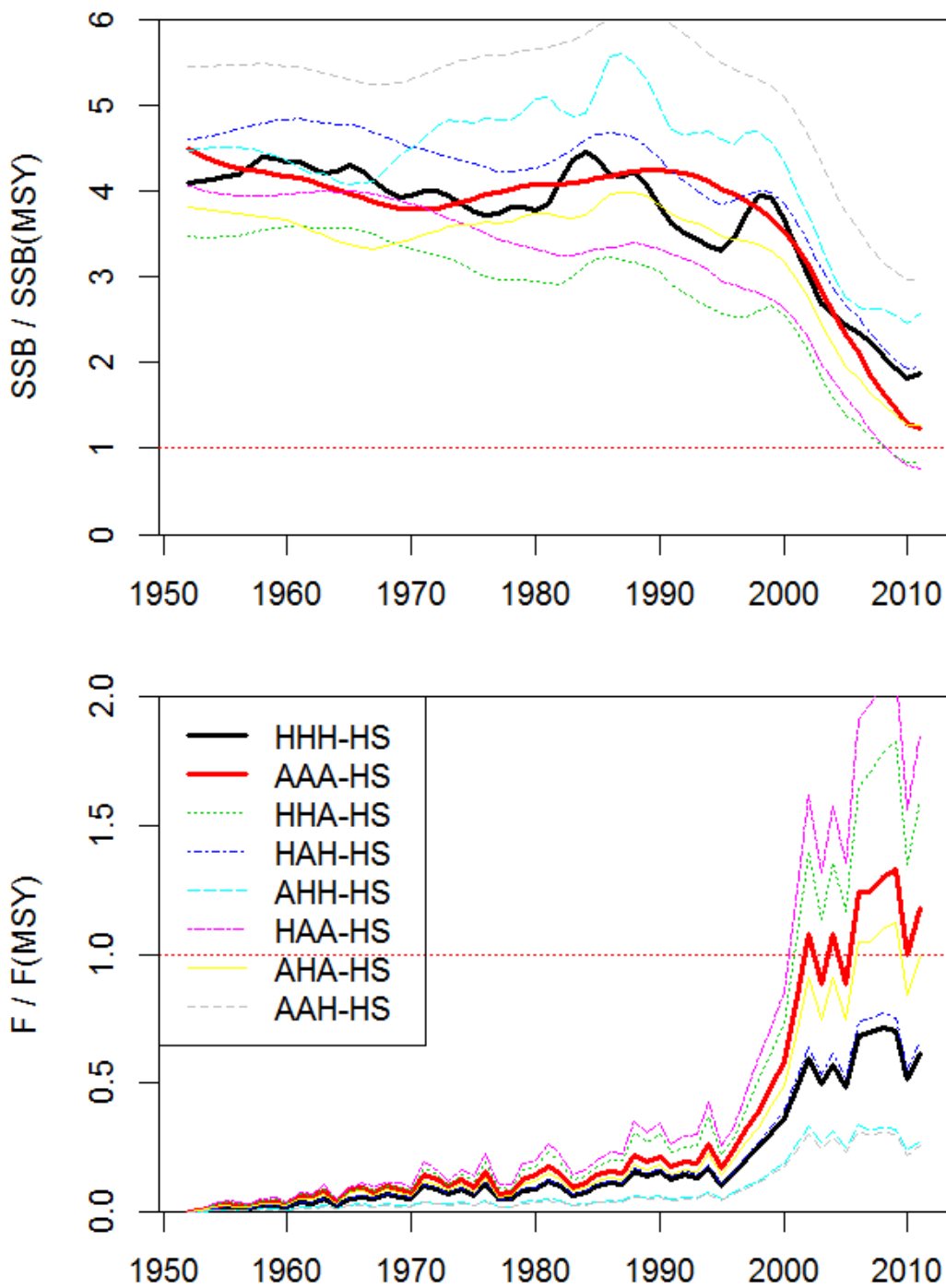


Figure 44 Time series of estimated stock status reference points for the Davies et al. (2013) reference model (derived from the Hawaiian life history parameters HHH-HS), and the analogous models (in terms of M) derived from the Australian life history parameters in 2013 (AAA-HS), and mixed combinations of Australian and Hawaiian life history parameters from the 2013 assessment. The mixed combinations are not considered realistic, but provide insight into the relative importance of growth, maturity and M . Model abbreviations are explained in Table 13 and Table 14.

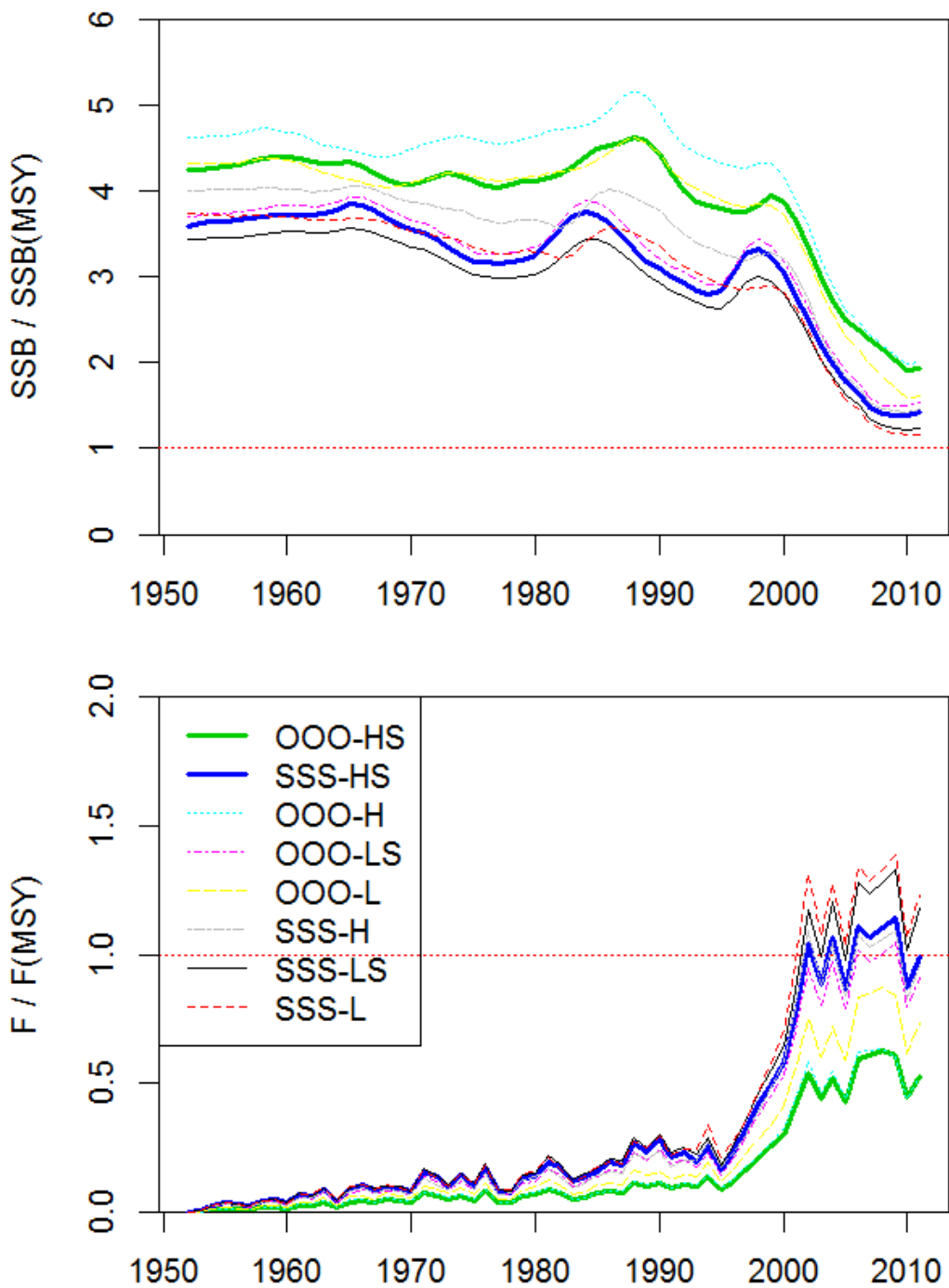


Figure 45 Time series of estimated stock status reference points for a range of models using the otolith-based and ray/spine-based growth and maturity estimates from this study, combined with the full range of M assumptions analogous to the assessment uncertainty grid from Davies et al. (2013). The otolith-based (OOO-HS) and ray/spine-based (SSS-HS) models are the closest analogues to the reference case model from 2013. Model abbreviations are explained in Table 13 and Table 14.

8 Recommendations for future assessments

1. The new maturity estimates from this study should be used for future assessments of swordfish in the east coast Australian fishery. The new estimates are very similar regardless of whether they are derived from otolith-based or ray-based age estimates. They also overcome a methodological bias with the previous Australian estimates, and are reasonably similar to the Hawaiian estimates (i.e., such that a geographical difference of the observed magnitude should not be surprising).
2. The new growth estimates from this study should be used for future assessments of swordfish in the east coast Australian fishery. The ray-based age interpretations presented here are consistent with other international labs, including the PISCF lab in Hawaii. To the extent that we believe the ray-based estimates, it makes sense to use the studies derived from the most geographically appropriate location, i.e., Hawaiian estimates should no longer be used for (at least the western part of) the SW Pacific. The ray-based estimates also appear to be consistent with otoliths for the first few years, which provides an independent corroboration of early growth.
3. There are strong arguments why otolith-based age estimates should be preferable to ray-based estimates, particularly for older individuals, and unless there are counter-arguments that we are not aware of, we recommend that otolith-based estimates should be included in future assessments. Nevertheless, in the absence of direct validation, and a general consensus within the swordfish ageing community, it may not be appropriate to entirely dismiss ray-based estimates at this time (though we would argue that they should be given a lower priority/weighting). We recommend that direct age validation work be considered, including a mark-recapture experiment.
4. Given the remaining sensitivity to growth estimates, and the clear evidence for sex dimorphism in swordfish, it is worth considering sex disaggregation in future assessments (e.g., Wang et al. 2007; Kolody & Herrera 2011), or pooling catch-at-length observations for ages $\sim 7+$.
5. We recommend that uncertainty in M should be represented in future assessments, though the specific approach used in past assessments should be revisited: i) it is not clear why the model with the most optimistic M should be emphasized as the reference case, ii) the functional form of the age-specific M vectors might be reconsidered (e.g., particularly the low values for young ages when there is spawning-related mortality), and iii) if sex-specific growth is pursued, sex-specific M would be worth considering as well.
6. There is evidence for spatial heterogeneity in growth and maturity in tuna and billfish species, though it is often unclear the extent to which this represents real biological differences as opposed to methodological differences (e.g., Kolody et al. 2015). For SW Pacific swordfish, there is tagging (Evans et al. 2014) and genetic (Reeb et al. 2000) evidence suggesting that large movements across the assessment domain might be rare. Accordingly, we would suggest that growth and maturity studies in other regions might

also be informative. However, we would consider this a lower assessment priority than resolving the fundamental uncertainty in population connectivity.

References

- Akaike H (1974) A new look at the statistical model identification. *IEEE Trans Autom Control* 19: 716–723.
- Arocha F (1997) The reproductive dynamics of swordfish *Xiphias gladius* L. and management implications in the northwestern Atlantic. Ph.D. thesis, University of Miami, Miami, FL.
- Arocha F (2007) Swordfish reproduction in the Atlantic Ocean: An overview. *Gulf Caribb Res* 19: 21–36.
- Bard FX, Compean-Jimenez G (1980) Consequences pour l'évaluation du taux d'exploitation du germon (*Thunnus alalunga*) Nord Atlantique d'une courbe de croissance déduite de la lecture des sections de rayon épinaux. *Col Vol Sci Pap ICCAT* 9: 365-375.
- Beamish RJ (1979) Differences in the age of Pacific hake (*Merluccius productus*) using whole otoliths and sectioned otoliths. *J Fish Res Board Can* 36: 141-151.
- Berkeley SA, Houde ED (1983) Age determination of broadbill swordfish, *Xiphias gladius*, from the straits of Florida, using anal fin spine sections. *US Dep Commer, NOAA Tech Rep NMFS* 8: 137-143.
- Boyce DG, Tittensor DP, Worm B (2008) Effects of temperature on global patterns of tuna and billfish richness. *Mar Ecol Prog Ser* 355: 267-276.
- Brouwer SL, Griffiths MH (2004) Age and growth of *Argyrozona argyrozona* (Pisces: Sparidae) in a marine protected area: an evaluation of methods based on whole otoliths, sectioned otoliths and mark-recapture. *Fish Res* 67: 1–12.
- Brown-Peterson NJ, Franks JS, Comyns BH, McDowell JR (2008) Do blue marlin spawn in the northern Gulf of Mexico? *Proceedings of the Gulf and Caribbean Fisheries Institute*, 60: 372–378.
- Brown-Peterson NJ, Wyanski DM, Saborido-Rey F, Macewicz BJ, Lowerre-Barbieri SK (2011) A standardized terminology for describing reproductive development in fishes. *Mar Coast Fish* 3: 52–70.
- Campana SE (1999) Chemistry and composition of fish otoliths: pathways, mechanisms and applications. *Mar Ecol Prog Ser* 188: 263-297.
- Campana SE (2001) Accuracy, precision and quality control in age determination, including a review of the use and abuse of age validation methods. *J Fish Biol* 59: 197-242. doi:10.1006/jfbi.2001.1668.
- Campana SE, Annand MC, McMillan I (1995) Graphical and statistical methods for determining the consistency of age determinations. *Trans Amer Fish Soc* 124: 131–138.
- Castro-Longoria R, Sosa-Nishizaki O (1998) Age determination of swordfish, *Xiphias gladius* L., from waters off Baja California, Mexico, using anal fin rays and otoliths. In: Barrett I, Sosa-Nishizaki, O, Bartoo N (Eds) *Biology and fisheries of swordfish, Xiphias gladius*. Papers from

the International Symposium on Pacific Swordfish, Ensenada, Mexico, 11-14 December 1994. US Dep Commer, NOAA Tech Rep NMFS 142, pp 231-238.

- Chang WYB (1982) A statistical method for evaluating the reproducibility of age determinations. *Can J Fish Aquat Sci* 39: 1208-1210.
- Clarke AD, Telmer KH, Shrimpton JM (2007) Elemental analysis of otoliths, fin rays and scales: a comparison of bony structures to provide population and life-history information for the Arctic grayling (*Thymallus arcticus*). *Ecol Freshw Fish* 16: 354–361.
- Clear N, Davis TL O, Carter T (2000) Developing techniques to estimate the age of bigeye tuna and broadbill swordfish off eastern Australia: a pilot project. FRDC Grant 98/113.
- Davies N, Pilling G, Harley S, Hampton J (2013) Stock assessment of swordfish (*Xiphias gladius*) in the southwest Pacific Ocean. WCPFC-SC9-2013/SA-WP-05.
- De la Serna JM, Ortiz JM, Macias D (1996) Observations on sex ratio, maturity and fecundity by length-class for swordfish (*Xiphias gladius*) captured with surface longline in the western Mediterranean. *Collect Vol Sci Pap ICCAT* 45: 115–140.
- DeMartini EE, Uchiyama JH, Humphreys RL, Sampaga JD, Williams HA (2007) Age and growth of swordfish (*Xiphias gladius*) caught by the Hawaii-based pelagic longline fishery. *Fish Bull* 105: 356–367.
- DeMartini EE, Uchiyama JH, Williams HA (2000) Sexual maturity, sex ratio, and size composition of swordfish, *Xiphias gladius*, caught by the Hawaii-based pelagic longline fishery. *Fish Bull* 98: 489-506.
- Dwyer KS, Walsh SJ, Campana SE (2003) Age determination, validation and growth of Grand Bank yellowtail flounder (*Limanda ferruginea*). *ICES J mar Sci* 60: 1123–1138. doi:10.1016/S1054–3139(03)00125-5.
- Ehrhardt NM, Robbins RJ, Arocha F (1996) Age validation and growth of swordfish, *Xiphias gladius*, in the northwest Atlantic. *Int Comm Conserv Atl Tunas, Coll Vol Sci Pap* 45(2): 358–367.
- Esteves E, Simoes P, da Silva HM, Pedro J (1995) Ageing of swordfish, *Xiphias gladius* Linnaeus, 1758, from the Azores, using sagittae, anal-fin spines and vertebrae. *Life and Marine Sciences* 13A: 39-51.
- Evans K, Abascal F, Kolody D, Sippel T, Holdsworth J, Maru P (2014) The horizontal and vertical dynamics of swordfish in the South Pacific Ocean. *J Exp Mar Biol Ecol* 450: 55-67.
- Farley JH, Clear NP, Leroy B, Davis TLO, McPherson G (2006) Age, growth and preliminary estimates of maturity of bigeye tuna, *Thunnus obesus*, in the Australian region. *Mar Freshwat Res* 57: 713–724. doi:10.1071/MF05255.
- Farley JH, Williams AJ, Clear NP, Davies CR, Nicol SJ (2013a) Age estimation and validation for South Pacific albacore tuna (*Thunnus alalunga*). *J Fish Biol* 82: 1523-1544. doi:10.1111/jfb.12077.
- Farley JH, Williams AJ, Hoyle SP, Davies CR, Nicol SJ (2013b) Reproductive dynamics and potential annual fecundity of South Pacific albacore tuna (*Thunnus alalunga*). *PLoS ONE* 8(4): e60577. doi:10.1371/journal.pone.0060577.

- Francillon-Vieillot H, de Buffrenil V, Castenet J, Geraudie J, Meunier FJ, Sire JY, Zylberberg L, de Ricqlès A (1990) Microstructure and mineralization of vertebrate skeletal tissues. In: Carter JG (ed), *Skeletal biomineralization: patterns, processes and evolutionary trends*, vol.1, p. 471–530. Van Nostrand Reinhold, New York, NY.
- Geffen AJ, de Pontual H, Wright PJ, Mosegaard H (2002) Life history events. In: *Manual of Fish Sclerochronology*. (Eds J Panfili, HD Pontual, H Troadec, PJ Wright.) pp. 99-104. (Ifremer-IRD coedition: Brest, France).
- Gonzalez-Garces A, Farina-Perez AC (1983) Determining age of young albacore, *Thunnus alalunga*, using dorsal spines. US Dept Comm, NOAA Tech Rep NMFS 8: 117-271.
- Griffiths SP, Fry GC, Manson FJ, Lou DC (2009) Age and growth of longtail tuna (*Thunnus tonggol*) in tropical and temperate waters of the central Indo-Pacific. *ICES J Mar Sci* 67:125–134. doi: 10.1093/icesjms/fsp223.
- Gunn JS, Clear NP, Carter TI, Rees AJ, Stanley CA, Farley JH, Kalish JM. (2008) Age and growth in southern bluefin tuna, *Thunnus maccoyii* (Castelnau): direct estimation from otoliths, scales and vertebrae. *Fisheries Research* 92: 207–220. doi:10.1016/j.fishres.2008.01.018.
- Hazin FHV, Hazin HG, Boeckmann CE, Travasson P (2002) Preliminary study on the reproductive biology of swordfish, *Xiphias gladius* (Linnaeus, 1758), in the southwestern equatorial Atlantic Ocean. *ICCAT Col Vol Sci Pap* 54 (5): 1560-1569.
- Hinton MG, Taylor RG, Murphy MD (1997) Use of gonad indices to estimate the status of reproductive activity of female swordfish, *Xiphias gladius*: a validated classification method. *Fish Bull* 95: 80-84.
- Hunter JR, Macewicz BJ (1985) Rates of atresia in the ovary of captive and wild northern anchovy, *Engraulis mordax*. *Fish Bull* 83: 119-136.
- Hunter JR, Macewicz BJ (2003). Improving the accuracy and precision of reproductive information used in fisheries. In: Report of the working group on Modern approaches to assess maturity and fecundity of warm- and cold-water fish and squids. Bergen, Norway 4-7 September 2001. Kjesbu OS, Hunter JR, Witthames PR (eds) *Fisken og Havet*. Nr. 12-2003, pp. 57-68.
- Kalish J, DeMartini E (1993) Determination of swordfish (*Xiphias gladius*) age based on analysis of radiocarbon in vertebral carbonate and collagen. In: Kalish JM (ed), *Use of the bomb radiocarbon chronometer to validate fish age*. Final Report FRDC Project 93/109. Fisheries Research and Development Corporation, Canberra, Australia, pp 340-351.
- Kolody D, Campbell R, Davies N (2008) A Multifan-CL stock assessment of south-west Pacific swordfish 1952-2007. Western and Central Pacific Fisheries Commission Working Paper WCPFC-SC4-2008/SA-WP-6 (rev. 1).
- Kolody D, Eveson JP, Hillary RM (2015) Modelling growth in tuna RFMO stock assessments: current approaches and challenges. doi:10.1016/j.fishres.2015.06.016.
- Kolody D, Herrera M (2011) An Age-, Sex- and Spatially-Structured Stock Assessment of the Indian Ocean Swordfish Fishery 1950-2009, including Special Emphasis on the South-West Region. IOTC-2011-WPB-17_Rev_1.

- Kolody D, Preece, AL, Davies CR, Hartog JR, Dowling NA (2010) Integrated evaluation of management strategies for tropical multi-species long-line fisheries. Final report for FRDC Project 2007/017, 213 pp.
- Lee DW, Prince ED, Crow ME (1983) Interpretation of growth bands on vertebrae and otoliths of Atlantic bluefin tuna, *Thunnus thynnus*. In: Prince ED, Pulos LM (Eds) Proceedings of the International Workshop on Age Determination of Oceanic Pelagic Fishes: Tunas, Billfishes and Sharks. US Dep Commer, NOAA Tech Rep NMFS 8, pp. 61–69.
- Lowerre-Barbieri SL, Ganas K, Saborido-Rey F, Murua H, Hunter RJ (2011) Reproductive timing in marine fishes: variability, temporal scales, and methods. *Mar Coastal Fish* 3: 71–91.
- Mejuto J, Garcia-Cortes B (2014) Reproductive activity of swordfish *Xiphias gladius*, in the Atlantic Ocean inferred on the basis of macroscopic indicators. *Revista de Biología Marina y Oceanografía* 1493): 427-447.
- Megalofonou P (2000) Age and growth of Mediterranean albacore. *J Fish Biol* 57: 700–715. doi: 10.1006/jfbi.2000.1345.
- Megalofonou P, Dean JM, De Metrio G, Wilson C, Berkely S. (1995) Age and growth of juvenile swordfish, *Xiphias gladiou linnaeus*, from the Mediterranean Sea. *J Exp Mar Biol Ecol* 188:79-88.
- Meunier FJ (2002) Skeleton. In: Manual of Fish Sclerochronology. (Eds J Panfili, HD Pontual, H Troadec, PJ Wright.) pp. 65-88. (Ifremer-IRD coedition: Brest, France).
- Mernier FJ, Panfili J (2002) Historical. In: Manual of Fish Sclerochronology. (Eds J Panfili, HD Pontual, H Troadec, PJ Wright.) pp. 23-28. (Ifremer-IRD coedition: Brest, France).
- Morales-Nin B, Panfili J (2002) Age estimation. In: Manual of Fish Sclerochronology. (Eds J Panfili, HD Pontual, H Troadec, PJ Wright.) pp. 91–110. (Ifremer-IRD coedition: Brest, France).
- Mugiya Y, Uchimura T (1989) Otolith resorption induced by anaerobic stress in goldfish, *Carassius auratus*. *J Fish Biol* 35(6): 813-818.
- Murua H, Saborido-Rey F (2003) Female reproductive strategies of marine fish species of the North Atlantic. *J Northwest Atl Fish Sci* 33: 23-31
- Neilson JD, Campana SE (2008) A validated description of age and growth of western Atlantic bluefin tuna (*Thunnus thynnus*). *Can J Fish Aquat Sci*. 65: 1523–1527. doi: 10.1139/F08-127.
- Nishimoto RN, DeMartini EE, Landgraf KC (2006) Suitability of sagittae for estimating annular ages of swordfish, *Xiphias gladius*, from the central North Pacific. Pacific Islands Fish. Sci Cent, Natl Mar Fish Serv, NOAA, Honolulu, HI 96822-2396. Pacific Islands Fish Sci Cent Admin Rep. H-06-04, 34 p.
- Pauly D (1980) On the interrelationships between natural mortality, growth parameters, and mean environmental temperature in 175 fish stocks. *J Cons CIEM* 39(2): 87-92.
- Poisson F, Fauvel C (2009) Reproductive dynamics of swordfish (*Xiphias gladius*) in the southwestern Indian Ocean (Reunion Island). Part 1: oocyte development, sexual maturity and spawning. *Aquat living Resour* 22: 45-58.

- Prince Ed, Lee DW, Wilson CA, Dean JM (1986) Longevity and age validation of a tag-recaptured Atlantic sailfish, *Istiophorus platypterus*, using dorsal spines and otoliths. *Fish Bull* 84: 493-502.
- Quelle P, González F, Ruiz M, Valeiras X, Gutierrez O, Rodriguez-Marin E, Mejuto J (2014) An approach to age and growth of South Atlantic swordfish (*Xiphias gladius*) stock. *ICCAT Collect Vol Sci Pap* 70(4): 1927-1944.
- Reeb CA, Arcangeli L, Block BA (2000) Structure and migration corridors in Pacific populations of the swordfish, *Xiphias gladius*, as inferred through analyses of mitochondrial DNA. *Mar Biol* 136: 1123–1131.
- Restrepo VR, Diaz GA, Walter JF, Neilson JD, Campana SE, Secor D, Wingate RL (2010) Updated estimate of the growth curve of Western Atlantic bluefin Tuna. *Aquat Living Resour* 23: 335–342. doi:10.1051/alr/2011004.
- Rideout RM, Tomkiewicz J (2011) Skipped Spawning in fishes: more common than you might think. *Marine and Coastal Fisheries: Dynamics, Management, and Ecosystem Science*, 3: 176-189.
- Robbins WD, Choat JH (2002) Age-based dynamics of tropical reef fishes; A guide to the processing, analysis and interpretation of tropical fish otoliths. Townsville, Australia, p 1-39.
- Rodríguez-Marín E, Clear N, Cort JL, Megalofonou P, Neilson JD, Neves dos Santos M, Olafsdottir D, Rodríguez-Cabello C, Ruiz M, Valeiras J (2007) Report of the 2006 ICCAT workshop for bluefin tuna direct ageing. *ICCAT Coll Vol Sci Pap* 60: 1349–1392.
- Schaefer KM (2001) Reproductive biology of tunas. In *Tuna: physiology, ecology and evolution*. Volume 19, *Fish Physiology*. (Eds B. A. Block and D. E. Stevens.) pp 225-269. Academic Press: New York, USA.
- Shapiro DY, Sadovy Y, McGehee MA (1993) Periodicity of sex change and reproduction in the red hind, *Epinephelus guttatus*, a protogynous grouper. *Bull Mar Sci* 53: 1151–1162.
- Shimose T, Tanabe T, Chen K-S, Hsu C-C (2009) Age determination and growth of Pacific bluefin tuna, *Thunnus orientalis*, off Japan and Taiwan. *Fish Res* 100: 134–139.
- Siskey MR, Lyubchich V, Liang D, Piccoli PM, Secor DH (2015) Periodicity of strontium: Calcium across annuli further validates otolith-ageing for Atlantic bluefin tuna (*Thunnus thynnus*). *Fish Res* 177: 13-17.
- Sun C, Wang S, Yeh S (2002) Age and growth of the swordfish (*Xiphias gladius* L.) in the waters around Taiwan determined from anal fin rays. *Fish Bull* 100: 822-835.
- R Core Team (2013) R: A language and environment for statistical computing. R Foundation for Statistical Computing, Vienna, Austria. <http://www.R-project.org/>.
- Taylor RG, Murphy M (1992) Reproductive biology of the swordfish *Xiphias gladius* in the Straits of Florida and adjacent waters. *Fish Bull* 90: 809–816.
- Tserpes G, Tsimenides N (1995) Determination of age and growth of swordfish, *Xiphias gladius* L., 1758, in the eastern Mediterranean using anal-fin spines. *Fish Bull* 93: 594–602.
- Uchiyama JH, Skillman RA, Sampaga JD, De Martini EE (1998) A preliminary assessment of the use of hard parts to age central Pacific swordfish, *Xiphias gladius*. In: Barrett I, Sosa-Nishizaki, O,

- Bartoo N (Eds) Biology and fisheries of swordfish, *Xiphias gladius*. Papers from the International Symposium on Pacific Swordfish, Ensenada, Mexico, 11-14 December 1994. US Dep Commer, NOAA Tech Rep NMFS 142: 261-273.
- Varghese SP, Vijayakumaran, K, Anrose A, Mhatre VD (2013) Biological aspects of swordfish, *Xiphias gladius* Linnaeus, 1758, caught during tuna longline survey in the Indian seas. Turkish J Fish Aquat Sci 13: 529-540.
- von Bertalanffy L (1938) A quantitative theory of organic growth (Inquiries on growth laws II). Human Biol 10: 181–213.
- Wang S-P, Sun C-L, Punt AE, Yeh S-Z (2007) Application of the sex-specific age-structured assessment method for swordfish, *Xiphias gladius*, in the North Pacific Ocean. Fish Res 84: 282–300.
- Wang S-P, Sun C-L, Yeh S-Z (2003) Sex ratios and sexual maturity of swordfish (*Xiphias gladius* L.) in the waters of Taiwan. Zool Stud 42: 529–539.
- West G. (1990) Methods of assessing ovarian development in fishes: a review. Mar Freshw Res 41: 199–222.
- Wilson CA, Dean JM (1983) The potential use of sagittae for estimating age of Atlantic swordfish, *Xiphias gladius*. US Dep Commer., NOAA Tech Rep NMFS 8: 151-156.
- Wright PJ, Panfili J, Morales-Nin B, Geffen AJ (2002). Types of calcified structures. In: Manual of Fish Sclerochronology. (Eds J Panfili, HD Pontual, H Troadec, PJ Wright.) pp. 31–57. (Ifremer-IRD coedition: Brest, France).
- Young J, Drake A (2002) Reproductive dynamics of broadbill swordfish (*Xiphias gladius*) in the domestic longline fishery off eastern Australia. FRDC Final Report for project 1999/108.
- Young J, Drake A (2004) Age and growth of broadbill swordfish (*Xiphias gladius*) from Australian waters. FRDC Final Report for project 2001/014.
- Young JW, Drake A, Brickhill M, Farley JH, Carter T (2003) Reproductive dynamics of broadbill swordfish, *Xiphias gladius*, in the domestic longline fishery off eastern Australia. Mar Freshwat Res 54: 315-32.
- Young J, Humphreys R, Uchiyama J, Clear N (2008) Comparison of maturity and ageing of swordfish from the Hawaiian and Australian waters. WCPFC-SC4-2008/BI-IP-2.

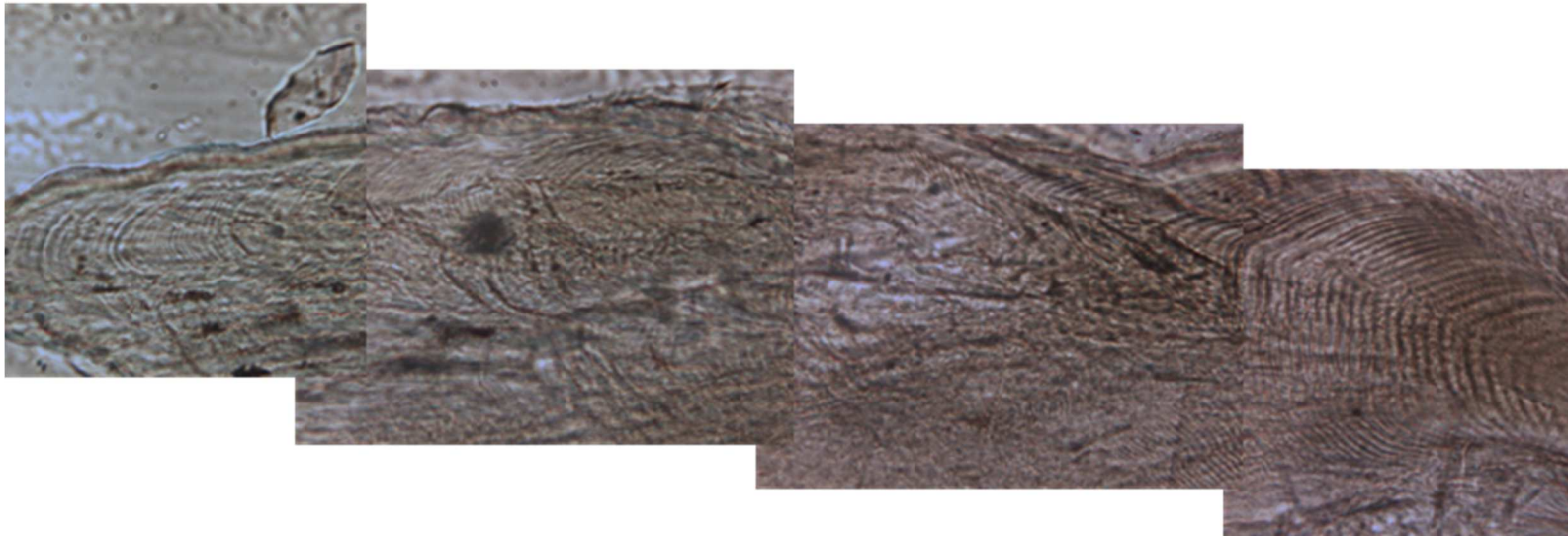
Appendix A Distally ground A) sagittae and B) lapilli and C) transverse ground sagittae from the same fish. The clearest count path is shown at higher magnification



A)

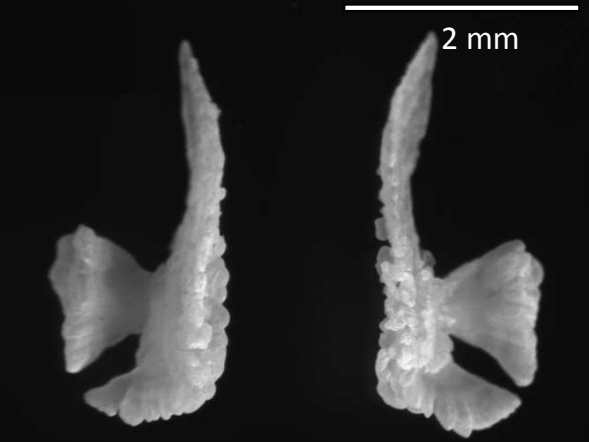


B)

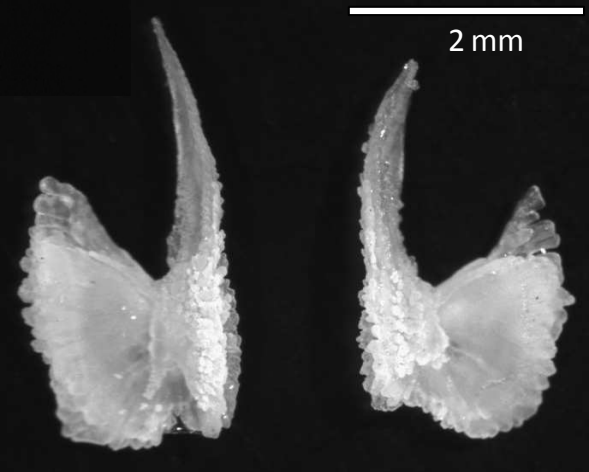


c)

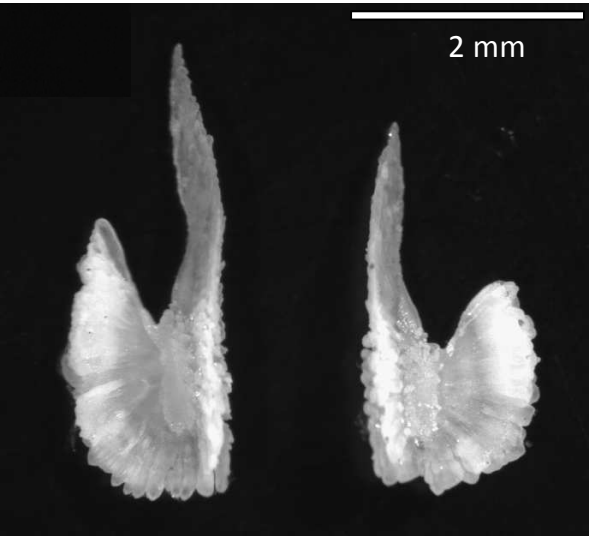
Appendix B Examples of the variability in swordfish sagittal otolith morphology among similar sized fish.



136 cm OFL fish.



132 cm OFL fish.



128 cm OFL fish.

Appendix C Daily age estimates versus annual age estimates from otoliths (transverse sections read at 640-1000x magnification with transmitted light).

Archive number	OFL	Otolith weight (mg)	Zone count	Readability	Comments	A - primordia to end of clear zones or opaque zone measurement (µm)	Count at measurement A	B - primordia to edge measurement (µm)	C - shoulder to edge measurement (µm)	Annual Age	Edge Type	Ageing comment
135	113	0.77	233	2	clear for first 90-100, probably reliable for first 150 to 170	561	166	885	664	2	I	
142	108	0.74	299	3	quite a few split zones - post 150 difficult and could be more	468	142	735	680	2	I	maybe 2 W
160	109	1.15	242	3	reasonable throughout	528	157	742	752	2	W	maybe 2 I or actually 2nd on edge
163	120	0.73		1	confident count out to 178 zones-structure poor thereafter	556	178	960	848	3	W	
248	106	0.93	268	3	good out to approx 170	524	157	773	643	1	W	
250	109	0.84	354	4	reasonable out to approx 140 - very fine zones probably not daily	495	181	787	674	3	N	maybe 2 Wide
253	104	0.56	290	3		502	170	679	668	1	W	
258	107	0.92	269	4	definite change at about 95-100 zones, zone become poor at approx 150	550	182	776	766	3	N	maybe 2 Wide - edge tricky
268	103	0.65	228	3		470	160	619	564	1	W	
274	102	0.77		1	can't age	490		763	733	2	W	
275	113	0.71	311	3	clear out to 180-200	549	178	808	664	2	W	
281	103	0.51	223	3		513	138	704	811	1	W	

286	117	0.71		1	can only age out to first zone 160-170	477		162	952	845	4	N	maybe 3 wide
291	114	0.87	374	2	can count out to 244 clear zones - rest not so confident	581		189	951	835	3	N	maybe some translucent just on edge
305	117	1.15	391	3	first 100 zones ok - difficult between 110-160 - outer zones possibly not daily	606		168	921	795	2	W	poss 3w
341	104	0.72	287	3	probably only 2N or 2I	650		205	929	894	3	N	maybe only 2 N or I
343	109	0.103	257	3		619		180	841	763	2	N	
349	106	0.59	309	2		532		125	736	824	2	I	
350	106	0.85		1	cant age past 150	495		148	834	826	3	N	
357	116	0.67	291	3		624		202					
407	117	0.67		1		550		185	890	836	2	W	
511	116	0.92			can't age past 98 zones				788	895	1	W	maybe 2 W
558	111	0.76	193	2		492		144	742	644	1	W	
559	102	0.91	386	3	clear out to 1st or 2nd opaque - outer zones reasonable also	585		227	941	902	2	W	
597	113	0.67	441	3	no areas that were unreadable - change in structure around 150-160	508		154	998	811	3	W	
617	76	0.2	196	3	abrupt change just in from edge - maybe first opaque	528		162	617	492	0	W	maybe 1 forming near/on edge
1750	102	0.46		1									
1753	104	0.89	323	3	structure relatively clear throughout	458		169	732	680	2	W	maybe 1 edge would be better
1785	82	0.58	228	4	ok for most - other otolith prep as distal, slightly better structure but similar age	558		179	637	796			

1806	75	0.37	146	2	not sure that outer zones are daily - if not maybe another 40	610	146	610	516	1	N	or 0 W
1812	94	0.5	246	2	not great - a few different layers	512	192	662	565	1	N	maybe 1 edge
1222	70	0.35	179	2	difficult past 130	529	179	529	525	0	W	
1223	76	0.51	167	2	reasonable	501	167	501	555	0	W	Maybe 1st on edge
1748	98	0.58	214	3	not too bad for most	663	185	701	585	1	N	Maybe 1 edge
1783	82	0.41	124	2	difficult after 80	487	124	688	512	0	W	poss 1 on edge
1224	80	0.41	174	4		497	174	497		1	N	
591	116	1.08	240	3	nice core. Lots of fine zones visible.	640	156	854	1176	2	N	
1225	96	0.61	305	3	Distal section age used as transverse section broken- Clear increments to near edge - no measurements taken – Count on transverse section = 278.					1	W	
LARGER OTOLITHS PREPARED FOR DAILY AGE COMPARISON												
211	210	2.81	459	4	Both broken in vial. Nailed core, rest difficult After 60 days close to unageable and perhaps not daily???					6	W	
228	230	2.26	512	4	Broken in vial. Missed core, but mid section better, edge still difficult.					11	W	
332	171	1.31	308	3	Off core, but rest good. May be out by ten days at core					5	w	
388	137	0.76	290	3	Nailed core, but faint towards edge. Had to assume last 30 zones					4	W	
336	194	2.06	486	2	Difficult					10	W	

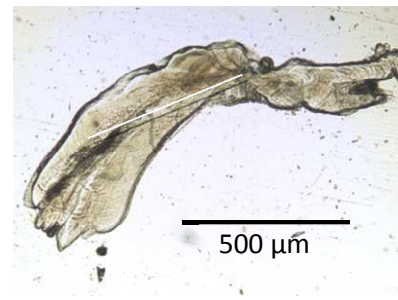
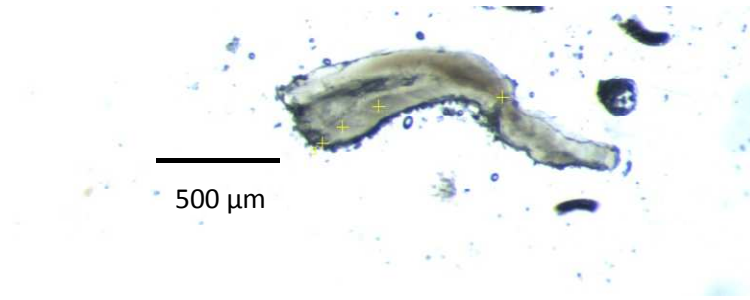
Appendix D Example images for some otoliths prepared for annual (left) and daily (right) examination. White line represents transect A (distance and count to a point that corresponds to either the marked change in microincrement structure or as indicated on the annual images, the first assumed annual zone).



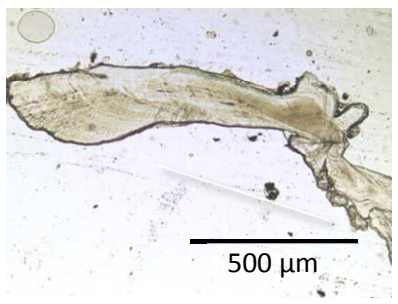
SWO #250 – 109cm (OFL), otolith weight 0.84mg. Daily zone count -354, Annual zone count – 3N. Count to the end of transect A = 189.



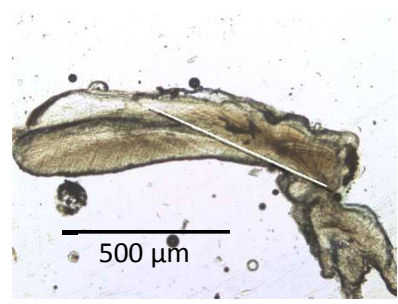
SWO #268 – 103cm (OFL), otolith weight 0.65mg. Daily zone count – 228, Annual zone count - 1W. Count to the end of transect A = 160.



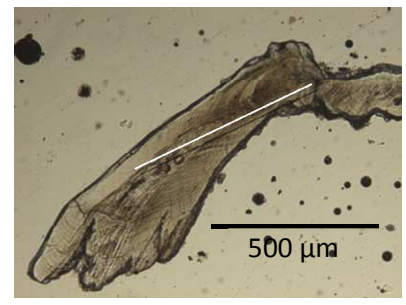
SWO #275 – 113cm (OFL), otolith weight 0.71mg. Daily zone count – 311, Annual zone count - 2W. Count to the end of transect A = 178.



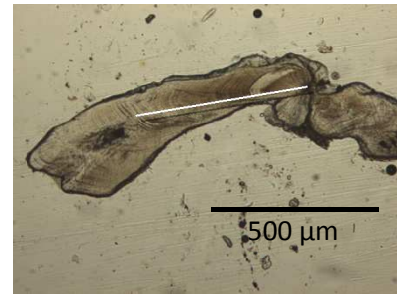
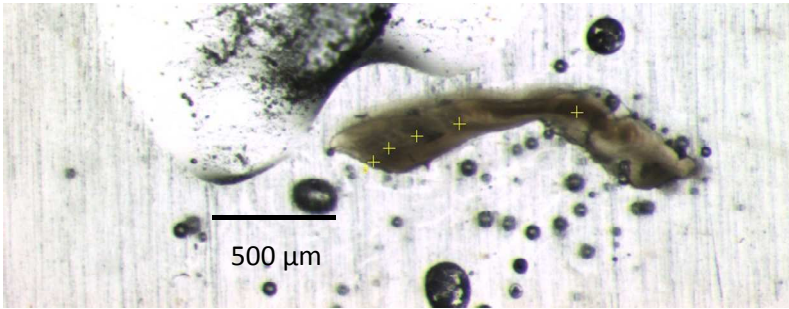
SWO #286 – 117cm (OFL), otolith weight 0.71 mg. Daily zone count N/A, Annual zone count - 4N. Count to the end of transect A = 162.



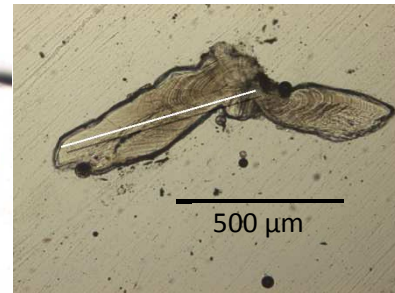
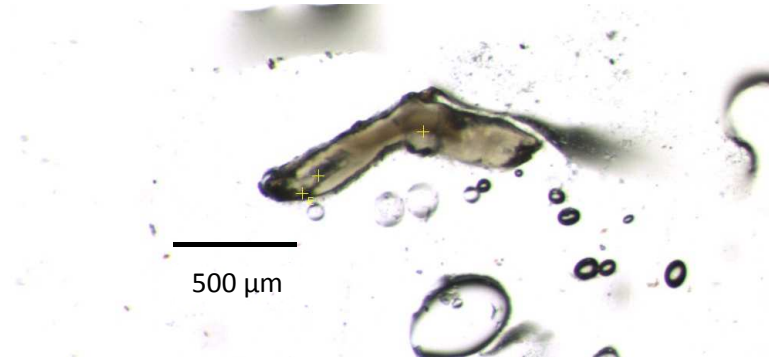
SWO #341 – 104cm (OFL), otolith weight 0.72mg. Daily zone count – 287, Annual zone count - 3N. Count to the end of transect A = 205.



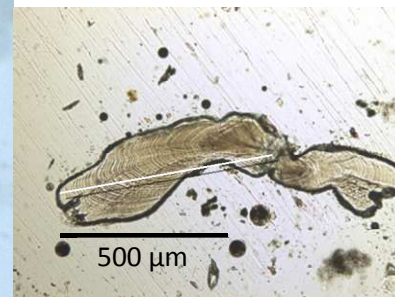
SWO 559 – 102cm (OFL), otolith weight 0.91mg. Daily zone count – 386, Annual zone count - 2W. Count to the end of transect A = 227.



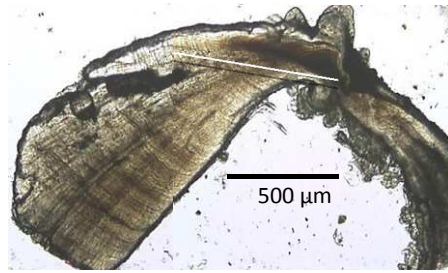
SWO 597 – 113cm (OFL), otolith weight 0.67mg. Daily zone count – 441, Annual zone count 3W. Count to the end of transect A = 154.



SWO #1222 – 70cm (OFL), otolith weight 0.35mg. Daily zone count 179, Annual zone count 0W. Count to the end of transect A = 179.



SWO #1806 – 75cm (OFL), otolith weight 0.37mg. Daily zone count 146, Annual zone count 0W. Count to the end of transect A = 146.

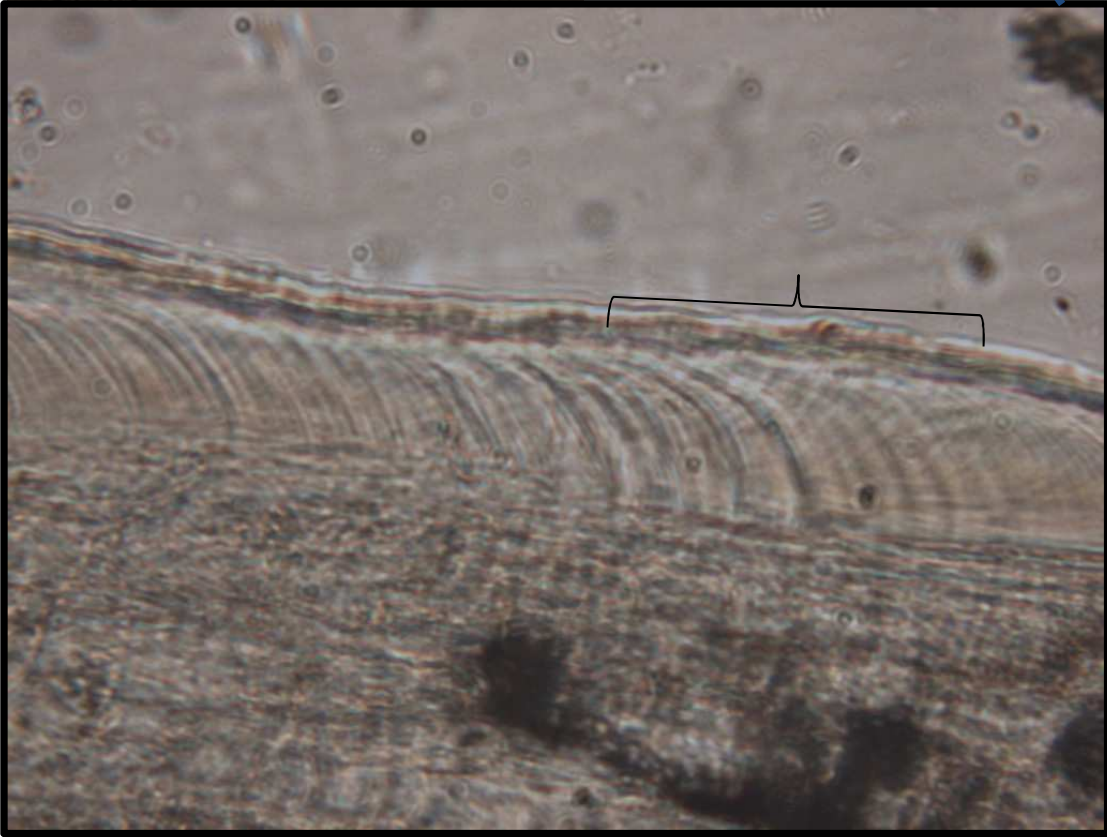
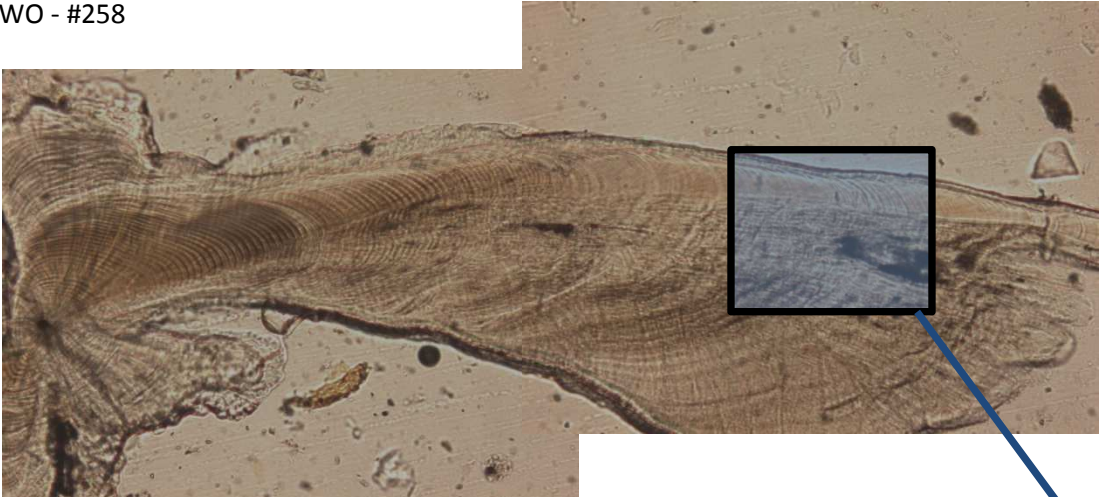


SWO 336 – (OFL), otolith weight 3.40mg. Daily zone count 486, Annual zone count 10W. Count to the end of transect A = 189.

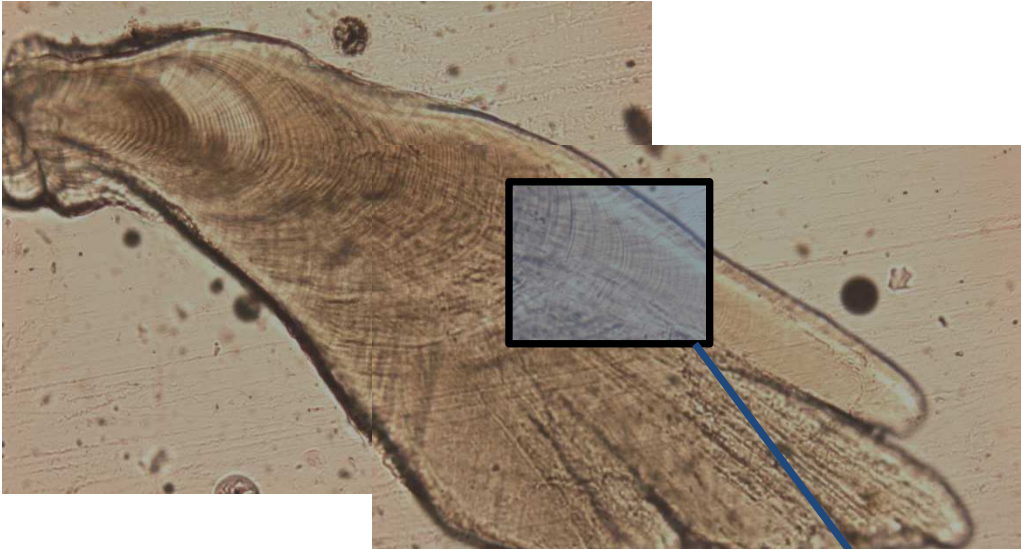
Appendix E Examples of the transition point in otoliths

Highlighted area under higher magnification (100x) of the transition point in the otolith.

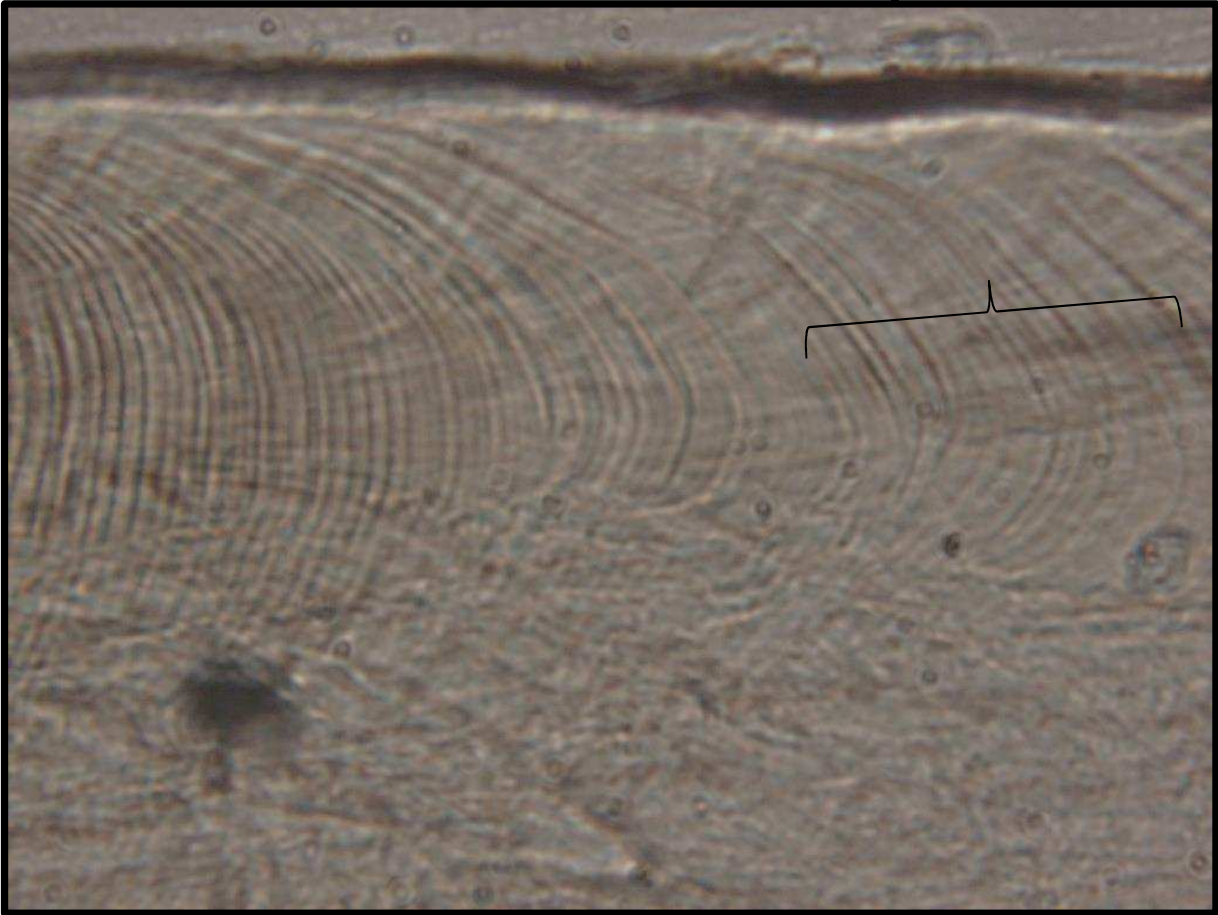
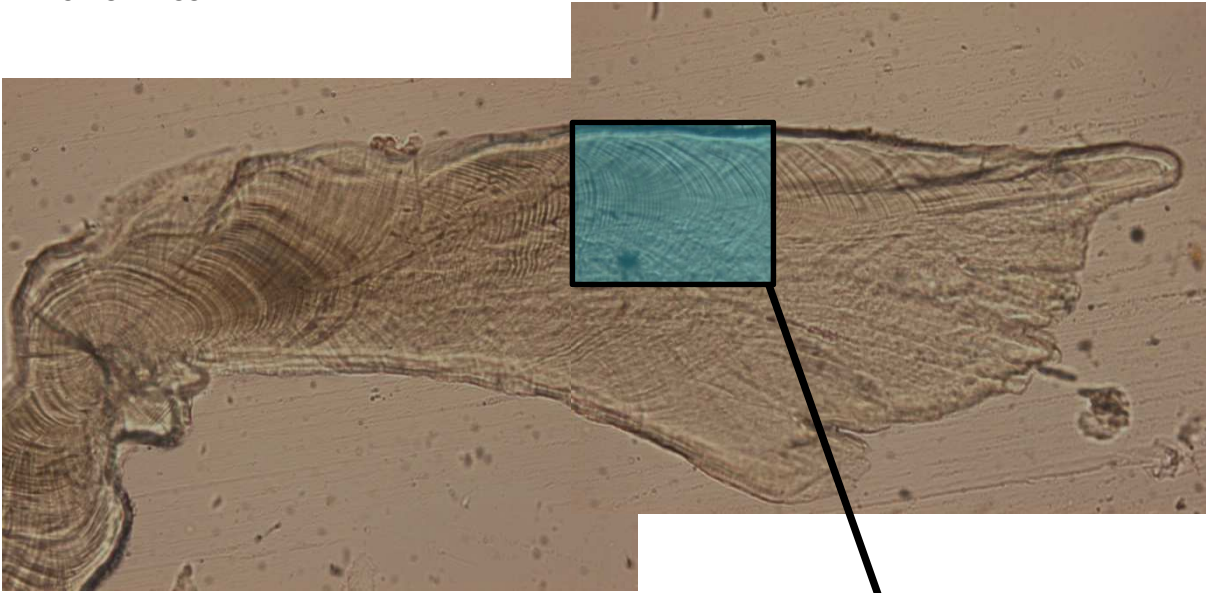
SWO - #258



SWO - #268

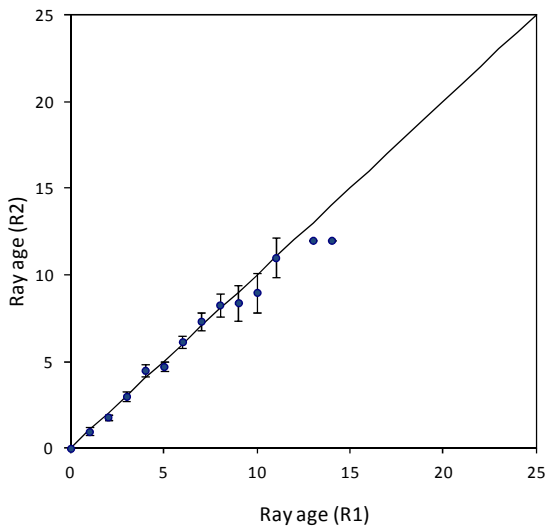


SWO - #253

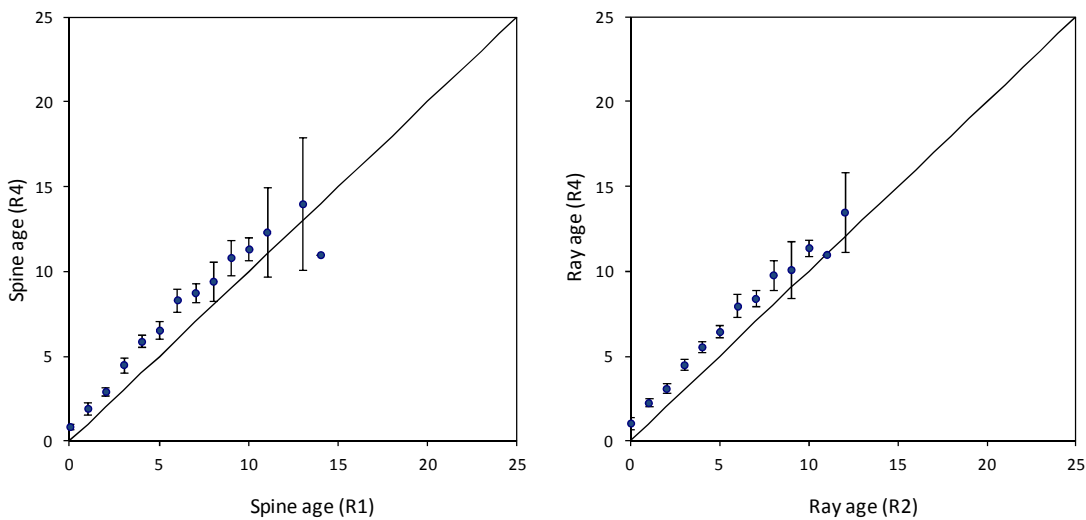


Appendix F Age bias plots (+/- CI) between readers (R1-R4) of rays and otoliths

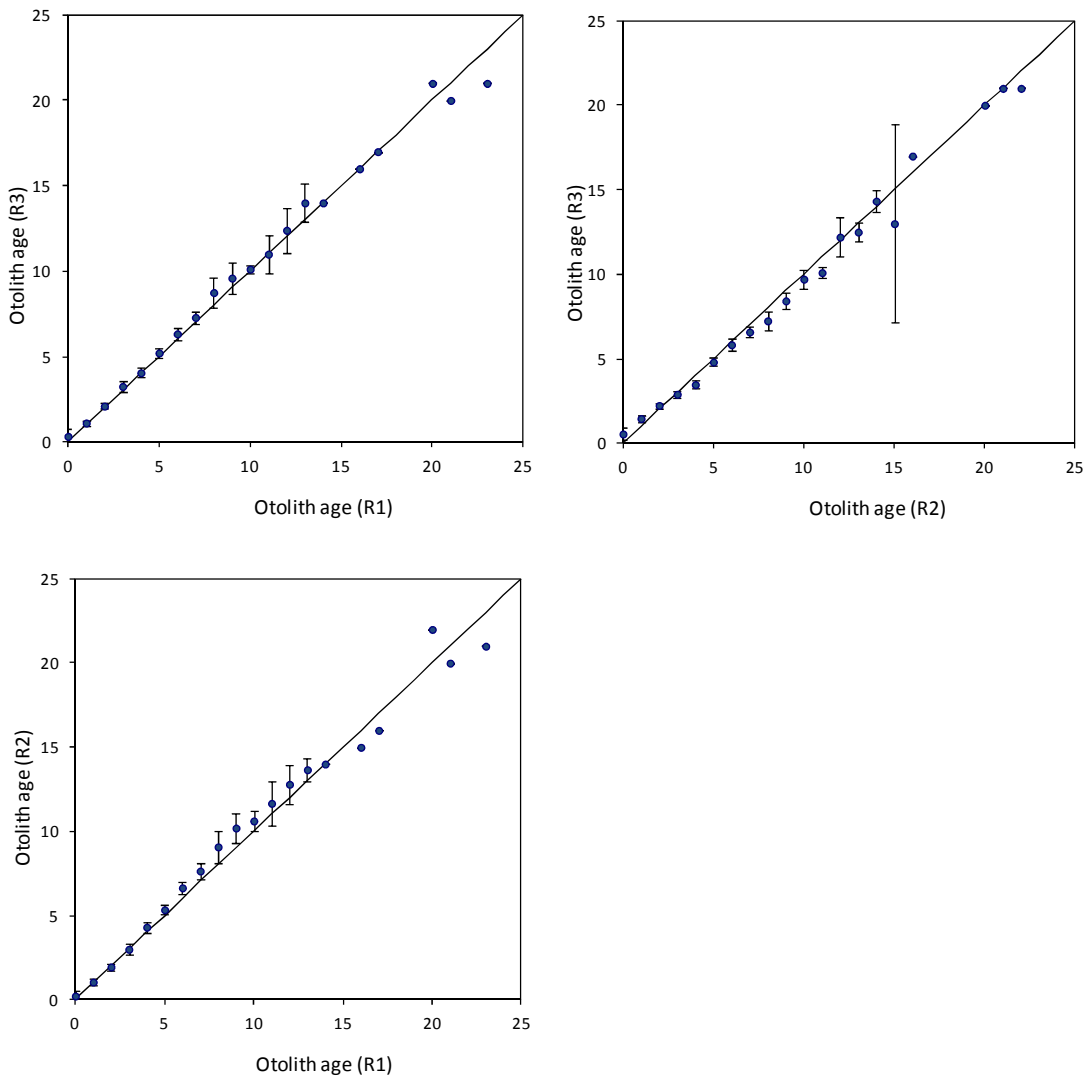
Apx Figure F.1. Age bias plot for rays between R1 and R2.



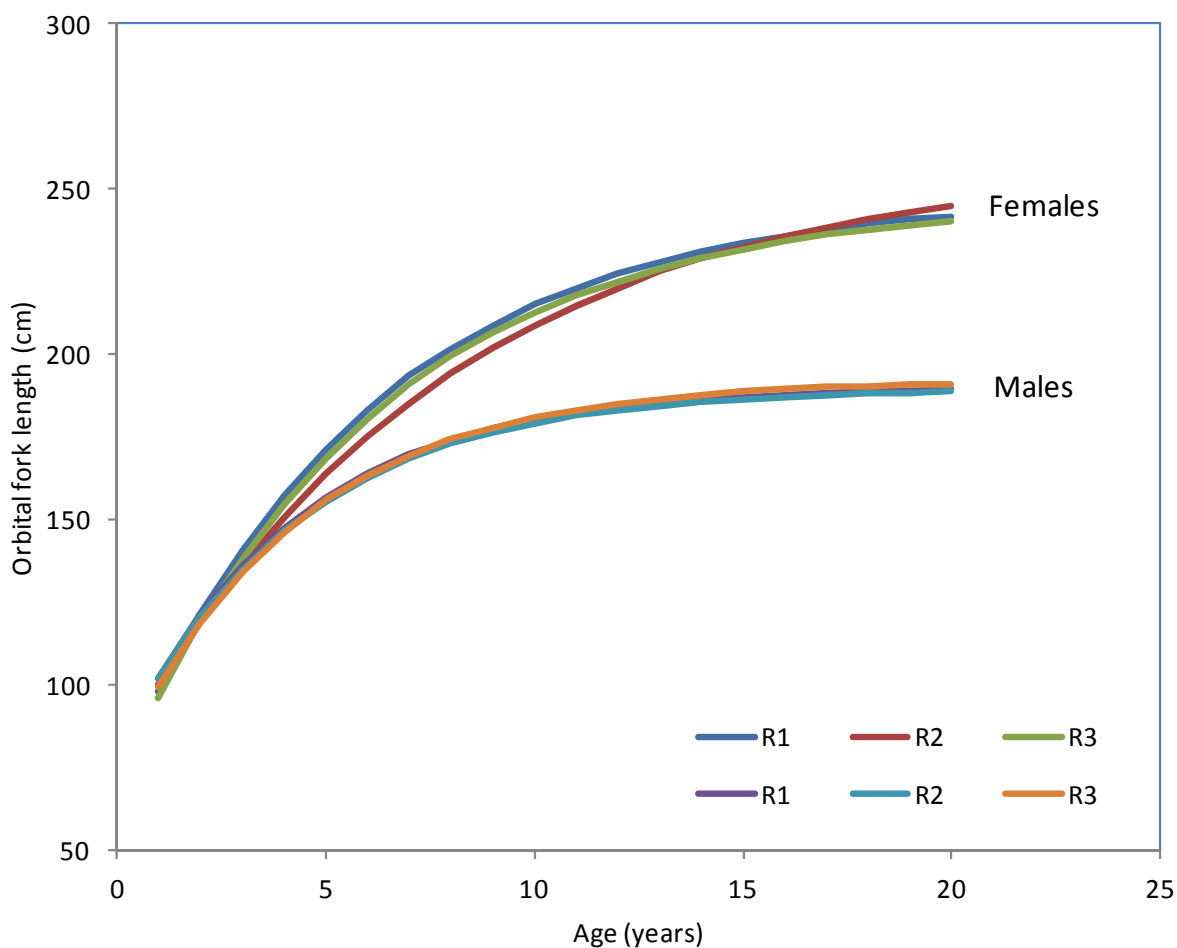
Apx Figure F.2. Age bias plots for rays between R1 or R2 and R4.



Apx Figure F.3. Age bias plots for otoliths between readers R1, R2 and R3.



Appendix G Comparison of von Bertalanffy growth curves to otolith-based age data from three readers (R1, R2 and R3).

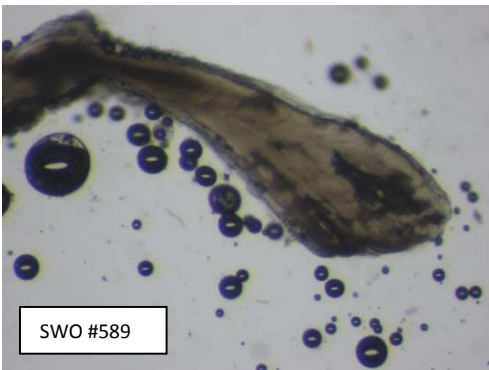
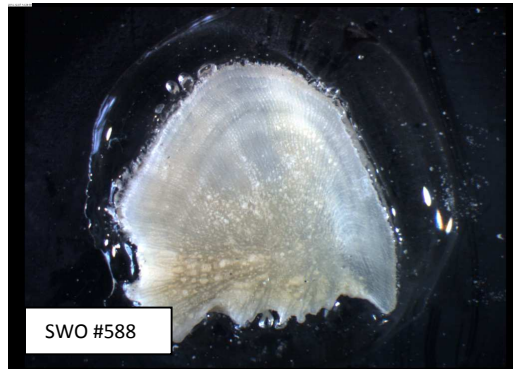


Appendix H Examples of the marginal state of clear otoliths and fin rays for each month that samples are available for. Where possible, hardparts were selected from the same fish.

January Otolith

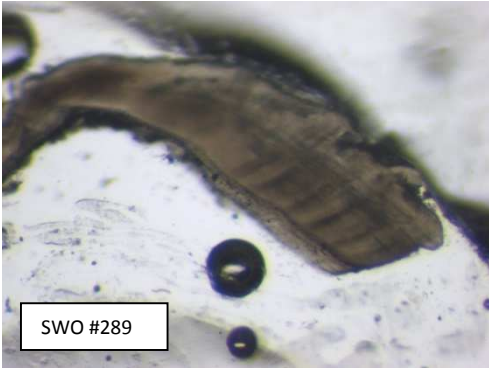


Fin ray



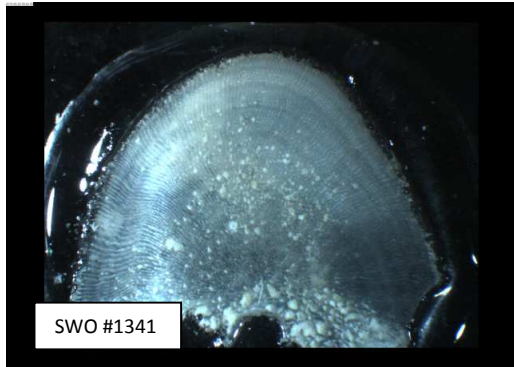
February



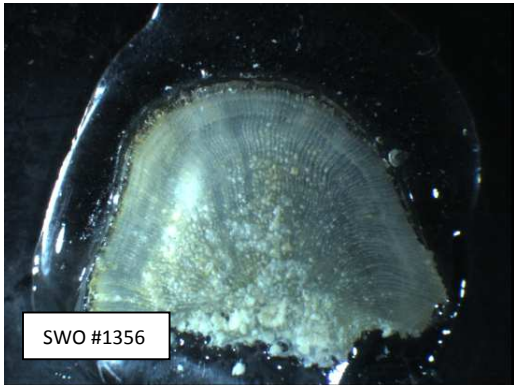


March

N/A

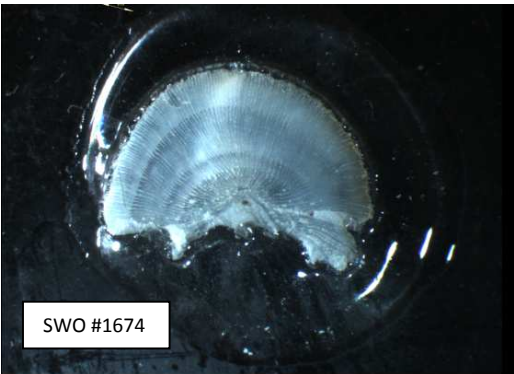


N/A

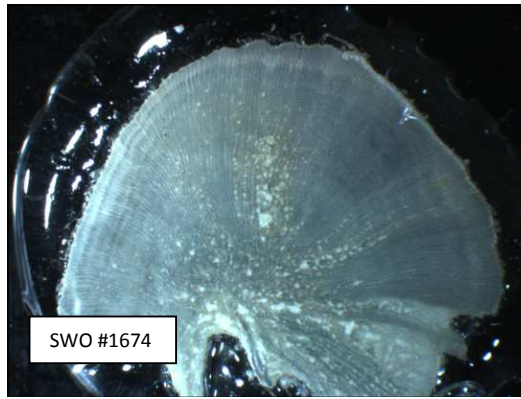


April

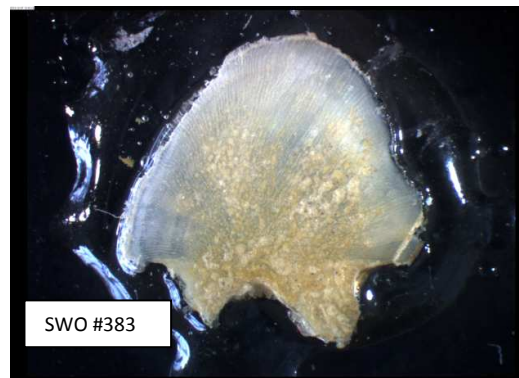
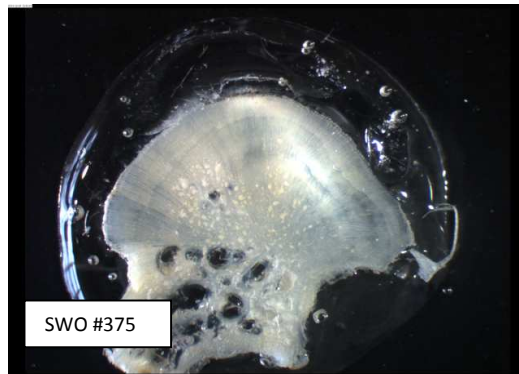
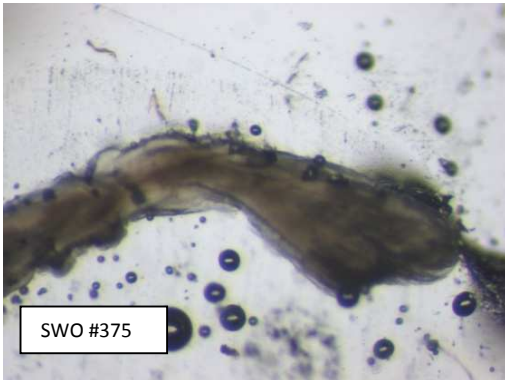
N/A



N/A

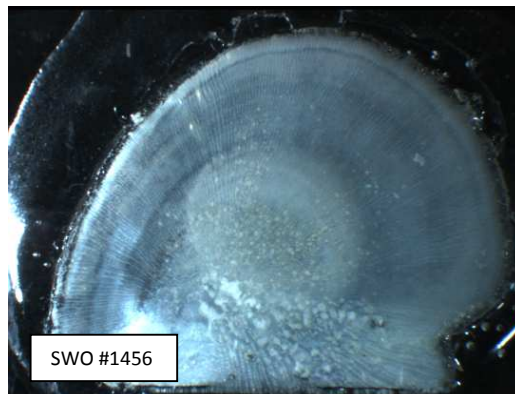


May



June

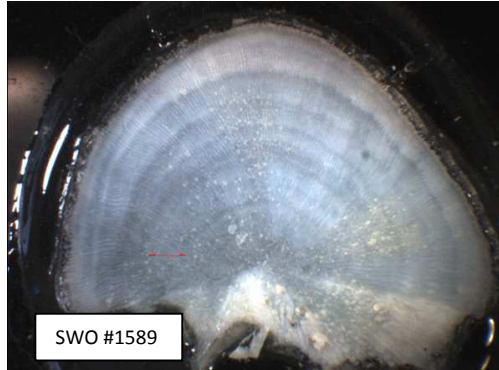
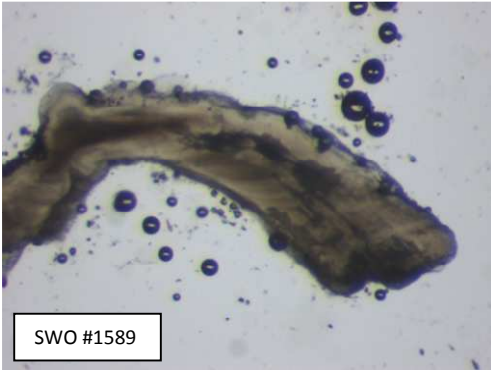
N/A



N/A



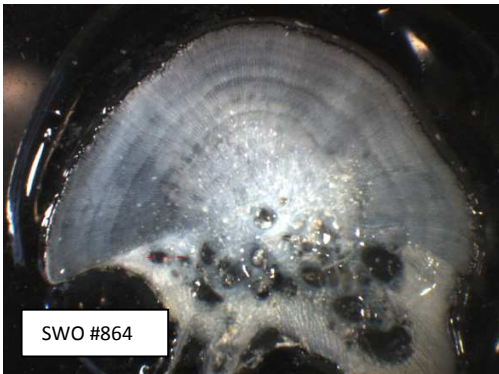
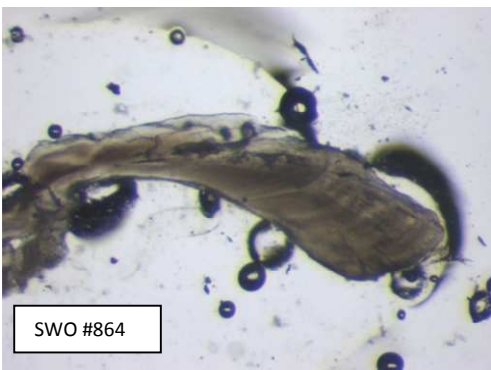
July



N/A

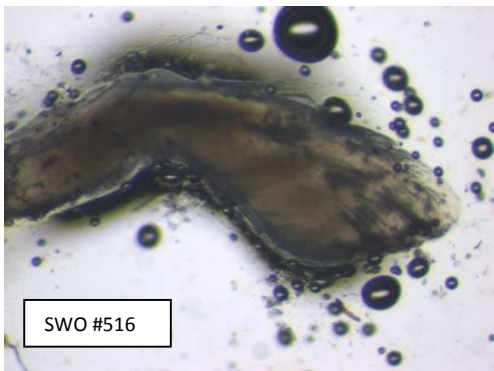


August

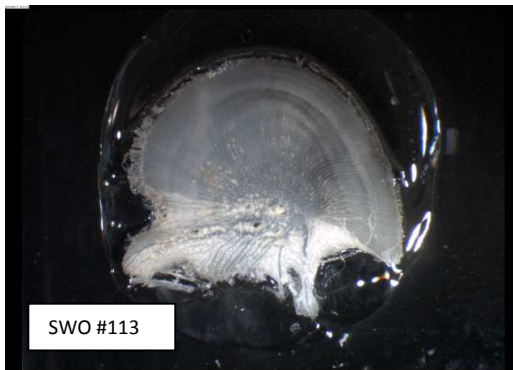


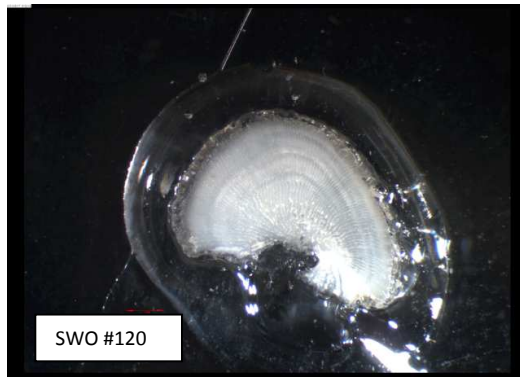


September

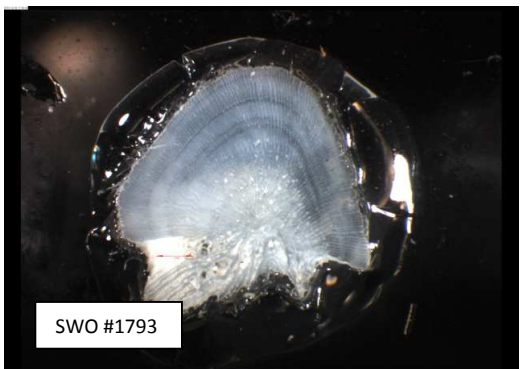
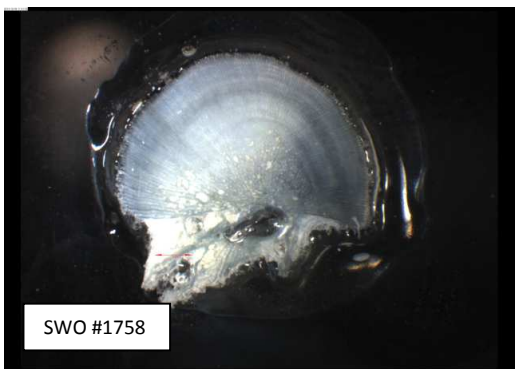
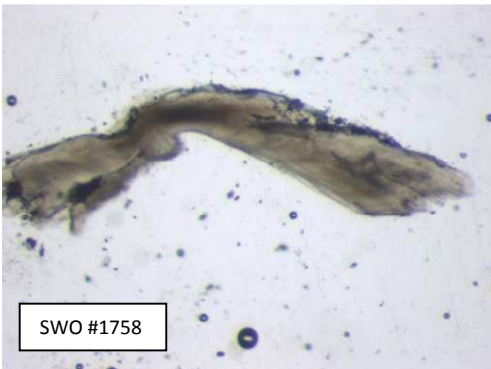


October

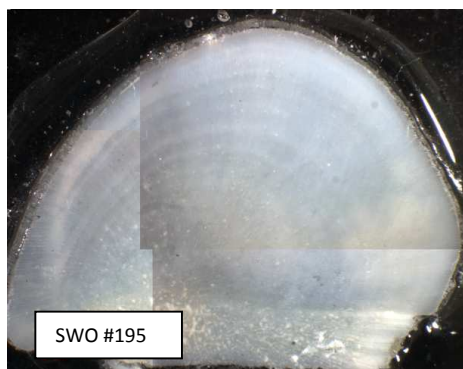
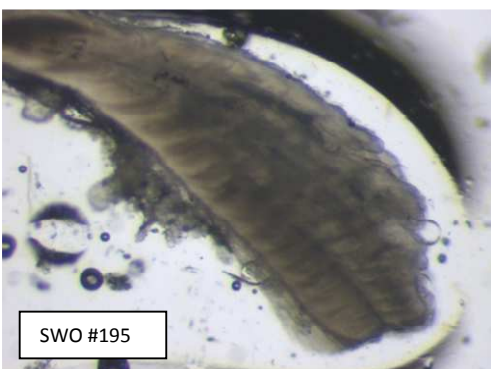




November



December





CONTACT US

t 1300 363 400
+61 3 9545 2176
e enquiries@csiro.au
w www.csiro.au

FOR FURTHER INFORMATION

Oceans and Atmosphere
Jessica Farley
t +61 3 6232 5189
e Jessica.farley@csiro.au
w www.csiro.au

AT CSIRO WE SHAPE THE FUTURE

We do this by using science to solve real issues. Our research makes a difference to industry, people and the planet.

As Australia's national science agency we've been pushing the edge of what's possible for over 85 years. Today we have more than 5,000 talented people working out of 50-plus centres in Australia and internationally. Our people work closely with industry and communities to leave a lasting legacy. Collectively, our innovation and excellence places us in the top ten applied research agencies in the world.

WE ASK, WE SEEK AND WE SOLVE